Age of Information in Multi-Hop Status Update Systems: Fundamental Bounds and Scheduling Policy Design

by

Shahab Farazi

A Thesis

Submitted to the Faculty

of the

WORCESTER POLYTECHNIC INSTITUTE

In partial fulfillment of the requirements for the

Degree of Doctor of Philosophy

in

Electrical and Computer Engineering

by

May 2020

APPROVED:

Professor Donald R. Brown III, Major Advisor, ECE Department, WPI

Professor Kaveh Pahlavan, ECE Department, WPI

Professor Andrew G. Klein, Engineering and Design Department, WWU

To my family.

Abstract

Freshness of information has become of high importance with the emergence of many real-time applications like monitoring systems and communication networks. The main idea behind all of these scenarios is the same, there exists at least a monitor of some process to which the monitor does not have direct access. Rather, the monitor indirectly receives updates over time from a source that can observe the process directly. The common main goal in these scenarios is to guarantee that the updates at the monitor side are as fresh as possible. However, due to the contention among the nodes in the network over limited channel resources, it takes some random time for the updates before they are received by the monitor. These applications have motivated a line of research studying the *Age of Information* (AoI) as a new performance metric that captures timeliness of information.

The first part of this dissertation focuses on the AoI problem in general multi-source multi-hop status update networks with slotted transmissions. Fundamental lower bounds on the instantaneous peak and average AoI are derived under general interference constraints. Explicit algorithms are developed that generate scheduling policies for status update dissemination throughout the network for the class of minimum-length periodic schedules under global interference constraints.

Next, we study AoI in multi-access channels, where a number of sources share the same server with exponentially distributed service times to communicate to a monitor. Two cases depending on the status update arrival rates at the sources are considered: (i) random arrivals based on the Poisson point process, and (ii) active arrivals where each source can generate an update at any point in time. For each case, closed-form expressions are derived for the average AoI as a function of the system parameters.

Next, the effect of energy harvesting on the age is considered in a single-source single-monitor status update system that has a server with a finite battery capacity. Depending on the server's ability to harvest energy while a packet is in service, and allowing or blocking the newly-arriving packets to preempt a packet in service, average AoI expressions are derived.

The results show that preemption of the packets in service is sub-optimal when the energy arrival rate is lower than the status update arrival rate.

Finally, the age of channel state information (CSI) is studied in fully-connected wireless networks with time-slotted transmissions and time-varying channels. A framework is developed that accounts for the amount of data and overhead in each packet and the CSI disseminated in the packet. Lower bounds on the peak and average AoI are derived and a greedy protocol that schedules the status updates based on minimizing the instantaneous average AoI is developed. Achievable average AoI is derived for the class of randomized CSI dissemination schedules.

Acknowledgements

I would like to thank everyone who has helped, inspired, or encouraged me to pursue this degree, including Professors, collaborators, family and friends.

I want to thank my family for all they have done for me, their unconditional love and endless support throughout my life.

I am incredibly fortunate to have Professor Richard Brown as my advisor. He has always been supportive of my research and has given me the freedom to pursue various topics. Despite his busy schedule, he has always made time for insightful discussions about the research and provided helpful pointers. The completion of this dissertation would not have been possible without his direction. The lessons that I have learned from working with him throughout my journey at WPI have helped me become a better researcher as well as a better person in life. This experience has been an honor and I will treasure it forever.

I would like to thank Professor Andrew Klein for his constant help and support throughout this endeavour. He always ensured his availability for discussions and shared with me his research expertise, guiding me to look at the problems with a new perspective and come up with original research ideas. I am forever grateful for the experiences and skills that I have gained from working with him, which I will take with me into my future career.

Many thanks to Professor Kaveh Pahlavan for accepting to be part of my PhD dissertation committee. Your time and your comments are very much appreciated.

Thanks to my labmates Rui and Kim at WPI who have made the lab a better workplace.

Biography

Shahab Farazi was born in the city of Quchan located in the northeastern part of Iran. During his childhood he discovered his love for math. In 2006, he took the national entrance exam for public universities, in the field of mathematics and physics. He applied to the electrical and computer engineering program at Khajeh Nasir Toosi University (KNTU) of Technology, for which he was accepted into. This led him to move to Tehran when he was 18 years old. After undergraduate school, he continued his pursuit of knowledge in the electrical and computer engineering field when he attended Iran University of Science and Technology for his Masters degree. Next, he decided to study abroad and applied for the PhD program at the electrical and computer engineering department at Worcester Polytechnic Institute (WPI). From the northeastern part of Iran to the northeastern part of the USA he began his next adventure. While at WPI, he worked as a research assistant on campus. The skills that he learned as a research assistant and from his classes he is eager to apply to his future career. As Shahab is finishing his studies at WPI, he is looking forward to the next step to acquire a job.

Contents

List of Figures

List of Tables

f

Chapter 1

Introduction.

Information freshness is of critical importance in a variety of communication and networked monitoring and control systems such as intelligent vehicular systems, channel state information feedback in wireless networks, and environmental monitoring as well as applications such as financial trading, online learning and internet of things. In these types of applications, stale information can lead to incorrect decisions, unstable control loops, and even compromises in safety and security. A recent line of research has considered information freshness from a fundamental perspective under an *Age of Information* (AoI) metric first proposed in [1]. The central idea is that there are one or more sources of information along with one or more monitors. A source generates timestamped status updates which are received by a monitor after some delay. The "age of information" is defined as the difference between the current time and the time stamp of the most recent successfully received update at the monitor. A common theme of the AoI literature is to study and optimize the statistics of AoI, i.e., average age or peak age, as a function of the system parameters and update strategies.

1.1 Motivation

Over the last few years, the need for having fresh information in multiple scenarios like network monitoring and intelligent vehicular transportation systems as well as lower latencies in

the range of a few milliseconds in the fifth generation of wireless communications technologies supporting cellular data networks (5G) has led to many studies in the AoI area. The early work in [2] considers a simple system model where a single source updates a monitor through a queue that has capacity of one packet and follows a first-come-first-served (FCFS) service discipline, as represented in Fig. 1.1. Even with this simple model, it was shown that minimizing the average AoI is non-trivial, due to the correlation of the system parameters like the inter-arrival times of the consecutive updates and the system times. Further, it was shown that minimizing the AoI is equivalent to finding a trade-off between highly frequent and too infrequent update generation rate at the source side. Since the former leads to updates getting stale due to large waiting times at the queue and the latter leads to the monitor not being updated for long periods, both of these two cases result in high AoI. The update generation rate at the source that minimizes the average AoI for the considered FCFS system was derived.

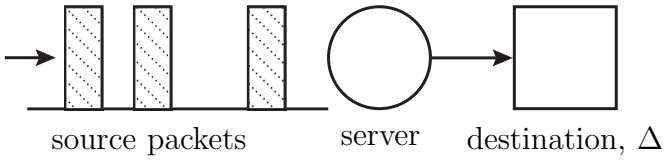

Figure 1.1: Simple single-source single-destination status update system.

The results in [1, 2] has opened the door for a lot of work in the AoI area. Single-source status update systems have been studied in [3–52]. The common approach in these works is using queuing theory where the channel between the source and destination is modeled by a server with a random service time.

Multi-source and/or multi-monitor extensions, also in the single-hop context, have been considered in [53–98]. These multi-source and/or multi-monitor settings often introduce additional delays in delivering updates in the single-hop setting through explicit contention for channel resources and interference constraints.

The multi-hop setting has received relatively little attention in the AoI literature despite

the early consideration of "piggybacking" status updates over multiple hops in vehicular networks in [99]. The analysis in [99–103] considers AoI in specific multi-hop network structures, e.g., line, ring, and/or two-hop networks. The schedules and performance metrics derived for these specific networks are not easily extended to more general settings. A general multi-hop network setting where a single-source disseminates status updates through a gateway to the network was considered in [104, 105]. Age-optimality was shown to be achievable, and the optimality results were shown to hold for any non-decreasing function of the age processes. Explicit algorithms were developed that achieve near optimal AoI performance. Allowing preemption with exponentially distributed service times, a preemptive last-generated first-served policy was proven to have smaller age across all nodes in the network than any other causal policy. These studies do not consider the effects of channel contention or interference constraints as they assume that all links in the network are modeled as interference-free. The work in [106, 107] considers a general network structure, but assumes a pre-defined source/monitor pairs, and analyzes achievable AoI under certain simplifying assumptions, e.g., stationary scheduling policies. Several extensions have been studied under different assumptions on channel state information availability in [108, 109]. Distributed scheduling policies for age minimization were developed in [110]. For a source sending updates to a destination over multiple hops and paths, the AoI minimization was studied given throughput constraints in [111]. The problem of designing a trajectory to optimize information gathering and dissemination in a general multi-hop setting was studied in [112]. A practical age control protocol to improve AoI in multi-hop IP networks was also recently proposed in [113].

In general, in terms of modelling the contention over the channel resources in status update systems, there exists two approaches within the AoI literature, (i) implicit contention and (ii) explicit contention. Considering the implicit contention point of view, the source-destination channel is modeled using tools from the queuing theory and the service times are random, based on the exponential distribution for example. On the other hand from the explicit contention point of view, the interference constraints throughout the network are

determined using tools from the graph theory and the service times are fixed.

Despite the work in [99–113], there is a gap in understanding the AoI in status update systems with a general multi-source multi-hop setting. Specifically, in the dissertation we look at the fundamental AoI bounds as a function of the system parameters under this setting and develop algorithms generating scheduling policies that disseminate status updates throughout the network. Further, observe that part of this dissertation deals with the AoI problem with a queuing theoretical perspective, while the remaining uses tools from the graph theory.

1.2 Dissertation Overview

The main body of this dissertation is organized into four chapters.

- Chapter 2 considers a general multi-source, multi-monitor, multi-hop setting with explicit interference constraints, but from a global perspective in the sense that (i) every node in the network is both a source and monitor of information and (ii) every node wishes to receive timely status updates from all other nodes in the network. This setting is appropriate in applications where nodes both generate status updates and monitor status updates from other nodes in the network, e.g., autonomous vehicles. Our only assumption on the network is that it is connected. We generalize the analysis to allow for arbitrary interference constraints and simultaneous transmissions of status updates, with explicit interference constraints expressed through the network's graph and a corresponding family of feasible activation sets. We derive general lower bounds on the instantaneous peak and average AoI under arbitrary interference constraints. These lower bounds are based on properties of each interference model's family of feasible activation sets. We develop an algorithm that generates explicit schedules for dissemination of status updates throughout any network with a connected topology based on the successive flooding tree algorithm. For networks with transmission errors,

we present two algorithms that generate schedules for dissemination of status updates throughout any given network with a connected topology under global interference constraints. For the schedules constructed by the algorithm without resampling by the root nodes of the flooding trees, we derive a closed-form expression that lower bounds the achieved average peak AoI.

- Chapter 3 considers the multiaccess status update networks with exponentially distributed service times and packet transmission errors. Two cases based on the packet arrivals at the sources are studied: (i) random arrivals based on the Poisson point process and (ii) at-will packet generations. For the random packet arrivals, average AoI is derived allowing self preemption of the packets in service. For the active sources, randomized stationary policy and round-robin policy are considered. For each scheduling policy, three packet management approaches are considered when errors occur, no retransmissions, retransmissions without resampling, and retransmissions with resampling. A closed-form expression for the average AoI of each case is derived as a function of the system parameters. Further, for the class of randomized stationary policies, source selection probabilities are optimized to minimize the weighted sum average AoI.
- Chapter 4 considers the age of information in a single-source status update system with energy constraints. Specifically, a source provides status updates to a destination through a server that has a battery with finite capacity, which is replenished by harvesting energy. Arrival times of the status updates at the source and energy units at the server are assumed to be random according to independent Poisson point processes, and service times are assumed to be exponentially distributed and independent of the status and energy arrivals. Average age expressions are derived under different settings based on the server's ability to harvest energy while a packet is in service and also, whether or not to preempt the packets in service.
- Chapter 5 considers the AoI problem in fully-connected wireless networks with time-

varying reciprocal channels and packetized transmissions. Specifically, a scenario where each node in the network wishes to maintain a table of global channel state information (CSI) is considered. Each node updates its global CSI table in two ways: (i) direct channel measurements through standard channel estimation techniques and (ii) indirect observations of channels through CSI dissemination from other nodes in the network. Information aging, i.e., CSI staleness, occurs due to timeslotting and contention for the common channel resources. New lower bounds are derived for the maximum and average CSI age of any protocol for any number of CSI estimates to be disseminated in each packet. A simple one-step greedy protocol is also proposed for any network size and any number of CSI estimates disseminated per packet.

- Chapter 6 concludes this dissertation and provides some future directions of work.

Table 1.1 represents the list of papers published from this work.

Table 1.1: List of publications.

Chapter 2	[1]	S. Farazi, A. G. Klein, and D. R. Brown III, "Age of information with unreliable transmissions in multi-source multi-hop status update systems," in Proc. ACSSC, pp. 2017–2021, Nov. 2019.
	[2]	S. Farazi, A. G. Klein, and D. R. Brown III, "Fundamental bounds on the age of information in general multi-hop interference networks," in Proc. INFOCOM Workshops, pp. 96–101, Apr. 2019.
	[3]	S. Farazi, A. G. Klein, and D. R. Brown III, "Fundamental bounds on the age of information in multi-hop global status update systems," JCN, vol. 21, no. 3, pp. 268-279, Jul. 2019.
	[4]	S. Farazi, A. G. Klein, J. A. McNeill, and D. R. Brown III, "On the age of information in multi-source multi-hop wireless status update networks," in Proc. SPAWC, pp. 1–5, Jun. 2018.
Chapter 3	[5]	S. Farazi, A. G. Klein, and D. R. Brown III, "Average age of information in update systems with active sources and packet delivery errors," IEEE Wireless Communications Letters, Mar. 2020.
	[6]	S. Farazi, A. G. Klein, and D. R. Brown III, "Average age of information in multi-source self-preemptive status update systems with packet delivery errors," in Proc. ACSSC, pp. 396–400, Nov. 2019.
Chapter 4	[7]	S. Farazi, A. G. Klein, and D. R. Brown III, "Age of information in energy harvesting status update systems: when to preempt in service?" in Proc. ISIT, pp. 2436–2440, Jun. 2018.
	[8]	S. Farazi, A. G. Klein, and D. R. Brown III, "Average age of information for status update systems with an energy harvesting server," in Proc. INFOCOM Workshops, pp. 112–117, Apr. 2018.
Chapter 5	[9]	S. Farazi, A. G. Klein, and D. R. Brown III, "Bounds on the age of information for global channel state dissemination in fully-connected networks," in Proc. ICCCN, pp. 1–7, Aug. 2017.
	[10]	A. G. Klein, S. Farazi, W. He and D. R. Brown III, "Staleness bounds and efficient protocols for dissemination of global channel state information," IEEE Trans. Wireless Comm., vol. 16, no. 9, pp. 5732-5746, Sep. 2017.
	[11]	S. Farazi, D. R. Brown III, and A. G. Klein, "On global channel state estimation and dissemination in ring networks," in Proc. ACSSC, pp. 1122–1127, Nov. 2016.
	[12]	S. Farazi, A. G. Klein, and D. R. Brown III, "On the average staleness of global channel state information in wireless networks with random transmit node selection," in Proc. ICASSP, pp. 3621–3625, Mar. 2016.
Other	[13]	S. Farazi, K. Chinkidjakarn, and D. R. Brown III, "Simultaneous distributed beamforming and nullforming with adaptive positioning," in Proc. GlobalSIP, pp. 129–132, Dec. 2016.
	[14]	S. Farazi, D. R. Brown III, and A. G. Klein, "Power allocation for three-phase two-way relay networks with simultaneous wireless information and power transfer," in Proc. ACSSC, pp. 812–816, Nov. 2015.

Chapter 2

Fundamental Bounds on the Age of Information in General Multi-hop Networks

This chapter considers a general multi-source, multi-monitor, multi-hop setting with explicit interference constraints. We assume that (i) every node in the network is both a source and a monitor of information, (ii) every node wishes to receive timely status updates from all other nodes in the network, and (iii) updates are disseminated with deterministic schedules. This work considers arbitrary interference constraints and simultaneous transmissions of status updates. The main contributions of this chapter are:

- We consider AoI in a general multi-source, multi-monitor, multi-hop setting with explicit interference constraints expressed through the network's graph and a corresponding family of feasible activation sets [114, 115].
- We derive general lower bounds on the instantaneous peak and average AoI under arbitrary interference constraints [116].
- We develop an explicit algorithm that generates status update dissemination schedules for any connected network topology under global interference constraints [114, 115].
- We develop two algorithms based on repetitive transmissions when transmission errors

occur under global interference constraints. The two algorithms differ in terms of whether the root nodes in each sequential flooding tree resample their local information when transmission errors occur. A lower bound on the average peak AoI as a function of fundamental graph properties is also derived for schedules generated by the algorithm without resampling by the root nodes [117].

2.1 System Model

We consider a wireless network where connectivity of nodes is modeled by a directed graph $\mathcal{G} = (\mathcal{V}, \mathcal{E})$ where the vertex set $\mathcal{V}$ represents the wireless nodes and the edge set $\mathcal{E}$ represents the channels between the nodes in the network. Edge $e_{i,j}$ is in set $\mathcal{E}$ when vertices i and j are adjacent (i.e., when there exists a channel between nodes i and j such that transmissions can be successfully delivered from node i to j). We denote the number of nodes as $N = |\mathcal{V}|$ and the set of one-hop neighbors of node i as $\mathcal{N}_1(i)$, i.e., $j \in \mathcal{N}_1(i) \Leftrightarrow e_{i,j} \in \mathcal{E}$. Our only assumption with regards to the topology of the network is that it is connected, i.e., there exists a path between any two distinct vertices $i, j \in \mathcal{V}$.

We assume a setting where each node $i \in \mathcal{V}$ is associated with a local process $H_i(t)$ as illustrated in a simple three-node setting in Fig. 2.1. No assumptions are made about these processes other than they are time-varying and each is of timely interest to all nodes in the network. In addition to its local process, each node $i \in \mathcal{V}$ has a table of "statuses" of all of the non-local processes in the network. We denote a status as the tuple $(H_j^{(i)}(t), \tau_j^{(i)}(t))$, where $H_j^{(i)}(t)$ and $\tau_j^{(i)}(t)$ denote the most recent sample value and the corresponding timestamp of process $H_j(t)$ known to node i at time t, respectively.

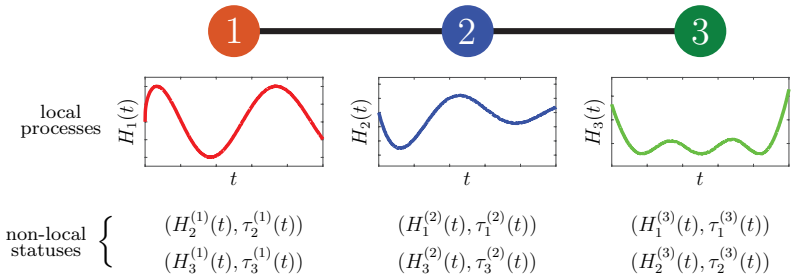

Figure 2.1: Example 3-node line network. Each node is associated with a local process and maintains tables of non-local statuses for the processes of other nodes in the network.

Since the processes $\{H_j(t)\}$ are time-varying and of timely interest to all nodes in the network, each node $i \in \mathcal{V}$ seeks to maintain a table of "fresh" statuses with recent timestamps. For simplicity, we assume each node can sample its own local process without delay such that $H_i^{(i)}(t) = H_i(t)$ and $\tau_j^{(i)}(t) = t$ for all $i \in \mathcal{V}$ and all t. The remaining statuses must be updated via broadcast transmissions containing status updates from other nodes in the system. We make the following assumptions regarding these broadcast transmissions:

1. Transmissions are time slotted, require one unit of time to complete, and are received at times $t = 1, 2, 3, \ldots$.
2. At least one node can reliably transmit a status update to its neighbors in each time slot. Depending on the interference model (as discussed in Section 2.3), more than one node may reliably transmit updates to its neighbors in each time slot subject to interference constraints.
3. Each transmission contains one status, i.e., one sample and its corresponding timestamp, of a process. The transmitting node may transmit the status of its own local process or its status of another node's process.
4. Transmissions from node i are received reliably by all nodes in the one-hop neighborhood of node i, denoted by $\mathcal{N}_1(i)$, while nodes outside the one-hop neighborhood receive nothing.

As each node in the network is both a source and a monitor of information, there are

inherent tradeoffs in how fresh the status at each node can be in this setting. For example, in the three-node network in Fig. 2.1, node 2 can keep nodes 1 and 3 updated with fresh status updates of $H_2(t)$ by transmitting new samples of its local process in every time slot. While statuses $H_2^{(1)}(t)$ and $H_2^{(3)}(t)$ remain fresh (we omit the timestamps here for notational convenience), statuses $H_1^{(2)}(t)$ and $H_3^{(2)}(t)$ become stale since node 2 does not receive updates from node 1 or node 3. Moreover, $H_3^{(1)}(t)$ and $H_1^{(3)}(t)$ also become stale since nodes 1 and 3 receive no status updates from each other in this example. To formalize these notions, we define the age metric for the status of process $H_j(t)$ at node i below.

Definition 1 (Age)**.** *Given the status of process j at node i denoted as $(H_j^{(i)}(t), \tau_j^{(i)}(t))$, the **age** of this status at time $t \geq \tau_j^{(i)}(t)$ is defined as $\Delta_j^{(i)}(t) \triangleq t - \tau_j^{(i)}(t)$.*

The age metric here is a multi-source multi-monitor generalization of the single-source single-monitor age metric first proposed in [2]. Note that the age $\Delta_j^{(i)}(t)$ is non-negative and is not defined for $t < \tau_j^{(i)}(t)$ or if no status update for process $H_j(t)$ has been received at node i. Under our previous assumption about the ability of each node to instantaneously sample its local process, the local age $\Delta_i^{(i)}(t) = 0$. While our model could be extended to include the effect of non-zero delay in sampling local processes, such delays would appear as a simple additive term in the various age expressions below; for simplicity, these local ages are ignored in the metrics defined in Section 2.2 and in the dynamic model describing the evolutions of the ages below.

Given Definition 1 and the assumed time slotted nature of the status updates in the system, we can describe the dynamics of each age in the system with a simple discrete time model. Specifically, given a status update from node i regarding process j, the age at each node $m \in \mathcal{V}$ with $m \neq j$ is updated at integer times $t = n$ according to

$$\Delta_j^{(m)}[n+1] = \begin{cases} 1 & m \in \mathcal{N}_1(i) \text{ and } i = j \\ \Delta_j^{(i)}[n] + 1 & m \in \mathcal{N}_1(i),\ i \neq j, \text{ and } \Delta_j^{(i)}[n] < \Delta_j^{(m)}[n] \\ \Delta_j^{(m)}[n] + 1 & \text{otherwise.} \end{cases} \tag{2.1}$$

In order for node $m \neq j$ to update its status of process j and reduce the corresponding age $\Delta_j^{(m)}(t)$, it must (i) receive the status update transmission, i.e., be within the one-hop neighborhood of the transmitting node, and (ii) the status update must be fresher than the current status at node m. Otherwise, the age simply increases by one. The first case in (2.1) corresponds to the case when node i transmits a status update of its local process $H_i(t)$. In this case, since transmissions require unit time to complete, the local age at the start of the transmission is $\Delta_i^{(i)}[n] = 0$ and the age when nodes $m \in \mathcal{N}_1(i)$ receive the status update is $\Delta_i^{(m)}[n+1] = 1$. The second case in (2.1) corresponds to the case when node i transmits a status update of a non-local process $H_j(t)$ with $j \neq i$. In this case, nodes receiving the transmission update their statuses to match that at node i if the status from node i is fresher. When no update is received or the update is staler than the current status at node m, i.e., the third case in (2.1), the age simply increases by one. Note that, for $t \in [n, n+1)$, since all (non-local) ages increase linearly with time, we can write $\Delta_j^{(m)}(t) = \Delta_j^{(m)}[n] + (t-n)$.

The scalar age update model in (2.1) can be straightforwardly extended to a vector age update model given by

$$\boldsymbol{\Delta}[n+1] = \boldsymbol{A}[n]\boldsymbol{\Delta}[n] + \mathbf{1}, \tag{2.2}$$

where $\boldsymbol{\Delta}[n] \in \mathbb{Z}^{N^2-N}$, $\boldsymbol{A}[n] \in \mathbb{Z}^{(N^2-N)\times(N^2-N)}$, and $\mathbf{1} \in \mathbb{Z}^{N^2-N}$ is a vector of ones. Note that the local ages $\Delta_i^{(i)}(t)$ are not included in $\boldsymbol{\Delta}[n]$ since they are always zero. From (2.1), it is clear that $\boldsymbol{A}[n]$ is a matrix with elements equal to zero or one. It is also evident that the rows of $\boldsymbol{A}[n]$ each have at most one element equal to one. From (2.1), we can derive several useful properties of the state update matrices $\boldsymbol{A}[n]$ in (2.2). Since the ordering of the ages in $\boldsymbol{\Delta}(t)$ is not specified, let $r(i,j)$ correspond to the row position of $\Delta_i^{(j)}(t)$ in $\boldsymbol{\Delta}(t)$. The following properties of $\boldsymbol{A}[n]$ are straightforward to verify:

I. Each row of $\boldsymbol{A}[n]$ is either equal to zero or has a single non-zero entry equal to one.

II. There are exactly δ_i all-zero rows in $\boldsymbol{A}[n]$ when node i transmits a status update of its local process $H_i(t)$. These occur at row indices $r(i,m)$ for all $m \in \mathcal{N}_1(i)$. This

corresponds to case 1 in (2.1).

III. There are no all-zero rows in $\boldsymbol{A}[n]$ when node i transmits a status update of a non-local process $H_j(t)$. There are, however, at most δ_i rows set to match row $r(j,i)$ of $\boldsymbol{A}[n]$, i.e., the transposed $r(j,i)$'th standard unit vector, when node i transmits a status update of a non-local process $H_j(t)$. This corresponds to case 2 in (2.1).

IV. If node m does not receive an update on process j at time $n+1$, then row $r(j,m)$ of $\boldsymbol{A}[n]$ is equal to the transposed $r(j,m)$'th standard unit vector. This corresponds to case 3 in (2.1).

V. For any integer $m \in \mathbb{N}$, $(\boldsymbol{A}[n])^m = \boldsymbol{A}[n]$.

This model and the properties will be useful in the analysis of the age metrics described below.

2.2 Age of Information Metrics and Schedules

In addition to the individual ages $\Delta_j^{(i)}(t)$ defined in Section 2.1, we are interested in characterizing certain statistics of the ages across the network. The most common age statistic studied in the literature is the average age, which we will consider here as well. In the single-source single-monitor literature, the average age is computed as an average over time. Here, we first consider the *instantaneous* peak and *instantaneous* average age, where the peak and average are calculated over the node indices at a fixed value of t. These are only defined when all of the constituent ages are defined, i.e., every node in the network has received at least one status update for every process. Hence, we denote by $\bar{t}$ a time such that all ages $\Delta_j^{(i)}(t)$ are defined. Given Definition 1 and $\bar{t}$, we now define the instantaneous peak age at any point in time $t \geq \bar{t}$.

Definition 2 (Instantaneous peak age)**.** *For any $t \geq \bar{t}$, the **instantaneous peak age** is defined as*

$$\Delta_{\text{peak}}(t) \triangleq \max \boldsymbol{\Delta}(t). \tag{2.3}$$

Note that t is fixed here and the maximum is computed over the $N^2 - N$ elements of the vector $\boldsymbol{\Delta}(t)$. Along the same lines, we define the instantaneous average age at any point $t \geq \bar{t}$ below.

Definition 3 (Instantaneous average age)**.** *For any $t \geq \bar{t}$, the* ***instantaneous average age*** *is defined as*

$$\Delta_{\text{avg}}(t) \triangleq \frac{\mathbf{1}^\top \boldsymbol{\Delta}(t)}{N^2 - N}. \tag{2.4}$$

Note that the instantaneous average age represents the average of the $N^2 - N$ ages of the non-local statuses, i.e., the zero-age local statuses are not included in the average.

We define a *schedule* as a sequence of transmissions indexed by integer time, transmitting node i, and process j. A schedule can be equivalently expressed as a series of state update matrices $\boldsymbol{A}[n]$ in (2.2). One of the main contributions of this chapter is in establishing fundamental limits on peak and average age for any schedule satisfying the assumptions listed in Section 2.1. To illustrate the concept of a schedule, we provide an example for the three-node line network shown in Fig. 2.1. The age vector in this example is defined as

$$\boldsymbol{\Delta}(t) = [\Delta_2^{(1)}(t), \Delta_3^{(1)}(t), \Delta_1^{(2)}(t), \Delta_3^{(2)}(t), \Delta_1^{(3)}(t), \Delta_2^{(3)}(t)]^\top. \tag{2.5}$$

An undefined age in $\boldsymbol{\Delta}(t)$ is denoted by "$-$". The initial state $\boldsymbol{\Delta}[0] = [-, -, -, -, -, -]^\top$. The notation TS$k$ below corresponds to time slot k, a transmission occurring over $t \in (k-1, k]$.

TS1: $(i = 1, j = 1)$ Suppose node 1 transmits a sample of its local process H_1 sampled at time $t = 0$. This update from node 1 is received by node 2 at $t = 1$, resulting in $\boldsymbol{\Delta}[1] = [-, -, 1, -, -, -]^\top$.

TS2: $(i = 2, j = 1)$ Suppose node 2 relays the update received in TS1 to node 3. This update (of process H_1) is received by node 3 at time $t = 2$, resulting in $\boldsymbol{\Delta}[2] = [-, -, 2, -, 2, -]^\top$. Note that node 1 ignores this transmission since it contains a status update regarding its local process.

TS3: $(i = 2, j = 2)$ Suppose node 2 now transmits a sample of its local process sampled at $t = 2$. This update from node 2 is received by nodes 1 and 3 at $t = 3$, resulting in $\boldsymbol{\Delta}[3] = [1, -, 3, -, 3, 1]^\top$.

TS4: $(i = 3, j = 3)$ Suppose node 3 transmits a sample of its local process sampled at time $t = 3$. This update from node 3 is received by node 2 at time $t = 4$, resulting in $\boldsymbol{\Delta}[4] = [2, -, 4, 1, 4, 2]^\top$.

TS5: $(i = 2, j = 3)$ Similar to TS2, suppose node 2 relays the update received in TS4 to node 1. This update is received by node 1 at $t = 5$, resulting in $\boldsymbol{\Delta}[5] = [3, 2, 5, 2, 5, 3]^\top$.

Note that all nodes have received updates for all processes at $t = 5$, hence we can set $\bar{t} = 5$ and compute instantaneous peak and average ages for all $t \geq \bar{t}$. This schedule can naturally be repeated to construct a periodic schedule for all $t \geq 0$. Table 2.1 summarizes this periodic schedule and Fig. 2.2 plots the evolution of the six relevant ages in $\boldsymbol{\Delta}(t)$ as a function of t for three periods of this schedule. The instantaneous peak and average ages for this schedule are shown in the fourth subplot of Fig. 2.2. Observe that all of the ages and the instantaneous age metrics are periodic in this example due to the periodicity of the schedule.

Table 2.1: Example schedule for the three-node line network in Fig. 2.1.

time slot	transmitting node index i	transmitted process index j
TS1, TS6, ...	1	1
TS2, TS7, ...	2	1
TS3, TS8, ...	2	2
TS4, TS9, ...	3	3
TS5, TS10, ...	2	3

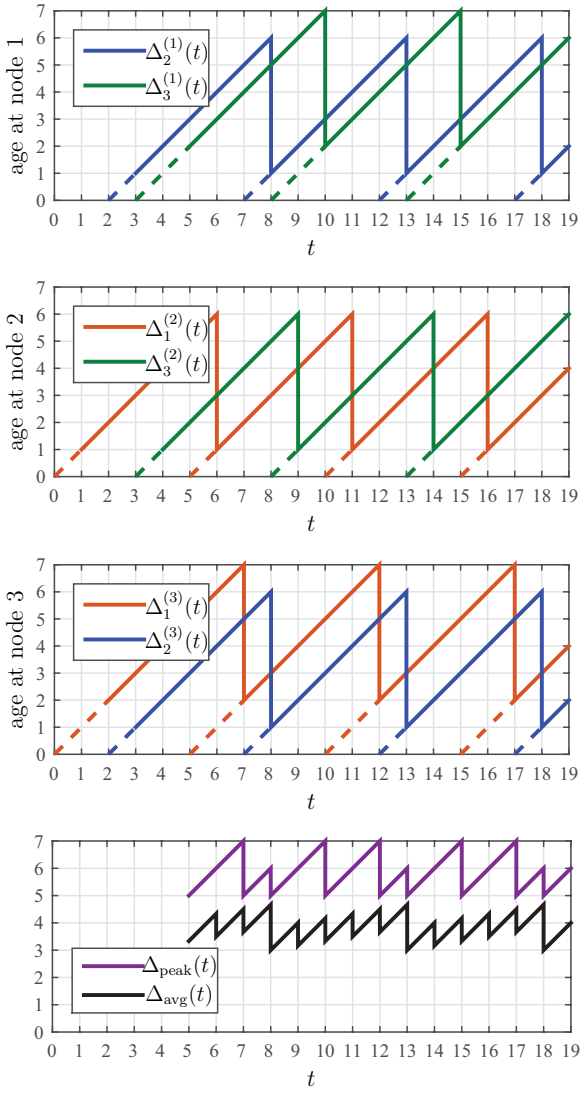

Figure 2.2: Instantaneous age metrics for the example schedule for a three-node line network in Fig. 2.1.

We conclude this section with two additional age metrics of interest. The peak and average ages over an arbitrary time interval $t \in [t_0, t_1)$ with $\bar{t} \leq t_0 < t_1$ are defined below.

Definition 4 (Peak age)**.** *The* ***peak age*** *for $t \in [t_0, t_1)$ with $\bar{t} \leq t_0 < t_1$ is defined as*

$$\Delta_{\text{peak}}(t_0, t_1) \triangleq \sup_{t_0 \leq t < t_1} \Delta_{\text{peak}}(t). \tag{2.6}$$

Definition 5 (Average age)**.** *The* ***average age*** *for* $t \in [t_0, t_1)$ *with* $\bar{t} \leq t_0 < t_1$ *is defined as*

$$\Delta_{\text{avg}}(t_0, t_1) \triangleq \frac{1}{t_1 - t_0} \int_{t_0}^{t_1} \Delta_{\text{avg}}(t)\ dt. \tag{2.7}$$

Note the supremum is used in (2.6) as $\Delta_{\text{peak}}(t)$ is a right-continuous piecewise linear function with discontinuities occurring at integer times when status updates are received. It is also worth mentioning here that Definition 4 differs from other definitions of "peak age" in the literature, e.g., [12, 106] define peak age as the average of the age peaks.

When we omit the time indices and use the notation Δ_{peak} and Δ_{avg}, this implies $t_0 = \bar{t}$ and $t_1 \to \infty$.

2.3 Interference Model Assumptions

This section introduces three interference models that determine the transmitting nodes during any time slot subject to interference constraints. Similar to [106], for any directed graph $\mathcal{G} = (\mathcal{V}, \mathcal{E})$, we call $f \subset \mathcal{E}$ a "feasible activation set" if all links in f can be activated simultaneously without interference. An edge $e_{i,j}$ is said to be "active" during a time slot if node i is transmitting and $j \in \mathcal{N}_1(i)$.

Specifically, we present interference models spanning from the most pessimistic model (*global interference* to the most optimistic model (*interference free* [104,105]). Between these extremes, we also describe a *topologically-dependent interference* model in which multiple nodes transmit simultaneously if they share no one-hop neighbors. Each of these settings will be analyzed in the sequel.

2.3.1 Global Interference Model

The global interference model pessimistically imposes the constraint that only one node can transmit during each time slot and the remaining $N - 1$ nodes in the network must remain

silent to avoid interference. In this setting, during any time slot there are a total of N feasible activation sets, given by $\mathcal{F}_{\mathsf{glob}} = \{f_1, \ldots, f_N\}$, where $f_i = \{\text{all } e_{\ell,j} \in \mathcal{E} \text{ s.t. } \ell = i\}$ is the set of directed edges exiting node i.

2.3.2 Interference Free Model

In contrast to the pessimistic global interference model, this model considers a setting in which all nodes can transmit simultaneously without interference. This optimistic "interference free" model has been considered previously in the context of AoI in [104, 105]. In this setting, each of the N nodes in the network can transmit in each time slot. The collection of all feasible activation sets $\mathcal{F}_{\mathsf{ifree}}$ in this setting can be expressed as $\mathcal{F}_{\mathsf{ifree}} = \bigcup_{k=1}^{N} \mathcal{F}_k$ where $\mathcal{F}_k$ is the collection of all sets of edges with k transmitting nodes. For example, $\mathcal{F}_1 = \mathcal{F}_{\mathsf{glob}}$ is the collection of all sets of edges with one transmitting node. Similarly, the collection of all sets of edges with two transmitting nodes $\mathcal{F}_2 = \{f_{1,2}, f_{1,3}, \ldots, f_{N-1,N}\}$, with $f_{i,j} = f_i \cup f_j$ and f_i as defined previously is the union of the sets of directed edges exiting nodes i and j. Note that $\mathcal{F}_N = \mathcal{E} \subset \mathcal{F}_{\mathsf{ifree}}$, i.e., the collection of all feasible activation sets in the interference free setting includes the set of all directed edges.

2.3.3 Topologically-Dependent Interference Model

In some networks, the global interference model may be overly pessimistic since multiple nodes may be able to transmit simultaneously due to frequency reuse, e.g., with sufficient spacing between some nodes, the use of multiple-access strategies, or other interference avoidance approaches. Similarly, the interference free model may be overly optimistic in some settings because nodes may not be able to separate simultaneously received updates or operate in full-duplex. As such, we consider a topologically-dependent interference model that falls between the pessimistic and optimistic models above. Specfically, if $\mathcal{N}_1(i) \cap \mathcal{N}_1(j) = \emptyset$, then i and j can transmit simultaneously without interference in this model.

Note that the collection of feasible activation sets in the topologically-dependent interfer-

ence setting includes all transmissions from a single node, i.e., $\mathcal{F}_{\mathsf{glob}} \subseteq \mathcal{F}_{\mathsf{tdi}}$. It also contains the collection of sets of edges of multiple transmitting nodes that share no common neighbors. As an example of the collection of feasible activation sets in topologically-dependent interference setting, consider the ring network in Fig. 2.3. Note that $\mathcal{F}_{\mathsf{tdi}} = \mathcal{F}_{\mathsf{glob}} \cup \{f_{1,4}, f_{2,5}, f_{3,6}\}$ where $f_{i,j} = f_i \cup f_j$ as defined previously. Hence, for the six-node ring network in Fig. 2.3, there are a total of nine feasible activation sets.

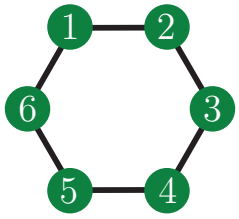

Figure 2.3: Example $N = 6$ ring network.

In general, since $\mathcal{F}_{\mathsf{glob}} \subseteq \mathcal{F}_{\mathsf{tdi}} \subset \mathcal{F}_{\mathsf{ifree}}$, the sets of possible schedules in each case has the same ordering. Hence, under optimized schedules, we can expect the age statistics under these different interference constraints to satisfy $\Delta_{\text{avg},\mathsf{glob}} \geq \Delta_{\text{avg},\mathsf{tdi}} \geq \Delta_{\text{avg},\mathsf{ifree}}$ and $\Delta_{\text{peak},\mathsf{glob}} \geq \Delta_{\text{peak},\mathsf{tdi}} \geq \Delta_{\text{peak},\mathsf{ifree}}$. These statistics are analyzed in the following section.

2.4 Fundamental Bounds on the Instantaneous Peak Age and Instantaneous Average Age

In this section, we present the main results consisting of lower bounds on the instantaneous peak and average age of information metrics in Definitions 2 and 3 under general interference constraints including the three interference models described in Section 2.3. The basic approach is to use a property of the feasible activation sets to lower bound the number of time slots required to update all statuses throughout the network. This leads to directly to a lower bound on the instantaneous peak age. Additional properties of the feasible activation sets are then used to derive a lower bound on the instantaneous average age.

As these lower bounds rely on certain properties of the graph $\mathcal{G}$ describing the network, we first review these properties and notation.

2.4.1 Preliminary Definitions and Notation

A set $\mathcal{S} \subset \mathcal{V}$ of vertices in a graph is called a *dominating set* if every vertex not in $\mathcal{S}$ is adjacent to a vertex in $\mathcal{S}$ [118]. A minimum connected dominating set (MCDS) $\mathcal{S} \subset \mathcal{V}$ is a dominating set satisfying (i) the subgraph induced by $\mathcal{S}$ is connected and (ii) $\mathcal{S}$ has the smallest cardinality among all connected dominating sets of $\mathcal{G}$. The cardinality of any MCDS is called *connected domination number* of $\mathcal{G}$ and is denoted by γ_c. Although, in general, graphs do not have a unique MCDS, all MCDSs of a graph $\mathcal{G}$ have the same cardinality γ_c [119, 120]. Because every vertex *not* in a given MCDS is a one-hop neighbor of a vertex in the MCDS, i.e., $\mathcal{N}_1(\mathcal{S}) = \mathcal{G}$ for any MCDS $\mathcal{S}$, a collection of vertices in a given MCDS is often referred to as the "backbone" of the network in the context of broadcast routing for ad-hoc networks [120].

A *leaf* vertex of graph $\mathcal{G}$ is any vertex $i \in \mathcal{V}$ with degree of one. To the best of our knowledge, although the notion of a leaf vertex is well defined and commonly understood, there is no commonly accepted name for the following graph object. As such, we define a "pseudo-leaf vertex" below.

Definition 6 (Pseudo-leaf vertex)**.** *A vertex $i \in \mathcal{V}$ is a **pseudo-leaf vertex** if it is not a member of any MCDS. That is, $i \in \mathcal{V}$ is a pseudo-leaf vertex if $i \notin \mathcal{U}$ where*

$$\mathcal{U} \triangleq \mathcal{S}_1 \cup \mathcal{S}_2 \cup \ldots \cup \mathcal{S}_M. \tag{2.8}$$

and $\mathcal{S}_k \subset \mathcal{V}$ for $k = \{1, 2, \ldots, M\}$ represent all possible MCDSs of $\mathcal{G}$. Further, we refer to the set of all pseudo-leaf vertices of $\mathcal{G}$ by $\mathcal{L} \triangleq \mathcal{V} - \mathcal{U}$.

Under this definition, every true leaf (i.e., every vertex with degree one) is also a pseudo-leaf. A graph may have additional non-leaf vertices that satisfy the conditions of a pseudo-leaf

vertex.

Finally, recall the degree δ_i of node $i \in \mathcal{V}$ is defined as the the number of edges of vertex i or, equivalently, the cardinality of the number of one-hop neighbors of node i, i.e., $\delta_i = |\mathcal{N}_1(i)|$. We define the maximum degree of the graph as $\delta_{\max} = \max_{i \in \mathcal{V}} \delta_i$.

To illustrate the key ideas, consider the 5-node network in Fig. 2.4 which has two MCDSs, shown as $\mathcal{S}_1$ and $\mathcal{S}_2$, both with cardinality $\gamma_c = 2$. While only node 1 is a true leaf vertex, nodes 1 and 5 are pseudo-leaf vertices as they are not members of any MCDS. The cardinality of the pseudo-leaf set is $|\mathcal{L}| = 2$. The maximum degree of this graph is $\delta_{\max} = \delta_2 = 3$. These graph parameters play an important role in the bounds developed in the following section.

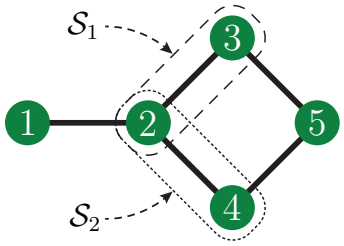

Figure 2.4: A 5-node "pan" network. The two MCDS's are shown as $\mathcal{S}_1 = \{2, 3\}$ and $\mathcal{S}_2 = \{2, 4\}$ with cardinality $\gamma_c = 2$. The set of pseudo-leaf vertices is $\mathcal{L} = \mathcal{V} - (\mathcal{S}_1 \cup \mathcal{S}_2) = \{1, 5\}$.

2.4.2 Lower Bounds on Instantaneous Peak and Instantaneous Average Ages

This section presents lower bounds on the instantaneous peak and instantaneous average ages for all $t \geq \bar{t}$ such that all of the constituent ages in $\boldsymbol{\Delta}(t)$ are defined. To facilitate the presentation of these bounds, we first present the following Lemma to characterize the number of time slots required to update all $N^2 - N$ statuses in the network given the global interference model.

Lemma 1 (Number of time slots to update all statuses)**.** *Given $\mathcal{G}$ with $N = |\mathcal{V}|$, there exists a schedule that updates all $N^2 - N$ statuses in the network in $T^*_{\mathsf{glob}} \triangleq N\gamma_c + |\mathcal{L}|$ time slots.*

Moreover, any schedule of length $T = T^* - K$ time slots for $K \in \{0, 1, \ldots, T^*_{\mathsf{glob}}\}$ updates at most $N^2 - N - K$ statuses.

Proof. We first show the sufficiency of T^*_{glob} time slots by construction. A schedule satisfying the conditions in Section 2.1 that updates all statuses in the network in T^*_{glob} time slots can be constructed by flooding the status from each node throughout the network sequentially for $i = 1, \ldots, N$, i.e., the local status of node i is transmitted to its one-hop neighbors and this status is retransmitted in subsequent time slots to the remaining nodes in the network via an optimal flooding tree constructed from the graph's MCDS [121]. As shown in [121, Theorem 1], the number of time slots required to propagate an update of $H_i(t)$ throughout the network is $\gamma_c + \mathbb{1}_{i \in \mathcal{L}}$ where $\mathbb{1}_{i \in \mathcal{L}}$ is an indicator function equal to one when i is a pseudo-leaf vertex and equal to zero otherwise. It follows that a schedule that performs this optimal flooding sequentially for each node $i = 1, \ldots, N$ requires $|\mathcal{L}|(\gamma_c + 1) + (N - |\mathcal{L}|)\gamma_c = N\gamma_c + |\mathcal{L}|$ time slots to complete and updates all statuses in the network.

To show the second part of the lemma (which also establishes the necessity of T^*_{glob} time slots to update all statuses), let $K = K_1 + \cdots + K_N$ with $K_i \in \{0, \ldots, \gamma_c + \mathbb{1}_{i \in \mathcal{L}}\}$ for all $i \in \{1, \ldots, N\}$. Let $\gamma_c + \mathbb{1}_{i \in \mathcal{L}} - K_i$ be the number of time slots allocated to propagate an update of $H_i(t)$. Observe that at least K_i nodes in the network do not receive an update of process $H_i(t)$. Hence at least $K = K_1 + \cdots + K_N$ statuses of the $N^2 - N$ total statuses in the network are not updated, which shows the desired result. □

Remarks:

1. A periodic version of a sequential flooding schedule of length T^*_{glob} described in the proof of Lemma 1 is presented in Section 2.5. Lemma 1 implies that there does not exist any periodic schedule with period less than T^*_{glob} time slots such that all statuses are updated.
2. For a fixed number of nodes N, it can be shown that T^*_{glob} obeys the inequality $N \leq T^*_{\mathsf{glob}} \leq N^2 - 2N + 2$, where the left side is true with equality for the complete graph and the right side is true with equality for the path graph. This suggests that

some network topologies require on the order of N time slots to update all statuses in the network, whereas others require on the order of N^2 time slots to update all statuses in the network. Unsurprisingly, the network topology has a significant impact on the minimum number of time slots T^*_{glob} required to update all statuses in the network.

Lemma 1 also implies certain properties about the state transition matrix for the discrete time model in (2.2). Given an initial age state of $\boldsymbol{\Delta}[n_0]$, the age vector at time $n \geq n_0,\ n \in \mathbb{Z}$ can be written as

$$\boldsymbol{\Delta}[n] = \boldsymbol{\Phi}[n, n_0]\boldsymbol{\Delta}[n_0] + \sum_{k=n_0}^{n-1} \boldsymbol{\Phi}[n, k+1]\mathbf{1} \tag{2.9}$$

where $\boldsymbol{\Phi}[n, m]$ is the discrete time time-varying state transition matrix defined as

$$\boldsymbol{\Phi}[n, m] = \begin{cases} \boldsymbol{A}[n-1]\boldsymbol{A}[n-2]\dots\boldsymbol{A}[m] & n - m > 0 \\ \boldsymbol{I}_{N^2-N} & n - m = 0 \\ \text{undefined} & n - m < 0 \end{cases}. \tag{2.10}$$

Now, we present the following Lemma that generalizes the result of Lemma 1 to all of the three interference models in Section 2.3.

Lemma 2 (Number of time slots required to update all statuses)**.** *For any schedule, updating all of the statuses throughout the network requires at least*

$$T^* \triangleq \left\lceil \frac{N\gamma_c + |\mathcal{L}|}{\nu} \right\rceil \tag{2.11}$$

time slots, where ν is the maximum number of simultaneously transmitting nodes over all feasible activation sets.

Proof. The global interference model is equivalent to setting $\nu = 1$ since all feasible activation sets correspond to a single transmitting node. For general interference models with ν corresponding to the maximum number of simultaneously transmitting nodes over all feasi-

ble activation sets, the desired result follows from considering ν simultaneous transmissions in each time slot. $\square$

For the interference models in Section 2.3, we have

$$\nu_{\mathsf{glob}} = 1, \tag{2.12a}$$

$$\nu_{\mathsf{ifree}} = N, \tag{2.12b}$$

$$\nu_{\mathsf{tdi}} = \chi, \tag{2.12c}$$

where χ is the maximum number of vertices with the same color over all distance-2 colorings of $\mathcal{G}$.

We now present the lower bounds on the instantaneous peak age of information.

Theorem 1 (Lower bound on instantaneous peak age)**.** *The instantaneous peak age of information for any schedule at time $t \geq \bar{t}$ is lower bounded by*

$$\Delta_{\text{peak}}(t) \geq \Delta^*_{\text{peak,inst}} \triangleq T^*. \tag{2.13}$$

Proof. For $t \geq \bar{t}$ and $t \in [n, n+1)$, we can write

$$\Delta_{\text{peak}}(t) = \max \boldsymbol{\Delta}[n] + (t-n), \tag{2.14a}$$

$$\geq \max \boldsymbol{\Delta}[n], \tag{2.14b}$$

$$\geq \boldsymbol{e}_i^\top \boldsymbol{\Delta}[n] \tag{2.14c}$$

for all $i \in \{1, \ldots, N^2 - N\}$. From (2.9), we can set $n_0 = 0$ and $n \geq \bar{t} \geq T^*$ to write

$$\boldsymbol{\Delta}[n] = \boldsymbol{\Phi}[n, 0]\boldsymbol{\Delta}[0] + \sum_{k=0}^{n-1} \boldsymbol{\Phi}[n, k+1]\mathbf{1}, \tag{2.15a}$$

$$= \sum_{k=0}^{n-1} \boldsymbol{\Phi}[n, k+1]\mathbf{1}, \tag{2.15b}$$

$$\geq \sum_{k=n-T^*}^{n-1} \mathbf{\Phi}[n, k+1]\mathbf{1}, \tag{2.15c}$$

where the equality follows from the fact that $n \geq \bar{t}$ implies all statuses have been updated by time n, i.e., $\mathbf{\Phi}[n, 0] = 0$, and the inequality follows from the fact that each term in the sum is non-negative. Observe that there are T^* terms in the sum and that that all $\mathbf{\Phi}[n, k+1]$ in the sum are non-zero. Hence, there must exist at least one i such that $\boldsymbol{e}_i^\top \mathbf{\Phi}[n, n - T^* + 1]\mathbf{1} = 1$. Moreover, from the properties of the $\mathbf{\Phi}$ matrix we have $\boldsymbol{e}_i^\top \mathbf{\Phi}[n, n - T^* + 1]\mathbf{1} = 1$, which implies $\boldsymbol{e}_i^\top \mathbf{\Phi}[n, k+1]\mathbf{1} = 1$ for all $k \in \{n - T^*, \ldots, n-1\}$. Hence, given i such that $\boldsymbol{e}_i^\top \mathbf{\Phi}[n, n - T^* + 1]\mathbf{1} = 1$, we can write

$$\Delta_{\text{peak}}(t) \geq \boldsymbol{e}_i^\top \sum_{k=n-T^*}^{n-1} \mathbf{\Phi}[n, k+1]\mathbf{1} = T^*, \tag{2.16}$$

which shows the desired result. □

For the interference models in Section 2.3, we have

$$\Delta^*_{\text{peak,inst,}\mathsf{glob}} = T^*_{\mathsf{glob}} = N\gamma_c + |\mathcal{L}|, \tag{2.17a}$$

$$\Delta^*_{\text{peak,inst,}\mathsf{ifree}} = T^*_{\mathsf{ifree}} = \gamma_c + \left\lceil \frac{|\mathcal{L}|}{N} \right\rceil, \tag{2.17b}$$

$$\Delta^*_{\text{peak,inst,}\mathsf{tdi}} = T^*_{\mathsf{tdi}} = \left\lceil \frac{N\gamma_c + |\mathcal{L}|}{\chi} \right\rceil. \tag{2.17c}$$

We now present the lower bounds on the instantaneous average age of information.

Theorem 2 (Lower bound on instantaneous average age)**.** *The instantaneous average age of information for any schedule is lower bounded by*

$$\Delta^*_{\text{avg,inst}} \triangleq \frac{\mathbf{1}^\top \boldsymbol{s}}{N^2 - N}, \tag{2.18}$$

where

$$\boldsymbol{s} \triangleq [\max(\boldsymbol{x}_1, \boldsymbol{y}_1), \max(\boldsymbol{x}_2, \boldsymbol{y}_2), \ldots, \max(\boldsymbol{x}_{T^*}, \boldsymbol{y}_{T^*})], \tag{2.19a}$$

$$\boldsymbol{x} \triangleq [N^2 - N, N^2 - N - \epsilon, \ldots, N^2 - N - (T^* - 1)\epsilon], \tag{2.19b}$$

$$\boldsymbol{y} \triangleq [T^*, T^* - 1, \ldots, 1] \tag{2.19c}$$

with ϵ corresponding to the maximum number of active edges over all feasible activation sets.

Proof. Along the same lines as Theorem 1, for $t \geq \bar{t}$ and $t \in [n, n+1)$, we can write

$$\Delta_{\text{avg}}(t) = \frac{\mathbf{1}^\top \boldsymbol{\Delta}[n]}{N^2 - N} + (t - n), \tag{2.20a}$$

$$\geq \frac{\mathbf{1}^\top \sum_{k=n-T^*}^{n-1} \boldsymbol{\Phi}[n, k+1]\mathbf{1}}{N^2 - N}, \tag{2.20b}$$

$$= \frac{\sum_{k=n-T^*}^{n-1} s[n, k+1]}{N^2 - N}, \tag{2.20c}$$

where the inequality follows from the fact that $t - n \geq 0$ and from following the same steps that led to (2.15c). The term $s[n, k+1]$ denotes the number of non-zero elements, i.e., the number of statuses not updated, in $\boldsymbol{\Phi}[n, k+1]$. Observe that

(P1) $s[n, n] = N^2 - N$ from the fact that $\boldsymbol{\Phi}[n, n] = \boldsymbol{I}_{N^2 - N}$.

(P2) $s[n, k+1] - s[n, k] \leq \epsilon$ since at most ϵ statuses can be updated in a time slot.

(P3) $s[n, n - T^* + K] \geq K$ for all $K \in \{1, \ldots, T^*\}$ from Lemma 1.

The minimal sequence $\boldsymbol{s} = [s[n, n], \ldots, s[n, n - T^* + 1]]$ satisfying these properties can be constructed by first defining

$$\boldsymbol{x} = [N^2 - N, N^2 - N - \epsilon, \ldots, N^2 - N - (T^* - 1)\epsilon], \tag{2.21a}$$

$$\boldsymbol{y} = [T^*, T^* - 1, \ldots, 1]\,. \tag{2.21b}$$

Note that $\boldsymbol{x}$ captures the constraints imposed by (P1) and (P2). Similarly $\boldsymbol{y}$ captures the

constraints imposed by (P3). Then

$$\boldsymbol{s} = [\max(\boldsymbol{x}_1, \boldsymbol{y}_1), \max(\boldsymbol{x}_2, \boldsymbol{y}_2), \ldots, \max(\boldsymbol{x}_{T^*}, \boldsymbol{y}_{T^*})] \tag{2.22a}$$

is the minimal sequence satisfying all of the properties, which establishes the lower bound and shows the desired result. □

For the interference models in Section 2.3, we have

$$\epsilon_{\mathsf{glob}} = \delta_{\max}, \tag{2.23a}$$

$$\epsilon_{\mathsf{ifree}} = |\mathcal{E}|, \tag{2.23b}$$

$$\epsilon_{\mathsf{tdi}} = \omega, \tag{2.23c}$$

where $\delta_{\max} = \max_{v \in \mathcal{V}} \deg(v)$ is the maximum degree of the graph and ω is the maximum number of active edges over all feasible activation sets in the topologically dependent interference model.

Referring to the three-node example in Section 2.1, we have $N = 3$, $\gamma_c = 1$ and $|\mathcal{L}| = 2$, $\delta_{\max} = 2$, and $\chi = 3$. These graph parameters imply $\Delta^*_{\text{peak,inst,}\mathsf{glob}} = 5$, $\Delta^*_{\text{peak,inst,}\mathsf{ifree}} = 2$, and $\Delta^*_{\text{peak,inst,}\mathsf{tdi}} = 5$ for the instantaneous peak age of information lower bounds and $\Delta^*_{\text{avg,inst,}\mathsf{glob}} = 2.67$, $\Delta^*_{\text{avg,inst,}\mathsf{ifree}} = 1.33$, and $\Delta^*_{\text{avg,inst,}\mathsf{tdi}} = 2.67$ for the instantaneous average age of information lower bounds. Figure 2.2 shows that the example periodic schedule considering the global interference model achieves the peak age lower bound of $\Delta^*_{\text{peak,inst,}\mathsf{glob}} = 5$ at times $t = \{5, 7, 8, 10, 12, 13, 15, 17, 18, \ldots\}$ and reaches a minimum value of $\Delta_{\text{avg}}(t) = 3$ at times $t = \{8, 13, 18, \ldots\}$. Hence, unlike the instantaneous peak age, there is a gap between the bound and the minimum instantaneous age achieved in this example.

2.5 Minimum-Length Periodic Schedules (MLPS) for Global Interference Model

In this section, we consider the class of periodic schedules in the global interference model with period T^*_{glob} as defined in Lemma 2. Such schedules have the property that $\boldsymbol{A}[n + kT^*_{\mathsf{glob}}] = \boldsymbol{A}[n]$ for all $n = 0, 1, \ldots, T^*_{\mathsf{glob}} - 1$ and all $k = 0, 1, \ldots$. The study of periodic schedules is motivated by the central goal of maintaining fresh statuses at each node in the network and by the recent results in [71] where round robin schedules, i.e., schedules in which a series of transmissions is repeated, were shown to be optimal in terms of minimizing peak age. As noted earlier, a periodic schedule with period $T < T^*_{\mathsf{glob}}$ cannot update all statuses and, consequently, this class of schedules is of little interest since some ages are never defined. Periodic schedules with period $T > T^*_{\mathsf{glob}}$ are also of limited interest since the time between updates of at least some statuses (and, hence, the corresponding peak ages of these statuses) will be larger than necessary. Due to the combinatorics of schedule design in the topologically-deterministic interference setting for general graphs, designing a schedule for the interference free model and topologically-dependent interference model is not trivial. Hence, we only focus on developing an algorithm for schedule design in the global interference model.

In the following, given the global interference model we first derive lower bounds on the peak and average age of information for all T^*_{glob}-periodic schedules that update all statuses in each period. While the instantaneous age bounds developed in Section 2.4.2 also serve as lower bounds over any period of a T^*_{glob}-periodic schedule, our focus here is on the development of bounds on the peak and average age over a period of the schedule according to Definitions 4 and 5. We then present an algorithm for constructing a specific T^*_{glob}-periodic schedule that updates all statuses in each period given any connected network topology assuming the global interference model. To analytically characterize the performance of this schedule, we upper bound its achieved age of information. This upper bound is then

compared with the previously developed lower bounds to show the achieved peak age is tight with respect to the lower bound on peak age for any network topology and and size N. We also show that the achieved average age is asymptotically tight to the lower bound on average age as $N \to \infty$.

2.5.1 Lower Bounds on Peak and Average Age for Minimum-Length Periodic Schedules in the Global Interference Model

To establish fundamental limits for the peak and average age of information for minimum-length periodic schedules, we first present the following useful Lemmas.

Lemma 3. *Given the global interference model, for any minimum-length periodic schedule that updates all $N^2 - N$ statuses, every status throughout the network is updated exactly once every T^*_{glob} time slots.*

Proof. Consider any minimum-length periodic schedule that updates all of the $N^2 - N$ statuses in the global interference model. From Lemma 1 recall that $\gamma_c + \mathbb{1}_{i \in \mathcal{L}}$ time slots are required to propagate an update of $H_i(t)$ throughout the network. The first of these time slots corresponds to dissemination of a fresh update of $H_i(t)$ by node i and the remaining $\gamma_c + \mathbb{1}_{i \in \mathcal{L}} - 1$ time slots correspond to retransmissions of the status by nodes other than node i. While nodes in the network may receive multiple transmissions containing the status of the $H_i(t)$ process, the status at each node $j \neq i$ is only updated once since subsequent updates contain the same status and are redundant. □

The main implication of Lemma 3 is that, for the class of minimum-length periodic schedules that update all $N^2 - N$ statuses in the network, all status updates at each node occur with period T^*_{glob}. No statuses are updated more frequently. So, over the interval $t \in [t', t' + T^*_{\mathsf{glob}})$, where t' is the time at which the status of process i is updated at node j, the age trajectory $\Delta_i^{(j)}(t)$ is simply $\Delta_i^{(j)}(t) = t - t' + \Delta_i^{(j)}$ where $\Delta_i^{(j)}$ is the age of status i at the time node j is updated. In other words, for T^*_{glob}-periodic schedules that update all

$N^2 - N$ statuses in the network, each age trajectory $\Delta_i^{(j)}(t)$ is identical except for time shifts and the "age offsets" $\Delta_i^{(j)}$.

These time shifts and age offsets are illustrated for the T^*_{glob}-periodic schedule for the three-node path network with $T^*_{\mathsf{glob}} = 5$ in Fig. 2.2 where $\Delta_2^{(1)} = 1$, $\Delta_3^{(1)} = 2$, $\Delta_3^{(2)} = 1$, $\Delta_1^{(2)} = 1$, $\Delta_2^{(3)} = 1$, and $\Delta_1^{(3)} = 2$. In general, note that the age offsets must satisfy $\Delta_i^{(j)} \geq d(i,j)$, where $d(i,j)$ is the distance in hops of the shortest path between nodes i and j. The following Lemma establishes an additional useful property of the age offsets $\Delta_i^{(j)}$ for networks with T^*_{glob}-periodic schedules.

Lemma 4. *Given the global interference model, for $i \in \mathcal{V}$ and a T^*_{glob}-periodic schedule that updates all of the $N^2 - N$ statuses,*

$$\max_{j \in \mathcal{V}} \Delta_i^{(j)} \geq \gamma_c + \mathbb{1}_{i \in \mathcal{L}}.$$

Proof. This result follows directly from Lemma 1, which establishes that $\gamma_c + \mathbb{1}_{i\in\mathcal{L}}$ time slots are required to propagate an update of the status of process i throughout the network. Hence, given $i \in \mathcal{V}$, there always exists a node $j \in \mathcal{V}$ such that status updates regarding process i are received with an age offset of at least $\gamma_c + \mathbb{1}_{i\in\mathcal{L}}$. □

Lemmas 3 and 4 imply that, over any interval $[t_0, t_0 + T^*_{\mathsf{glob}})$ and fixing $i \in \mathcal{V}$, there exists at least one age trajectory $\Delta_i^{(j)}(t)$ satisfying $\sup_{t\in[t_0,t_0+T^*_{\mathsf{glob}})} \Delta_i^{(j)}(t) \geq \gamma_c + \mathbb{1}_{i\in\mathcal{L}} + T^*_{\mathsf{glob}}$. This forms the basis for Theorem 3 below, which establishes a lower bound on the peak age of information for T^*_{glob}-periodic schedules.

Theorem 3 (Lower bound on Δ_{peak} of minimum-length periodic schedules, given the global interference model)**.** *Given the global interference model, the peak age of information for any T^*_{glob}-periodic schedule over any interval $[t_0, t_0 + T^*_{\mathsf{glob}})$ with $\bar{t} \leq t_0$ is lower bounded by*

$$\Delta_{\text{peak}}(t_0, t_0 + T^*_{\mathsf{glob}}) \geq \Delta^*_{\text{peak},\mathsf{glob}} \triangleq T^*_{\mathsf{glob}} + \gamma_c + \mathbb{1}_{|\mathcal{L}|\geq 1}. \tag{2.24}$$

Proof. From Definition 4 with $\bar{t} \leq t_0$ we can write

$$\Delta_{\text{peak}}(t_0, t_0 + T^*_{\mathsf{glob}}) = \sup_{t_0 \leq t < t_0 + T^*} \Delta_{\text{peak}}(t), \tag{2.25a}$$

$$= \sup_{t_0 \leq t < t_0 + T^*_{\mathsf{glob}}} \max_{i,j \in \mathcal{V}} \Delta_i^{(j)}(t), \tag{2.25b}$$

$$= \max_{i,j \in \mathcal{V}} \sup_{t_0 \leq t < t_0 + T^*_{\mathsf{glob}}} \Delta_i^{(j)}(t), \tag{2.25c}$$

$$\overset{\text{(a)}}{=} \max_{i,j \in \mathcal{V}} \left(T^*_{\mathsf{glob}} + \Delta_i^{(j)} \right), \tag{2.25d}$$

$$= T^*_{\mathsf{glob}} + \max_{i \in \mathcal{V}} \max_{j \in \mathcal{V}} \Delta_i^{(j)}, \tag{2.25e}$$

$$\overset{\text{(b)}}{\geq} T^*_{\mathsf{glob}} + \gamma_c + \mathbb{1}_{|\mathcal{L}| \geq 1}, \tag{2.25f}$$

where (a) follows from Lemma 3. Inequality (b) follows from Lemma 4 and the fact that $\max_{i \in \mathcal{V}} \mathbb{1}_{i \in \mathcal{L}} = \mathbb{1}_{|\mathcal{L}| \geq 1}$. □

The lower bound on peak age established in Theorem 3 has an intuitive interpretation. The T^*_{glob} component is a consequence of the common period between updates for all statuses in the network. The $\gamma_c + \mathbb{1}_{|\mathcal{L}| \geq 1}$ component is a consequence of the maximum amount of time required to propagate a status throughout the network. Note that the only inequality in the derivation of the lower bound is from Lemma 4. This suggests a strategy for constructing minimum-length periodic schedules to achieve the peak age bound with equality. This is discussed in detail in Section 2.5.2. In fact, for the three node example in Section 2.1, we can compute $\Delta^*_{\text{peak},\mathsf{glob}} = 7$, which is achieved with equality as seen in Fig. 2.2.

Since $T^*_{\mathsf{glob}} = N\gamma_c + |\mathcal{L}|$, we can express the lower bound on peak age as $\Delta^*_{\text{peak},\mathsf{glob}} = (N+1)\gamma_c + |\mathcal{L}| + \mathbb{1}_{|\mathcal{L}| \geq 1}$. The role of γ_c, i.e., the connected domination number of the graph, is more evident in this expression. In graphs with $\gamma_c = 1$, e.g., a star graph or a complete graph, $\Delta^*_{\text{peak},\mathsf{glob}} \sim \mathcal{O}(N)$. In graphs where $\gamma_c \sim \mathcal{O}(N)$, e.g., a path graph or a ring graph, $\Delta^*_{\text{peak},\mathsf{glob}} \sim \mathcal{O}(N^2)$.

The following theorem establishes a lower bound on the average age for networks with

minimum-length periodic schedules.

Theorem 4 (Lower bound on Δ_{avg} of of minimum-length periodic schedules, given the global interference model)**.** *Given the global interference model, the average age of information for any T^*_{glob}-periodic schedule over any interval $[t_0, t_0 + T^*_{\mathsf{glob}})$ with $\bar{t} \leq t_0$ is lower bounded by*

$$\Delta_{\text{avg},\mathsf{glob}}(t_0, t_0 + T^*_{\mathsf{glob}}) \geq \Delta^*_{\text{avg},\mathsf{glob}} \triangleq \frac{T^*_{\mathsf{glob}}}{2} + \bar{d}, \tag{2.26}$$

where

$$\bar{d} \triangleq \frac{1}{N^2 - N} \sum_{\substack{i,j \in \mathcal{V} \\ i \neq j}} d(i,j) \tag{2.27}$$

is the average distance of the network, and $d(i,j)$ is the distance in hops of the shortest path between nodes i and j.

Proof. From Definition 3 and Definition 5, we can write

$$\Delta_{\text{avg},\mathsf{glob}}(t_0, t_0 + T^*_{\mathsf{glob}}) = \frac{1}{T^*_{\mathsf{glob}}(N^2 - N)} \sum_{\substack{i,j \in \mathcal{V} \\ j \neq i}} \int_{t_0}^{t_0 + T^*_{\mathsf{glob}}} \Delta_i^{(j)}(t) dt, \tag{2.28a}$$

$$\overset{\text{(a)}}{=} \frac{1}{T^*_{\mathsf{glob}}(N^2 - N)} \sum_{\substack{i,j \in \mathcal{V} \\ j \neq i}} \int_{0}^{T^*_{\mathsf{glob}}} (\Delta_i^{(j)} + t) dt, \tag{2.28b}$$

$$\overset{\text{(b)}}{\geq} \frac{1}{N^2 - N} \sum_{\substack{i,j \in \mathcal{V} \\ j \neq i}} \left(d(i,j) + \frac{T^*_{\mathsf{glob}}}{2} \right), \tag{2.28c}$$

$$= \frac{T^*_{\mathsf{glob}}}{2} + \bar{d}, \tag{2.28d}$$

where (a) follows from Lemma 3 and (b) follows from the fact that $\Delta_i^{(j)} \geq d(i,j)$. □

Like the lower bound on peak age, the lower bound on average age has an intuitive interpretation. The $\frac{T^*_{\mathsf{glob}}}{2}$ component is a consequence of the common period between updates for all statuses in the network. The $\bar{d}$ component is a consequence of the average amount of

time required to propagate statuses throughout the network. For the three node example in Section 2.1, the lower bound on average age can be calculated as $\Delta^*_{\text{avg,glob}} = \frac{5}{2} + \frac{8}{6} \approx 3.83$, which is achieved with equality since $\Delta_i^{(j)} = d(i,j)$ for all i, j in this case. This bound is not achievable in general, however, since it is not always possible to achieve $\Delta_i^{(j)} = d(i,j)$ for all i, j (see, e.g., an $N = 5$ node path network).

2.5.2 Algorithm for T^*_{glob}-Periodic Schedule Design, Given the Global Interference Model

This section formalizes the main idea suggested by Lemma 1 to develop a sequential flooding algorithm that generates a periodic minimum-length schedule for a given network topology, given the global interference model. Recall from the proof of Lemma 1 that propagation of $H_i(t)$ throughout the network can be accomplished with an initial transmission by node i of its zero-delay status update, and then subsequent transmissions that propagate that status update to remaining nodes via multiple hops from nodes in a MCDS. By repeating this approach and disseminating status updates from each of the N processes in turn, a length T^*_{glob} schedule emerges which can then be repeated in a periodic fashion to continuously propagate fresh status updates throughout the network. An algorithm that details this approach is summarized in Algorithm 1, where Depth-First Search$(\mathcal{G}[\mathcal{S}], i)$ denotes an ordered list of vertices generated by performing an in-order depth-first search of the graph induced by $\mathcal{S}$

where the search starts at root vertex i.

Algorithm 1: Schedule design to disseminate status updates throughout the network for the global interference model

1 initialize time, $t \leftarrow 0$;
2 **for** node $i = 1 : N$ **do**
3 **if** $\exists$ MCDS $\bar{\mathcal{S}}$ s.t. $i \in \bar{\mathcal{S}}$ **then**
4 $\mathcal{S} \leftarrow \bar{\mathcal{S}}$;
5 **else**
6 $\mathcal{S} \leftarrow \bar{\mathcal{S}} \cup \{i\}$, for any MCDS $\bar{\mathcal{S}} \subset \mathcal{V}$;
7 **end**
8 $\mathcal{S}_{\text{sorted},i} = \text{Depth-First Search}(\mathcal{G}[\mathcal{S}], i)$;
9 node i generates a fresh sample of H_i;
10 **for** $m = 1 : |\mathcal{S}_{\text{sorted},i}|$ **do**
11 $j = \mathcal{S}_{\text{sorted},i}(m)$;
12 node j transmits $H_i^{(j)}(t)$;
13 $t \leftarrow t + 1$;
14 **end**
15 **end**
16 go to line 2;

Observe that the schedule generated by Algorithm 1 obeys the following properties: (i) it uses exactly T^*_{glob} transmissions to update all tables throughout the network, (ii) it is periodic, and (iii) all statuses throughout the network get updated exactly once during each period. While our algorithm makes use of the depth-first search to traverse the graph induced by the MCDS, we note that an alternate graph traversal approach (e.g., breadth-first search) could be used here. Moreover, the specific choice of graph search used does not impact the bounds presented below.

2.5.3 Guaranteed Peak and Average Age of Schedules Generated by Algorithm 1

Since Algorithm 1 implements optimal sequential flooding, it achieves $\max_{j\in\mathcal{V}} \Delta_i^{(j)} = \gamma_c + \mathbb{1}_{i\in\mathcal{L}}$ for all $i \in \mathcal{V}$. Hence, the inequality in Lemma 4 used in the derivation of the lower bound on peak age in Theorem 3 is achieved with equality for schedules generated by Algorithm 1. Unlike peak age, the achieved average age of schedules generated by Algorithm 1 will not coincide with the lower bound in Theorem 4 since the inequality $\Delta_i^{(j)} \geq d(i,j)$ cannot be

achieved with equality in general. In this section, we derive an *upper* bound, i.e., a performance guarantee, on the achieved average age of schedules generated by Algorithm 1. This is followed by a characterization of the gap between the upper and lower bounds developed previously.

Theorem 5 (Upper bound on achievable average age)**.** *For any interval* $[t_0, t_0 + T^*_{\mathsf{glob}})$ *with* $t_0 \geq \bar{t}$*, the average age of the schedule generated by Algorithm 1 satisfies*

$$\Delta_{\text{avg,Alg.1}}(t_0, t_0 + T^*_{\mathsf{glob}}) \leq \Delta_{\text{avg,ub}} \triangleq \frac{T^*_{\mathsf{glob}}}{2} + \gamma_c + \frac{|\mathcal{L}|}{N}. \tag{2.29}$$

Proof. The proof follows from the fact Algorithm 1 implements optimal sequential flooding with age offsets satisfying $d(i,j) \leq \Delta_i^{(j)} \leq \gamma_c + \mathbb{1}_{i\in\mathcal{L}}$. The lower bound on $\Delta_i^{(j)}$ holds for any schedule and was used in Theorem 4. Using the upper bound here, we can write

$$\begin{aligned}
\Delta_{\text{avg,Alg.1}}(t_0, t_0 + T^*_{\mathsf{glob}}) &\leq \frac{1}{N^2 - N} \sum_{\substack{i,j\in\mathcal{V} \\ j\neq i}} \frac{T^*_{\mathsf{glob}}}{2} + \gamma_c + \mathbb{1}_{i\in\mathcal{L}}, && \text{(2.30a)} \\
&= \frac{T^*}{2} + \gamma_c + \frac{1}{N^2 - N} \sum_{\substack{i,j\in\mathcal{V} \\ j\neq i}} \mathbb{1}_{i\in\mathcal{L}}, && \text{(2.30b)} \\
&= \frac{T^*_{\mathsf{glob}}}{2} + \gamma_c + \frac{|\mathcal{L}|}{N}. && \text{(2.30c)}
\end{aligned}$$

□

Corollary 1 below characterizes the gap between the upper bound on the achieved average age in Theorem 5 and the average age lower bound in Theorem 4.

Corollary 1. *The gap between upper bound on the average age of the schedule generated by Algorithm 1 and the lower bound in Theorem 4 satisfies* $\Delta_{\text{avg,ub}} - \Delta^*_{\text{avg,}\mathsf{glob}} < N - 2$.

Proof. From (2.26) and (2.29) we can write

$$\Delta_{\text{avg,ub}} - \Delta^*_{\text{avg,glob}} = \gamma_c + \frac{|\mathcal{L}|}{N} - \bar{d}, \tag{2.31a}$$

$$\overset{(a)}{\leq} N - 2 + \frac{|\mathcal{L}|}{N} - \bar{d}, \tag{2.31b}$$

$$\overset{(b)}{<} N - 1 - \bar{d}, \tag{2.31c}$$

$$\overset{(c)}{<} N - 2, \tag{2.31d}$$

where (a) is from $\gamma_c \leq N - 2$, (b) is from $\frac{|\mathcal{L}|}{N} < 1$, and (c) is from $\bar{d} \geq 1$. All of these inequalities are general properties of graphs. □

The result presented by Corollary 1 shows that the gap grows at most linearly with respect to the number of nodes, N. Next, we show that the schedule generated by Algorithm 1 is asymptotically optimal in terms of the average age when N is large.

Corollary 2. *The ratio of the average age of the schedule generated by Algorithm 1 to the average age lower bound in Theorem 4 goes to one as $N \to \infty$.*

Proof. We can use the average age upper bound of Theorem 5 and a sandwiching argument to prove the desired result. From (2.26) and (2.29) we can write

$$\lim_{N\to\infty} \frac{\Delta_{\text{avg,ub}}}{\Delta^*_{\text{avg,glob}}} = \lim_{N\to\infty} \frac{\frac{T^*_{\text{glob}}}{2} + \gamma_c + \frac{|\mathcal{L}|}{N}}{\frac{T^*_{\text{glob}}}{2} + \bar{d}}, \tag{2.32a}$$

$$= 1 + \lim_{N\to\infty} \frac{\gamma_c + \frac{|\mathcal{L}|}{N} - \bar{d}}{\frac{T^*_{\text{glob}}}{2} + \bar{d}}, \tag{2.32b}$$

$$= 1 + \lim_{N\to\infty} \frac{\frac{T^*_{\text{glob}}}{N} - \bar{d}}{\frac{T^*_{\text{glob}}}{2} + \bar{d}}, \tag{2.32c}$$

$$\leq 1 + \lim_{N\to\infty} \frac{2}{N}, \tag{2.32d}$$

$$= 1, \tag{2.32e}$$

where the inequality in the last step results from the fact that $\frac{\frac{T^*_{\text{glob}}}{N} - \bar{d}}{\frac{T^*_{\text{glob}}}{2} + \bar{d}} \leq (\frac{T^*_{\text{glob}}}{N})/(\frac{T^*_{\text{glob}}}{2})$ since

$\bar{d} \geq 0$. Moreover, since $\frac{\Delta_{\text{avg,Alg.1}}(t_0,t_0+T^*_{\mathsf{glob}})}{\Delta^*_{\text{avg},T^*}} \geq 1$ for all N, we have

$$\lim_{N\to\infty} \frac{\Delta_{\text{avg,Alg.1}}(t_0, t_0 + T^*_{\mathsf{glob}})}{\Delta^*_{\text{avg,glob}}} = 1. \tag{2.33}$$

□

While the upper bound in Theorem 5 makes the pessimistic assumption that all nodes have a worst-case age offset of $\Delta_i^{(j)} = \gamma_c + \mathbb{1}_{i\in\mathcal{L}}$, the result in Corollary 2 shows that this pessimistic assumption is inconsequential asymptotically.

2.5.4 Schedule Design for the Global Interference Model with Transmission Errors

In this section we provide two algorithms that generate schedules for refreshing all of the status update parameters throughout the network with any arbitrary topology. The main idea for the schedule design is similar to the development of a sequential flooding tree in Algorithm 1 that generates a periodic minimum-length schedule for a given network topology except that nodes retransmit status updates until all "modified" one-hop neighbors have received at least one successful update of the process. Since transmission errors may occur, we assume a retransmission policy where each node i retransmits a status update until the update has been received successfully by all nodes in the modified one-hop neighborhood of node i, denoted by set $\bar{\mathcal{N}}_1(i)$. This process is then repeated for the $H_2(t)$ process and so on until an update of the $H_N(t)$ process is successfully received at least once by all nodes in the network. This process then starts over again with node 1. In the following we formalize the notion of modified one-hop neighborhood and provide an example to further clarify the schedule design.

Without loss of generality assume that the indices of the nodes in the sequential flooding tree that disseminates updates of the $H_i(t)$ process form set $\mathcal{S}_{\text{sorted},i}$. The first index in this

sorted set represents node i, since every time in order to refresh the H_i statuses throughout the network, first a fresh update is required to be disseminated by node i. Algorithm 2 describes how this sorted set is obtained. For the m^{th} element in the sorted set $\mathcal{S}_{\text{sorted},i}$, $m \in \{1, 2, \ldots, |\mathcal{S}_{\text{sorted},i}|\}$, where $|\mathcal{S}_{\text{sorted},i}| = \gamma_c + \mathbf{1}_{i\in\mathcal{L}}$ and $i \in \mathcal{V}$, we define the modified one-hop neighborhood of node $j = \mathcal{S}_{\text{sorted},i}(m)$ as

$$\bar{\mathcal{N}}_1(j) \triangleq \left[\mathcal{N}_1(j) - \bigcup_{m'=1}^{m-1} \mathcal{N}_1(\mathcal{S}_{\text{sorted},i}(m'))\right] - \{i\}. \tag{2.34}$$

In other words based on (2.34), node j does not need to refresh the statuses at the nodes that have been updated by the previous nodes in the sequential flooding tree. We also define the cardinality of the modified one-hop neighborhood in (2.34) as

$$J_{i,m} \triangleq |\bar{\mathcal{N}}_1(\mathcal{S}_{\text{sorted},i}(m))|. \tag{2.35}$$

There are some subtleties to this schedule that can be illustrated by considering an example in the setting shown in Figure 2.4. Suppose node 1 successfully transmits a status update to node 2 and that MCDS $\mathcal{S}_1$ is used for sequential flooding. Node 2 retransmits the update until both node 3 and node 4 successfully receive the update once. Although node 1 is in the one-hop neighborhood of node 2, it is not in the *modified* one-hop neighborhood of node 2 since node 1 has already been updated (directly). Similarly, when node 3 retransmits the update, it only requires node 5 to successfully receive the update once. Although node 2 is in the one-hop neighborhood of node 3, node 2 received the update (indirectly) earlier in this schedule. In this example we have $\mathcal{S}_{\text{sorted},1} = \{1, 2, 3\}$, $\mathcal{N}_1(1) = \{2\}$, $\mathcal{N}_1(2) = \{1, 3, 4\}$, $\mathcal{N}_1(3) = \{2, 5\}$, $\bar{\mathcal{N}}_1(1) = \{2\}$, $\bar{\mathcal{N}}_1(2) = \{3, 4\}$, $\bar{\mathcal{N}}_1(3) = \{5\}$, $J_{1,1} = 1$, $J_{1,2} = 2$, and $J_{1,3} = 1$.

We consider two variations of the sequential flooding tree schedule for updating the statuses throughout the network. The only difference is with regards to the root node in each of the sequential flooding trees. In the first variation, we assume the root node i retransmits without resampling $H_i(t)$ until all of its neighbors successfully receive an update.

In the second variation, we assume that root node i resamples $H_i(t)$ in each retransmission until all of its neighbors successfully receive an update. Note that each neighbor may receive a different sample of $H_i(t)$ in the second variation. The former case is easier to analyze, whereas the latter case provides better performance.

In the following, Algorithm 2 and Algorithm 3 summarize these two approaches.

Algorithm 2: Schedule design *without resampling* by root nodes

```
1  initialize time, t ← 0;
2  for node i = 1 : N do
3  |  if ∃ MCDS S̄ s.t. i ∈ S̄ then
4  |  |  S ← S̄;
5  |  else
6  |  |  S ← S̄ ∪ {i}, for any MCDS S̄ ⊂ V;
7  |  end
8  |  S_sorted,i = Depth-First Search(G[S], i);
9  |  node i generates a fresh sample of H_i;
10 |  for m = 1 : |S_sorted,i| do
11 |  |  j = S_sorted,i(m);
12 |  |  t' ← t;
13 |  |  while ∃ n ∈ N̄_1(j) s.t. n has not received a packet during interval (t', t] or
   |  |   t' == t do
14 |  |  |  node j transmits H_i^(j)(t');
15 |  |  |  t ← t + 1;
16 |  |  end
17 |  end
18 end
19 go to line 2;
```

Observe that "Depth-First Search$(\mathcal{G}[\mathcal{S}], i)$" in Algorithm 2 describes an ordered list of vertices generated by performing a depth-first search of the graph induced by $\mathcal{S}$ where the search starts at root node i. The schedule generated by Algorithm 2 is periodic in the absence of packet errors; however, when packet errors are present it is not periodic in general.

Algorithm 3: Schedule design *with resampling* by root nodes

initialize time, $t \leftarrow 0$;
for node $i = 1 : N$ **do**
  if $\exists$ MCDS $\bar{\mathcal{S}}$ s.t. $i \in \bar{\mathcal{S}}$ **then**
    $\mathcal{S} \leftarrow \bar{\mathcal{S}}$;
  else
    $\mathcal{S} \leftarrow \bar{\mathcal{S}} \cup \{i\}$, for any MCDS $\bar{\mathcal{S}} \subset \mathcal{V}$;
  end
  $\mathcal{S}_{\text{sorted},i} =$ Depth-First Search$(\mathcal{G}[\mathcal{S}], i)$;
  for $m = 1 : |\mathcal{S}_{\text{sorted},i}|$ **do**
    $j = \mathcal{S}_{\text{sorted},i}(m)$;
    $t' \leftarrow t$;
    while $\exists\ n \in \bar{\mathcal{N}}_1(j)$ s.t. n has not received a packet during interval $(t', t]$ **or** $t' == t$ **do**
      if $j == i$ **then**
        node j generates a fresh sample of H_i;
      end
      node j transmits $H_i^{(j)}(t)$;
      $t \leftarrow t + 1$;
    end
  end
end
go to line 2;

Similarly, the schedule generated by Algorithm 3 is not periodic in general.

2.5.5 Lower Bound on the Average Peak Age of Information of the Schedules Generated by Algorithm 2

In this section, we present an expression that lower bounds the *average peak AoI* for the schedules generated by Algorithm 2. Before proceeding, we first define the average peak AoI. Figure 2.5 represents an example age $\Delta_i^{(j)}(t)$ for some i and j where $i, j \in \mathcal{V},\ i \neq j$. The age value immediately before arrival of the q^{th} update of the H_i process at node j is

$$A_i^{(j)}(q) = a_i^{(j)}(q-1) + \tau_i^{(j)}(q), \tag{2.36}$$

where $a_i^{(j)}(q)$ represents the age of the q^{th} update at its arrival time at node j and $\tau_i^{(j)}(q)$ represents the interarrival time of the $(q-1)^{\text{th}}$ and q^{th} updates for $q \in \{1, 2, \ldots\}$. The initial age is denoted by $a_i^{(j)}(0)$.

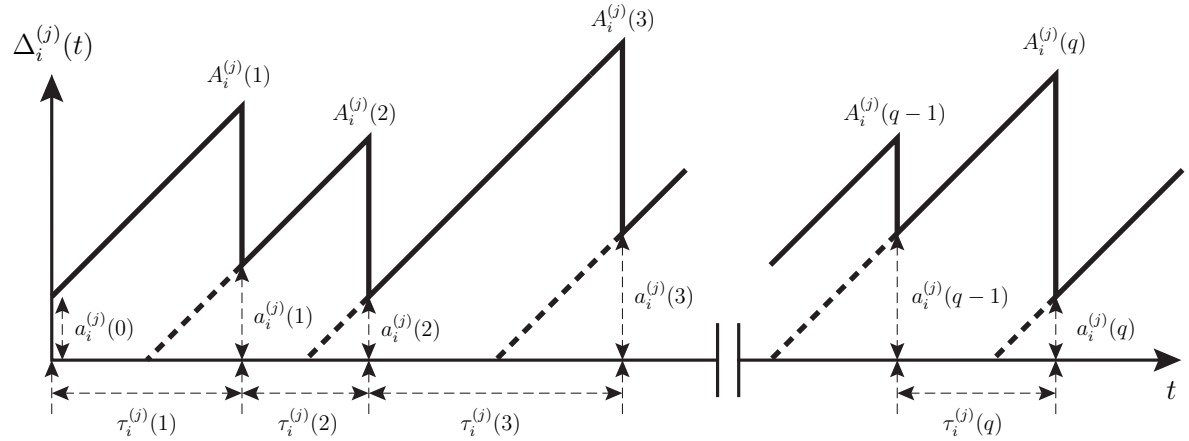

Figure 2.5: An example age $\Delta_i^{(j)}(t)$ for some i and j where $i, j \in \mathcal{V},\ i \neq j$.

We define the average peak AoI over the $N^2 - N$ indirectly observed statuses throughout the network as

$$\bar{\Delta}_{\text{peak}} \triangleq \frac{1}{(N^2 - N)} \sum_{\substack{i,j \in \mathcal{V} \\ i \neq j}} \bar{\Delta}_i^{(j)}, \tag{2.37}$$

where

$$\bar{\Delta}_i^{(j)} = \lim_{Q \to \infty} \frac{1}{Q} \sum_{q=1}^{Q} A_i^{(j)}(q). \tag{2.38}$$

Theorem 6 represents a lower bound on the average peak AoI of the schedules generated by Algorithm 2.

Theorem 6. *The average peak AoI of the $N^2 - N$ indirectly observed statuses throughout*

the network for the schedules generated by Algorithm 2 is lower bounded by

$$\bar{\Delta}^{*}_{\text{peak}} = \bar{d} + \sum_{i=1}^{N} \sum_{m=1}^{\gamma_c + \mathbf{1}_{i\in\mathcal{L}}} \sum_{n=1}^{J_{i,m}} \binom{J_{i,m}}{n} \frac{(-1)^{n+1}}{(1-\epsilon^n)}. \tag{2.39}$$

Proof. From (2.36) and (2.37) we can write

$$\bar{\Delta}_{\text{peak}} = \frac{1}{(N^2-N)} \sum_{\substack{i,j\in\mathcal{V} \\ i\neq j}} \left[\lim_{Q\to\infty} \frac{1}{Q} \sum_{q=1}^{Q} a_i^{(j)}(q-1) + \tau_i^{(j)}(q) \right], \tag{2.40a}$$

$$\geq \bar{d} + \underbrace{\frac{1}{(N^2-N)} \sum_{\substack{i,j\in\mathcal{V} \\ i\neq j}} \left[\lim_{Q\to\infty} \frac{1}{Q} \sum_{q=1}^{Q} \tau_i^{(j)}(q) \right]}_{\triangleq \bar{\tau}}, \tag{2.40b}$$

$$= \bar{d} + \bar{\tau}, \tag{2.40c}$$

where (2.40b) is obtained considering (2.27) and the fact that $a_i^{(j)}(q) \geq d(i,j)$ for all i, j and q, and $\bar{\tau}$ in (2.40c) is obtained in Corollary 3. This completes the proof. □

Corollary 3 represents an expression for $\bar{\tau}$, which we refer to as the average interarrival time.

Corollary 3. *The average interarrival time of the $N^2 - N$ statuses throughout the network for the schedules generated by Algorithm 2 is given by*

$$\bar{\tau} = \sum_{i=1}^{N} \sum_{m=1}^{\gamma_c + \mathbf{1}_{i\in\mathcal{L}}} \sum_{n=1}^{J_{i,m}} \binom{J_{i,m}}{n} \frac{(-1)^{n+1}}{(1-\epsilon^n)}. \tag{2.41}$$

Proof. Without loss of generality, consider dissemination of the H_i process throughout the network for $i \in \mathcal{V}$. The H_i process should be disseminated by the nodes in the sorted set $\mathcal{S}_{\text{sorted},i}$ in the schedule generated by Algorithm 2. Denote the indices of the nodes in this sorted set by $m \in \{1, \ldots, \gamma_c + \mathbf{1}_{i\in\mathcal{L}}\}$, and the number of transmissions by the m^{th} node to

update the nodes in $\bar{\mathcal{N}}_1(\mathcal{S}_{\text{sorted},i}(m))$ by $k_{i,m}$. For $\ell = \{1, 2, \ldots\}$ we get

$$\Pr\{k_{i,m} = \ell\} = (1-\epsilon^{\ell})^{J_{i,m}} - (1-\epsilon^{\ell-1})^{J_{i,m}}. \tag{2.42}$$

From (2.42) we can write

$$\begin{aligned}
\mathrm{E}[k_{i,m}] &= \sum_{\ell=1}^{\infty} \ell \Pr\{k_{i,m} = \ell\}, && \text{(2.43a)}\\
&= \sum_{\ell=1}^{\infty} \ell[(1-\epsilon^{\ell})^{J_{i,m}} - (1-\epsilon^{\ell-1})^{J_{i,m}}], && \text{(2.43b)}\\
&= \sum_{\ell=1}^{\infty} \ell \left\{ \sum_{n=0}^{J_{i,m}} \binom{J_{i,m}}{n} [(-\epsilon^{\ell})^n - (-\epsilon^{\ell-1})^n] \right\}, && \text{(2.43c)}\\
&= \sum_{n=1}^{J_{i,m}} \binom{J_{i,m}}{n} (-1)^n \left(1 - \frac{1}{\epsilon^n}\right) \left[\sum_{\ell=1}^{\infty} \ell(\epsilon^n)^{\ell} \right], && \text{(2.43d)}\\
&= \sum_{n=1}^{J_{i,m}} \binom{J_{i,m}}{n} (-1)^n \left(1 - \frac{1}{\epsilon^n}\right) \frac{\epsilon^n}{(1-\epsilon^n)^2}, && \text{(2.43e)}\\
&= \sum_{n=1}^{J_{i,m}} \binom{J_{i,m}}{n} \frac{(-1)^{n+1}}{(1-\epsilon^n)}. && \text{(2.43f)}
\end{aligned}$$

Now, observe the number of transmissions required by any of the nodes in a given sequential flooding tree in a schedule generated by Algorithm 2 is independent of the number of transmissions by any other transmitting node. Considering the result in (2.43f) over all $m \in \{1, \ldots, \gamma_c + \mathbf{1}_{i \in \mathcal{L}}\}$ and $i \in \mathcal{V}$, the average interarrival time in (2.41) is obtained. □

For $\epsilon = 0$, note that $\mathrm{E}[k_{i,m}] = 1$, which gives $\bar{\tau} = N\gamma_c + |\mathcal{L}|$. This result is consistent with Lemma 1.

2.6 Numerical Results

This section presents numerical examples that serve to illustrate and verify the bounds on the peak and average age of information in Sections 2.4 and 2.5, and that permit comparison

Table 2.2: AoI Bounds for Canonical Graph Topologies

topology	$\lvert\mathcal{L}\rvert$	γ_c	$\delta_{\max}$	$\bar{d}$	$\Delta^*_{\text{peak,inst,glob}}$	$\Delta^*_{\text{peak,glob}}$	$\Delta^*_{\text{avg,inst,glob}}$	$\Delta^*_{\text{avg,glob}}$
complete	0	1	N–1	1	N	N+1	$\frac{N+1}{2}$	$\frac{N+2}{2}$
cycle	0	N–2	2	$\frac{N^2}{4(N-1)}$, N even $\frac{N+1}{4}$, N odd	N^2–2N	N^2–N–2	$\frac{N^3-4N^2+6N-1}{2(N-1)}$	$\frac{2N^3-5N^2+4N}{4(N-1)}$, N even $\frac{2N^2-3N+1}{4}$, N odd
path	2	N–2	2	$\frac{N+1}{3}$	N^2–2N+2	N^2–N+1	$\frac{N^4-4N^3+10N^2-13N+8}{2N(N-1)}$	$\frac{3N^2-4N+8}{6}$
star 	N–1	1	N–1	$\frac{2(N-1)}{N}$	2N–1	2N+1	$\frac{N^3+N^2-2N+2}{2N(N-1)}$	$\frac{2N^2+3N-4}{2N}$
pan ($N>5$) 	1	N–3	3	$\frac{N^3-N^2+6N-8}{4N(N-1)}$, N even $\frac{N^2+7}{4N}$, N odd	N^2–3N+1	N^2–2N–1	$\frac{N^4-6N^3+14N^2-9N+2}{2N(N-1)}$	$\frac{2N^4-7N^3+7N^2+4N-8}{4N(N-1)}$, N even $\frac{2N^3-5N^2+2N+7}{4N}$, N odd

with the achieved peak and average age of the schedule generated by Algorithm 1.

2.6.1 Application of Bounds to Canonical Graph Topologies, Given the Global Interference Model

To illustrate computation of the various bounds, and to observe the impact of topology on the AoI, we list in Table 2.2 the bounds for some canonical graph topologies [122, 123] as a function of the number of nodes N. The table shows that for topologies like complete and star where $\gamma_c \ll N$ and $\delta_{\max}$ is of order of N, the age of information is of order of N, too. On the other hand for topologies like cycle, path, and pan where γ_c is of order of N and $\delta_{\max} \ll N$, the age of information is of order of N^2.

2.6.2 All Connected Topologies with $3 \leq N \leq 9$ Nodes, Given the Global Interference Model

For every connected network topology with $3 \leq N \leq 9$ nodes, we make use of a database [124] that exhaustively enumerates all connected network topologies with isomorphs removed.

Instantaneous Peak and Instantaneous Average Age

Figure 2.6 shows the lower bounds on the instantaneous peak and instantaneous average age of information in Theorems 1 and 2, as well as the minimum instantaneous peak and instantaneous average age achieved by the periodic schedule generated by Algorithm 1. For every graph topology in the database, the minimum instantaneous peak age achieved by Algorithm 1 is equal to the lower bound on instantaneous peak age, i.e., $\min_{t \geq \bar{t}} \Delta_{\text{peak,Alg.1}}(t) = \Delta^*_{\text{peak,inst,glob}}$, so Theorem 1 serves as a tight lower bound on schedules generated by Algorithm 1. Meanwhile, for the instantaneous average age, there is generally a gap between the lower bound from Theorem 2 and the minimum instantaneous average age achieved by Algorithm 1. To investigate this gap, we consider the ratio computed by dividing the achieved minimum instantaneous average age by the lower bound, and have found that for all networks with a connected topology having $3 \leq N \leq 9$ nodes, schedules generated by Algorithm 1 obey

$$1 \leq \frac{\min_{t \geq \bar{t}} \Delta_{\text{avg,Alg.1},k}(t)}{\Delta^*_{\text{avg,inst,glob}}(k)} \leq 1.783, \tag{2.44a}$$

$$\frac{1}{K} \sum_{k=1}^{K} \frac{\min_{t \geq \bar{t}} \Delta_{\text{avg,Alg.1},k}(t)}{\Delta^*_{\text{avg,inst,glob}}(k)} \approx 1.563, \tag{2.44b}$$

where we index by network topology $k = \{1, \ldots, K\}$ with $K = 273,191$ representing the total number of such networks. This leads to the following three observations: (i) only for the fully-connected network topologies, where $\gamma_c = 1$, Algorithm 1 achieves the lower bound on instantaneous average age, (ii) in the worst case, Algorithm 1 yields a minimum instantaneous average age that is 78.3% above the lower bound, and (iii) averaging over all K topologies, Algorithm 1 is 56.3% above the lower bound.

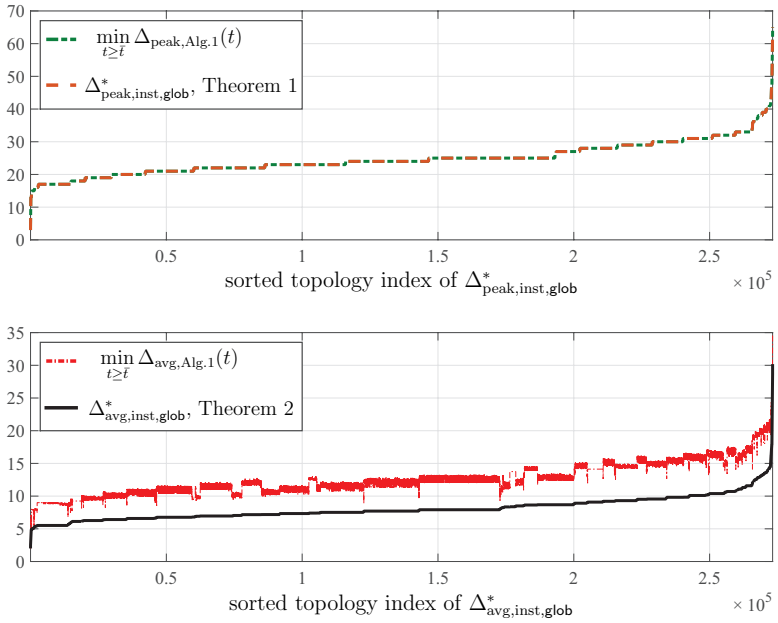

Figure 2.6: Lower bounds on the instantaneous peak and instantaneous average age of information in Theorems 1 and 2, compared to the minimum instantaneous peak and instantaneous average age of information achieved by the schedule in Algorithm 1.

Peak and Average Age for T^*_{glob}-Periodic Schedules

Figure 2.7 compares the lower bounds on peak and average age of information for T^*_{glob}-periodic schedules in Theorems 3 and 4 with the peak and average age of information achieved by the schedule generated by Algorithm 1, as well as the upper bound on achievable average age of schedules generated by Algorithm 1 given by Theorem 5. The results verify that, indeed, $\Delta_{\text{peak,Alg.1}} = \Delta^*_{\text{peak,glob}}$ for all of the considered topologies. In addition, for all $k = \{1, \ldots, K\}$ we have $\Delta^*_{\text{avg,glob}}(k) \leq \Delta_{\text{avg,Alg.1}}(k) \leq \Delta_{\text{avg,ub}}(k)$, thus verifying Theorems 4 and 5. Moreover, the numerical results on average age obey

$$1 \leq \frac{\Delta_{\text{avg,Alg.1}}(k)}{\Delta^*_{\text{avg,glob}}(k)} \leq 1.035, \tag{2.45a}$$

$$\frac{1}{K} \sum_{k=1}^{K} \frac{\Delta_{\text{avg,Alg.1}}(k)}{\Delta^*_{\text{avg,glob}}(k)} \approx 1.008, \tag{2.45b}$$

where as above we index by network topology $k = \{1, \ldots, K\}$. Again, this leads to three observations: (i) for network topologies with small γ_c, the average age of Algorithm 1 is very close or achieves the lower bound on the average age of T^*-periodic schedules, (ii) in the worst case, Algorithm 1 yields a minimum average age that is 3.5% above the lower bound, and (iii) averaging over all K topologies, Algorithm 1 is 0.8% above the lower bound. Moreover, we note that Corollary 2 implies that for schedules generated by Algorithm 1, these ratios approach 1 as N grows large. Finally, we note that the achievable peak age is roughly twice the achievable average age, i.e., $\Delta_{\text{peak,Alg.1}}(k) \approx 2\Delta_{\text{avg,Alg.1}}(k)$ for all $k = \{1, \ldots, K\}$.

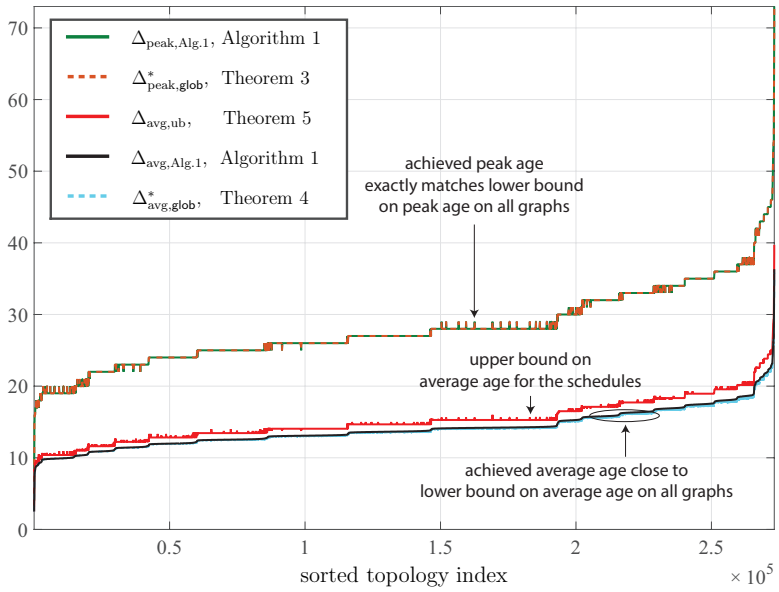

Figure 2.7: Achievable peak and average age of the schedule generated by Algorithm 1 for all networks with a connected topology and $3 \leq N \leq 9$. The age values are arranged in an increasing order for the achievable average age.

Figure 2.8 represents the gap between the achieved average age of the schedule generated by Algorithm 1 and the lower bound on the average age in Theorem 4 compared to the upper bound of $N - 2$ in Corollary 1 for all of the connected network topologies with $3 \leq N \leq 9$. The results show that the upper bound in Corollary 1 is conservative and for most of the topologies the schedule generated by Algorithm 1 achieves close to the lower bound on the average age.

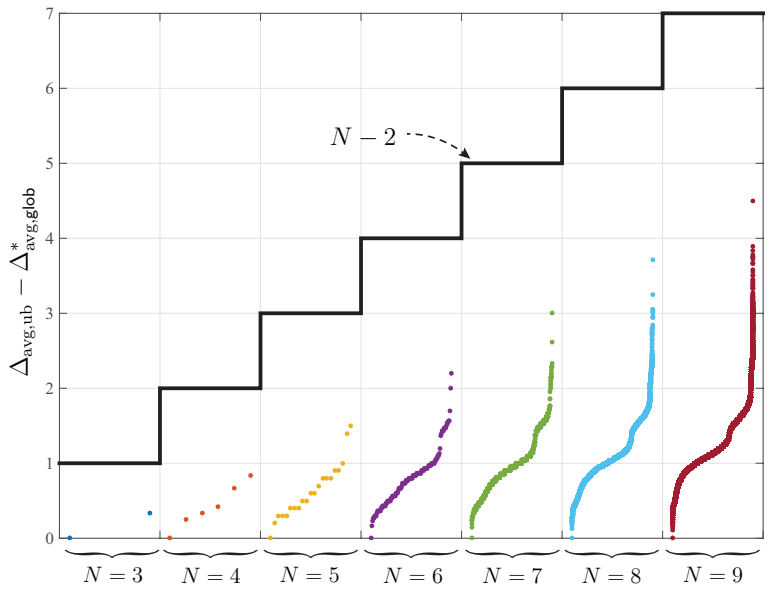

Figure 2.8: The achieved gap between the upper bound on the average age of the schedule generated by Algorithm 1 and the lower bound on the average age for all networks with a connected topology and $3 \leq N \leq 9$ compared to the upper bound in Corollary 1.

2.6.3 Comparing the Age of Information for the Three Interference Models in Ring Networks

This section presents numerical examples for the specific case of ring networks (i.e., cycle graphs) that serve to illustrate the bounds on peak and average age in Section 2.5.1. As mentioned earlier, due to the different combinatorics of schedule design in the interference free model and topologically-dependent interference model for general graphs, we do not present general schedule constructions algorithms here. Instead, we restrict our attention to status update schedules in the specific case of ring networks to illustrate the main points. For an N-node ring network, note that $|\mathcal{E}| = 2N$, $\gamma_c = N-2$, $\mathcal{L} = \emptyset$, $\chi = \left\lfloor \frac{N}{3} \right\rfloor$, $\delta_{\max} = 2$, and $\epsilon = 2\nu$.

We first present a schedule for the global interference model below. The modulus operator

$$\sigma_{p,q}(\{(i_1,j_1),\ldots,(i_r,j_r)\}) \triangleq \{(i_1+p \mod N, j_1+q \mod N), \ldots, (i_r+p \mod N, j_r+q \mod N)\},$$

is used to simplify the notation. Also, for any x if $x+p \mod N = 0$ ($x+q \mod N = 0$), set $x+p \mod N = N$ ($x+q \mod N = N$). Schedule A below is a special case of the general minimum-length periodic schedules designed by Algorithm 1 for ring networks.

Schedule A: ring with global interference model.

Let $1 : \{(1,1)\}$ be the schedule during time slot 1. For the next time slots $n = 2, 3, \ldots, N(N-2)$, the schedule is obtained by $n : \sigma_{p,q}(\{(1,1)\})$, where $p = n - 1 - \left\lfloor \frac{n-1}{N-2} \right\rfloor (N-3)$ and $q = \left\lfloor \frac{n-1}{N-2} \right\rfloor$.

In schedule A, node 1's status update is first disseminated clockwise around the ring (requiring $N-2$ transmissions), then node 2's status update is disseminated around the ring, and so on, until node N's status update has been disseminated around the ring at which point the process repeats with node 1. It is straightforward to confirm that Schedule A is a minimum-length periodic schedule with period $T = N(N-2) = T^*_{\mathsf{glob}}$.

For the $N = 6$ ring network in Fig. 2.3, Schedule A generates

$$
\begin{array}{llllll}
1:\{(1,1)\}, & 2:\{(2,1)\}, & 3:\{(3,1)\}, & 4:\{(4,1)\}, & 5:\{(2,2)\}, & 6:\{(3,2)\}, \\
7:\{(4,2)\}, & 8:\{(5,2)\}, & 9:\{(3,3)\}, & 10:\{(4,3)\}, & 11:\{(5,3)\}, & 12:\{(6,3)\}, \\
13:\{(4,4)\}, & 14:\{(5,4)\}, & 15:\{(6,4)\}, & 16:\{(1,4)\}, & 17:\{(5,5)\}, & 18:\{(6,5)\}, \\
19:\{(1,5)\}, & 20:\{(2,5)\}, & 21:\{(6,6)\}, & 22:\{(1,6)\}, & 23:\{(2,6)\}, & 24:\{(3,6)\}.
\end{array}
$$

Schedule B: ring with interference free model.

Let $1 : \{(1,1),(2,2),\ldots,(N,N)\}$ be the schedule during time slot 1. For the next time slots $n = 2, 3, \ldots, N-2$, the schedule is obtained by $n : \sigma_{p,q}(\{(1,1),(2,2),\ldots,(N,N)\})$, where $p = 0$ and $q = 1 - n$.

In schedule B, all N nodes begin by transmitting their local status updates in parallel. In the next $N-3$ time slots, each node continually relays the status update sent by their counter-clockwise neighbor, after which point the process repeats again with each node transmitting a fresh update of their local process. It is straightforward to confirm that Schedule B is a minimum-length periodic schedule with period $T = N - 2 = T^*_{\mathsf{ifree}}$.

For the $N = 6$ ring network in Fig. 2.3, Schedule B generates

$$
\begin{aligned}
&1 : \{(1,1),(2,2),(3,3),(4,4),(5,5),(6,6)\},\\
&2 : \{(1,6),(2,1),(3,2),(4,3),(5,4),(6,5)\},\\
&3 : \{(1,5),(2,6),(3,1),(4,2),(5,3),(6,4)\},\\
&4 : \{(1,4),(2,5),(3,6),(4,1),(5,2),(6,3)\}.
\end{aligned}
$$

Schedule C: ring with topologically-dependent interference model.

Let $1 : \{(1,1),(4,4),\ldots,(3K-3,3K-3)\}$ be the schedule during time slot 1, where $K \triangleq \lfloor \frac{N}{3} \rfloor$. For the next time slots $n = 2,3,\ldots,(3+\mathrm{mod}(N,3))(N-2)$, the schedule is obtained by $n : \sigma_{p,q}(\{(1,1),(4,4),\ldots,(3K-3,3K-3)\})$, where $p = n-1-\lfloor \frac{n-1}{N-2} \rfloor (N-3)$ and $q = \lfloor \frac{n-1}{N-2} \rfloor$.

In schedule C, every third node around the ring transmits simultaneously to avoid interference; in other words, given a distance-2 coloring of the graph, all nodes of the same color transmit simultaneously. For example, for the $N = 6$ ring network in Fig. 2.3 there are 3 colors. All nodes of a given color begin by transmitting their local status updates simultaneously, and over the next $N-3$ time slots these updates are disseminated in simultaneously, clockwise around the ring. Then, the next group of nodes of a given color take their turn, followed by the third and final group of same-colored nodes. After this, the process repeats by returning to the first color. It is straightforward to confirm that Schedule C is a minimum-length periodic schedule with period $T = 3(N-2) = T^*_{\mathsf{tdi}}$ for $N = 3k$ and $k \in \{1,2,3,\ldots\}$.

For the $N = 6$ ring network in Fig. 2.3, Schedule C generates

$$
\begin{aligned}
&1 : \{(1,1),(4,4)\}, \quad 2 : \{(2,1),(5,4)\}, \quad 3 : \{(3,1),(6,4)\}, \quad 4 : \{(4,1),(1,4)\},\\
&5 : \{(2,2),(5,5)\}, \quad 6 : \{(3,2),(6,5)\}, \quad 7 : \{(4,2),(1,5)\}, \quad 8 : \{(5,2),(2,5)\},\\
&9 : \{(3,3),(6,6)\}, \quad 10 : \{(4,3),(1,6)\}, \quad 11 : \{(5,3),(2,6)\}, \quad 12 : \{(6,3),(3,6)\}.
\end{aligned}
$$

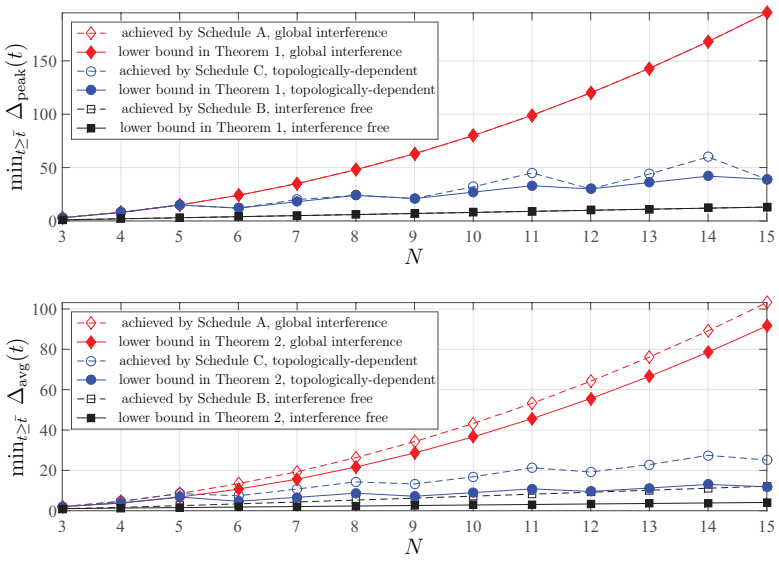

Figure 2.9: Lower bounds and achievable peak and average age for ring networks with $N = \{3, 4, \ldots, 15\}$.

Figure 2.9 compares the instantaneous peak and average age lower bounds presented in Theorems 1 and 2 with the minimum achievable instantaneous peak and average age of the schedules generated by Schedules A, B, and C for ring networks with $N \in \{3, 4, \ldots, 15\}$, where the minimum is taken over all times $t \geq \bar{t} = T^*$. To compute the minimum instantaneous peak and average ages, since the schedules are periodic, it is sufficient to consider only one interval of length T^* after having defined ages at all nodes, e.g., interval $[T^*, 2T^*]$. The results confirm that the instantaneous peak and average age for the interference free model and the topologically-dependent interference model are of order of N as Theorems 1 and 2 show.

2.6.4 Achieved Average Peak AoI of Algorithm 2 and Algorithm 3 Compared to Theorem 6

This section presents numerical examples to illustrate the achieved average peak AoI of the schedules generated by Algorithm 2 and Algorithm 3 and compares the achieved ages with the lower bound in Theorem 6. Figure 2.10 and Figure 2.11 represent the achieved average

peak AoI for fully-connected networks (K_N) and ring networks (C_N), respectively, versus the number of nodes $N \in \{3, \ldots, 10\}$ and for error probabilities $\epsilon \in \{0, 0.25, 0.5\}$. For the simulation lines, both Algorithm 2 and Algorithm 3 are run over an interval of 10^5 time slots. The results show that the achieved average peak AoI is an strictly increasing function of the number of nodes N and error probability ϵ. When $\epsilon = 0$, the schedules generated by Algorithm 2 and Algorithm 3 are identical and have the same average peak AoI.

For the fully-connected network case in Figure 2.10, each transmitting node needs to update the tables at its $N - 1$ neighbors. For the ring network network case in Figure 2.11, each transmitting node has at most 2 neighbors that it needs to update. As a result, when $\epsilon > 0$, resampling by root nodes as specified in Algorithm 2 tends to lead to a more significant reduction in the achieved average peak AoI in fully-connected networks than in ring networks when compared to the average peak AoI of schedules generated by Algorithm 1.

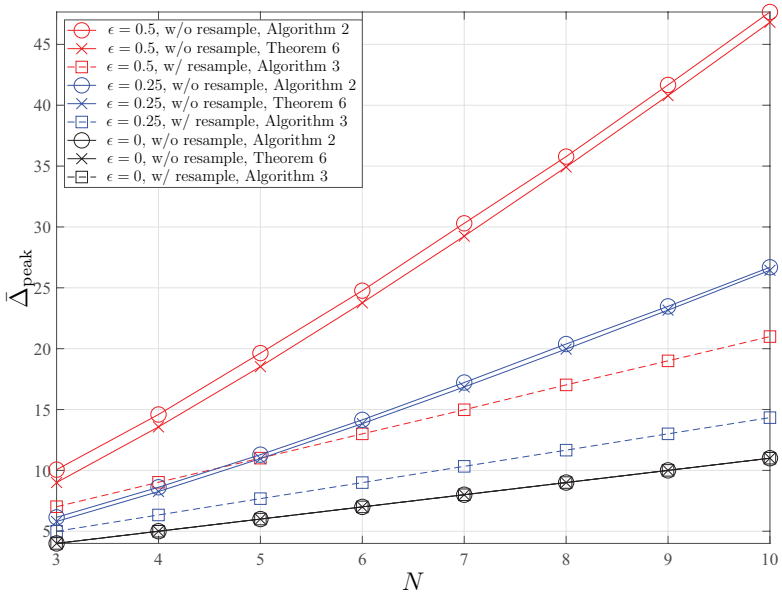

Figure 2.10: Achieved average peak AoI versus the number of nodes N and error probabilities $\epsilon \in \{0, 0.25, 0.5\}$ for fully-connected networks K_N.

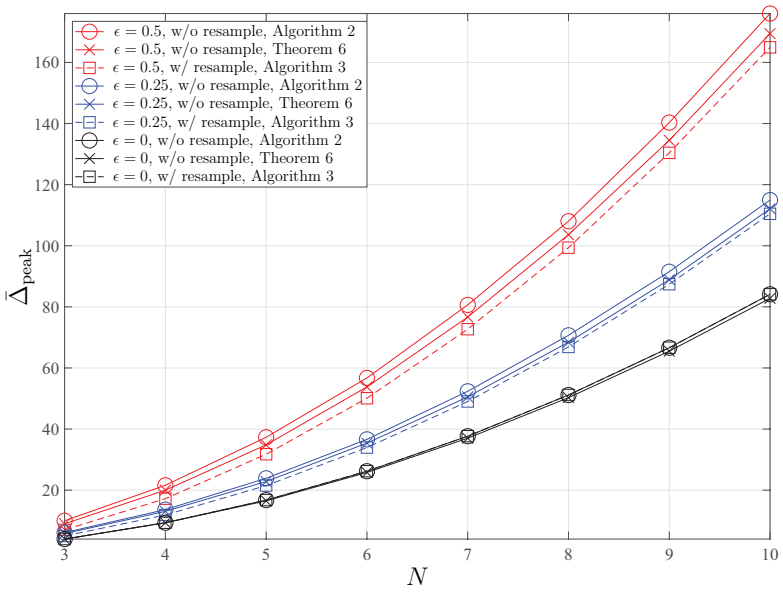

Figure 2.11: Achieved average peak AoI versus the number of nodes N and error probabilities $\epsilon \in \{0, 0.25, 0.5\}$ for ring networks C_N.

2.7 Conclusion

This chapter studied the age of information problem in a general multi-source multi-hop partially-connected wireless network with nodes communicating over time slotted transmissions. We derived fundamental results that lower bound the performance of any status update dissemination schedule in terms of the peak and average age of information metrics for three interference scenarios (i) global interference model (ii) interference free model, and (iii) topologically-dependent interference model. Taking a graph theoretical approach on the impact of network topology on the age of information, we found that the AoI depends on fundamental graph parameters such as the connected domination number and average shortest path length. We presented an algorithm that generates minimum-length periodic schedules for dissemination of the status updates among the nodes in the network with a connected topology, given the global interference model. We derived upper bounds on the

achieved peak and average age of the schedules designed by the proposed algorithm, which showed that these schedules exactly achieve the peak age bound and also achieve the average age bound within an additive gap scaling linearly with the size of the network. Under global interference constraints, we developed two algorithms based on repetitive transmissions in presence of error. A lower bound on the average peak AoI was derived for schedules generated by the algorithm without resampling by the root nodes. Numerical examples were presented to quantify the gap between the achieved age and the lower bounds.

Chapter 3

Age of Information in Multiaccess Networks with Transmission Errors

Several recent papers have considered the effect of packet delivery errors on AoI [11,19,39,40, 61, 71, 77, 85, 125, 126]. The single-source single-destination setting was first studied in [11]. The average AoI was derived for scheduled access with feedback and slotted ALOHA-like random access over multiaccess channels in [61]. A single-source multi-destination setting was considered in [71] where a single base station source sends status updates to a number of destinations through packets with a fixed transmission time over unreliable channels. It was shown that a greedy policy, which schedules a transmission to the destination with the highest current age is average age optimal in the absence of error. In [77, 126], the opposite setting was studied where a network of nodes transmits status updates to a base station while simultaneously satisfying throughput constraints. In this setting, stationary randomized policies are derived to minimize the weighted sum AoI assuming a unit-delay channel from each source to the destination.

In the first part of this chapter, we look at the AoI of multiaccess channels with active packet generation, where the sources send information packets to a destination through a server with unreliable transmissions. This scenario is similar to the multi-source single-destination setting considered in [61, 77]. A key difference, however, is that the service times

in our model are assumed to be random according to the exponential distribution. Another key difference is that we consider both stationary randomized policies as well as round-robin policies under three different packet retransmission policies when errors occur. Table 3 summarizes the key differences between the results in this paper compared to [11,61,71,77]. The main contributions of this section are twofold: (i) we derive closed-form expressions for each source's long-term average AoI from the perspective of the destination, and (ii) we derive optimal source selection probabilities that minimize the weighted sum average AoI for stationary randomized policies [127].

In the second part of this chapter we study the multiaccess setting motivated by Yates and Kaul in [68], where the AoI was studied under various assumptions about whether the server was first-come first-served (FCFS) or last-come last-served (LCFS) and, for the latter case, whether new updates could preempt packets currently in service or only in waiting. We study an LCFS system with the key assumption that source $\mathcal{S}_i$ can only preempt its own packets in service [128]. To distinguish this approach from the approach in [68], we refer to this as "self preemption" and the model of Yates and Kaul as "global preemption". We further generalize the model by allowing for transmission errors from the server with fixed probability $0 \leq \epsilon < 1$. Using tools from stochastic hybrid systems (SHS), we derive a closed-form expression for average AoI experienced by each source in terms of the status update arrival rates $\{\lambda_1, \ldots, \lambda_N\}$, service rate μ, and the transmission error probability ϵ. We show, somewhat surprisingly, that global preemption in service (referred to as LCFS-S in [68]) provides uniformly better AoI than self preemption in service for all sources in the system when $\epsilon = 0$.

3.1 System Model

We consider a status update system with N source nodes $\mathcal{S}_1, \mathcal{S}_2, \ldots, \mathcal{S}_N$ and one destination node $\mathcal{D}$ as represented in Figure 3.1. The sources intend to share information about their

Table 3.1: Comparing the average AoI analysis in [11, 61, 71, 77] with this work.

	single/multi-source/destination	status update arrival rate at the source(s)	service rate	stationary randomized policy			round-robin policy		
				no retransmission	retransmission w/o resampling	retransmission w/ resampling	no retransmission	retransmission w/o resampling	retransmission w/ resampling
[11]	single-source single-destination	Poisson	Exponential	—	—	—	—	—	—
[61]	multi-source single-destination	at the beginning of each time slot	constant / time-slotted	—	—	✓	—	—	✓
[71]	single-source multi-destination	at the beginning of each frame	constant / time-slotted	✓	—	—	—	✓	—
[77]	multi-source single-destination	at will / instantaneously	constant / time-slotted	✓	—	—	—	—	—
This work	multi-source single-destination	at will / instantaneously	Exponential	✓	✓	✓	✓	✓	✓

time-varying state with the destination. A server with service rate μ according to the exponential distribution delivers packets to the destination. We assume that a packet in service has a transmission error (is not delivered) with fixed probability $0 \leq \epsilon < 1$.

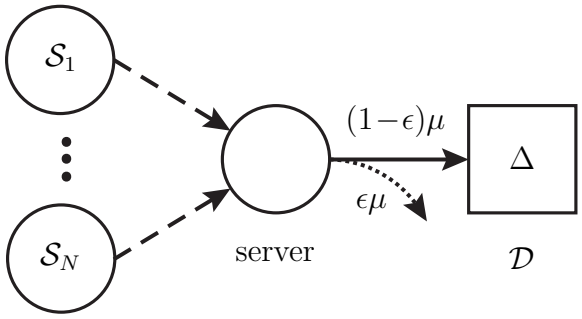

Figure 3.1: The multi-source status update system with unreliable transmissions.

3.2 Average AoI in Multiaccess Channels with Active Sources

We assume that the time required to sample a status update is negligible and that each source can generate packets containing status updates "at will" as in [40, 125]. The packets are sent to the destination through a server with service rate μ according to the exponential distribution. Service times are assumed to be i.i.d.. We further assume that upon service

completion, a packet is lost with probability ϵ. The destination sends instantaneous and error-free feedback to the server after every service completion indicating whether the transmission was successful or not. The following sections discuss the two scheduling policies considered in this section: (i) the stationary randomized policy and (ii) the round-robin policy.

3.2.1 Stationary randomized policy

We assume a fixed probability mass function $\mathcal{P} = \{p_1, ..., p_N\}$ with $p_i > 0$ corresponding to the probability that source $\mathcal{S}_i$ is selected to transmit. We denote the indices of the transmitted packets over time by $j \in \mathbb{J} = \{1, 2, ...\}$ and $m_j \in \mathbb{I}$ as the source of the j^{th} packet. If the j^{th} packet is successfully delivered, the next source m_{j+1} is simply drawn randomly from $\mathcal{P}$. If the j^{th} packet is lost, then we consider three packet management approaches:

A1. **No Retransmission**: The server ignores errors and simply draws source m_{j+1} from $\mathcal{P}$ as if no error occurred. We refer to this case as "RND_NR".

A2. **Retransmission Without Resampling**: The server sets $m_{j+1} = m_j$ and retransmits the *original* packet from $\mathcal{S}_{m_j}$. We refer to this case as "RND_ARQ".

A3. **Retransmission With Resampling**: The server sets $m_{j+1} = m_j$ and transmits a *fresh* packet from $\mathcal{S}_{m_j}$. We refer to this case as "RND_ASQ".

Theorem 7 presents the average AoI for the stationary randomized schedule policies.

Theorem 7. *The average AoI Δ_i of the status updates of source $i \in \mathbb{I}$ for the multi-source system with active sources and service completion with error probability ϵ under the stationary randomized policies is equal to*

$$\Delta_{i,\text{RND\_NR}} = \frac{1 + (1-\epsilon)p_i}{\mu(1-\epsilon)p_i}, \tag{3.1a}$$

$$\Delta_{i,\text{RND\_ARQ}} = \frac{1 + p_i}{\mu(1-\epsilon)p_i}, \tag{3.1b}$$

$$\Delta_{i,\text{RND\_ASQ}} = \Delta_{i,\text{RND\_NR}}. \tag{3.1c}$$

Proof sketch. We use tools from Stochastic Hybrid Systems (SHS) [68] to derive the average age. Due to space limitations, most of the algebraic derivations are omitted here. A Markov chain representation of the discrete state $q(t) \in \mathcal{Q}$ of the system regarding $\Delta_i(t)$ for case RND_NR is shown in Fig. 3.2. Table 3.2 represents the exponential rate and the transition map for each link ℓ with continuous state $[x_0, x_1]$, where x_0 represents the age of the $\mathcal{S}_i$'s state at $\mathcal{D}$ and x_1 stores the age to be used after an age reset when $\mathcal{S}_i$ successfully delivers a packet (link 0). For notational convenience, we denote

$$\mathbf{D}_0 = \begin{bmatrix} 1 & 0 \\ 0 & 0 \end{bmatrix}, \ \mathbf{D}_1 = \begin{bmatrix} 0 & 0 \\ 1 & 0 \end{bmatrix}, \text{ and } \mathbf{D}_2 = \begin{bmatrix} 1 & 0 \\ 0 & 1 \end{bmatrix}. \tag{3.2}$$

Figure 3.2: The Markov chain of the status update system regarding $\Delta_i(t)$ for case RND_NR. Link $\ell = 0$ corresponds to a successfully delivered packet for $\mathcal{S}_i$. Link $\ell = 1$ corresponds to an unsuccessfully delivered packet for $\mathcal{S}_i$ as well a successful or unsuccessful packet from any other source.

Table 3.2: Transition rates and maps for case RND_NR.

ℓ	$q_\ell \to q'_\ell$	$\lambda^{(\ell)}$	$\mathbf{x}\mathbf{A}_\ell$	$\mathbf{A}_\ell$	$\mathbf{v}_{q_\ell}\mathbf{A}_\ell$
0	$0 \to 0$	$\mu(1-\epsilon)p_i$	$[x_1, 0])$	$\mathbf{D}_1$	$[v_{01}, 0]$
1	$0 \to 0$	$\mu(1-(1-\epsilon)p_i)$	$[x_0, 0])$	$\mathbf{D}_0$	$[v_{00}, 0]$

Since there is only one state in Fig. 3.2, the stationary distribution of the Markov chain is trivial and we can write the single balance equation (Theorem 4, [68]) as

$$\mu\bar{\mathbf{v}}_0 = \mathbf{b} + \lambda^{(0)}\bar{\mathbf{v}}_{q_0}\mathbf{A}_0 + \lambda^{(1)}\bar{\mathbf{v}}_{q_1}\mathbf{A}_1 \tag{3.3}$$

where $\mathbf{b} = [1, 1]$ and $\bar{\mathbf{v}} = [\bar{v}_{00}, \bar{v}_{01}]$. Substituting the quantities from Table 3.2 and solving for v_{00} yields

$$\bar{v}_{00} = \frac{1 + (1-\epsilon)p_i}{\mu(1-\epsilon)p_i}, \tag{3.4}$$

which shows (3.1a).

We use a similar analysis for the RND_ARQ and RND_ASQ cases. Both of these cases can be represented by the Markov chain in Fig. 3.3. The system enters state 0 after any successful transmission. The system enters state 1 after an unsuccessful transmission from $\mathcal{S}_i$ and the system enters state 2 after an unsuccessful transmission from $\mathcal{S}_j$ for $j \neq i$. Links 0 and 4 correspond to successful transmissions by $\mathcal{S}_i$. Links 2 and 3 correspond to unsuccessful transmissions by $\mathcal{S}_i$. The remaining links correspond to successful and unsuccessful transmissions from $\mathcal{S}_j$ for all $j \neq i$.

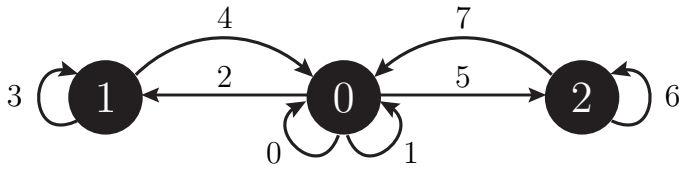

Figure 3.3: The Markov chain for cases RND_ARQ and RND_ASQ.

Table 3.3 shows the transition rates for case RND_ARQ. The table for RND_ASQ is identical except for links 2 and 3 where, for RND_ASQ, we have $\mathbf{A}_2 = \mathbf{A}_3 = \mathbf{D}_0$ and $\mathbf{x}\mathbf{A}_2 = \mathbf{x}\mathbf{A}_3 = [x_0, 0]$. For RND_ASQ we also have $\mathbf{v}_{q_2}\mathbf{A}_2 = [v_{00}, 0]$ and $\mathbf{v}_{q_3}\mathbf{A}_3 = [v_{10}, 0]$. These differences are due to the fact that, since RND_ASQ always transmits a fresh sample, links 2 and 3 reset the stored age in x_1. A similar analysis as above can be applied to solve for the steady state distribution of the Markov chain as

$$\bar{\boldsymbol{\pi}} = [\bar{\pi}_0 \ \bar{\pi}_1 \ \bar{\pi}_2] = \begin{bmatrix} 1-\epsilon & \epsilon p_i & \epsilon(1-p_i) \end{bmatrix}. \tag{3.5}$$

and then solving the balance equations for $\mathbf{v}_0$, $\mathbf{v}_1$, and $\mathbf{v}_2$ and then compute $\Delta_i = v_{00} + v_{10} + v_{20}$ to arrive at (3.1b) and (3.1c).

Table 3.3: Transition rates and maps for case RND_ARQ.

ℓ	$q_\ell \to q'_\ell$	$\lambda^{(\ell)}$	$\mathbf{x}\mathbf{A}_\ell$	$\mathbf{A}_\ell$	$\mathbf{v}_{q_\ell}\mathbf{A}_\ell$
0	$0 \to 0$	$\mu(1-\epsilon)p_i$	$[x_1, 0]$	$\mathbf{D}_1$	$[v_{01}, 0]$
1	$0 \to 0$	$\mu(1-\epsilon)(1-p_i)$	$[x_0, 0]$	$\mathbf{D}_0$	$[v_{00}, 0]$
2	$0 \to 1$	$\mu\epsilon p_i$	$[x_0, x_1]$	$\mathbf{D}_2$	$[v_{00}, v_{01}]$
3	$1 \to 1$	$\mu\epsilon$	$[x_0, x_1]$	$\mathbf{D}_2$	$[v_{10}, v_{11}]$
4	$1 \to 0$	$\mu(1-\epsilon)$	$[x_1, 0]$	$\mathbf{D}_1$	$[v_{11}, 0]$
5	$0 \to 2$	$\mu\epsilon(1-p_i)$	$[x_0, 0]$	$\mathbf{D}_0$	$[v_{00}, 0]$
6	$2 \to 2$	$\mu\epsilon$	$[x_0, 0]$	$\mathbf{D}_0$	$[v_{20}, 0]$
7	$2 \to 0$	$\mu(1-\epsilon)$	$[x_0, 0]$	$\mathbf{D}_0$	$[v_{20}, 0]$

In general, for any fixed system parameters, we have $\Delta_{i,\text{RND\_ARQ}} \geq \Delta_{i,\text{RND\_NR}} = \Delta_{i,\text{RND\_ASQ}}$. The fact that the achieved average age is identical between cases RND_NR and RND_ASQ can be understood intuitively by noting that the destination always receives a *fresh* sample with both RND_NR and RND_ASQ. Moreover, the rates of successful packets from $\mathcal{S}_i$ are the same in both cases, i.e., for RND_ASQ, the sum of links 0 and 4 weighted by the steady state probabilities of the Markov chain can be computed as $\bar{\pi}_0\lambda^{(0)} + \bar{\pi}_1\lambda^{(4)} = \mu(1-\epsilon)^2 p_i + \mu\epsilon(1-\epsilon)p_i = \mu(1-\epsilon)p_i$, which is the same as link 0 in RND_RR.

Optimal Randomized Stationary Policy for Minimizing Weighted Sum Average AoI

In this section we find the optimal source selection probabilities $p_1^*, \ldots, p_N^*$ that minimize the general weighted sum average AoI among all stationary randomized policies. Considering Theorem 7, this problem can be formulated as

$$\min_{p_i} \text{WSAoI}, \qquad \text{s.t.} \sum_{i=1}^{N} p_i = 1, \tag{3.6}$$

where

$$\text{WSAoI}_{\text{RND\_NR}} = \text{WSAoI}_{\text{RND\_ASQ}} \triangleq \sum_{i=1}^{N} \frac{\alpha_i[1+(1-\epsilon)p_i]}{\mu N(1-\epsilon)p_i}, \tag{3.7a}$$

$$\text{WSAoI}_{\text{RND\_ARQ}} \triangleq \sum_{i=1}^{N} \frac{\alpha_i[1+p_i]}{\mu N(1-\epsilon)p_i}, \tag{3.7b}$$

and $\alpha_i \geq 0$ denotes the fixed wight for source i. Without loss of generality we assume $\sum_{i=1}^{N} \sqrt{\alpha_i} = 1$. Theorem 8 represents the optimal solution for the problem in (3.6).

Theorem 8. *For the RND policies, the optimal p_i is*

$$p^*_{i,\text{RND\_NR}} = p^*_{i,\text{RND\_ARQ}} = p^*_{i,\text{RND\_ASQ}} = \sqrt{\alpha_i}. \tag{3.8}$$

Proof: Considering (3.7a)-(3.7b), the Hessian matrix of WSAoI can be written as

$$\mathbf{H}(\text{WSAoI}) = \text{diag}\left(\frac{2\alpha_1}{\mu N(1-\epsilon)p_1^3}, ..., \frac{2\alpha_N}{\mu N(1-\epsilon)p_N^3}\right). \tag{3.9}$$

Since $\alpha_i > 0$ we have $|\mathbf{H}(\text{WSAoI})| > 0$, which means that WSAoI is a convex function of $p_1, \ldots, p_N$ and there exist a set of optimal p_i values that minimize WSAoI. From (3.7a) we define the following Lagrangian multiplier function

$$\mathcal{L}(p_i, \lambda) = \frac{1}{N}\sum_{i=1}^{N} \frac{\alpha_i[1+p_i(1-\epsilon)]}{\mu p_i(1-\epsilon)} + \lambda(\sum_{i=1}^{N} p_i - 1). \tag{3.10}$$

Taking the partial derivative of (3.10), we get

$$\frac{\partial \mathcal{L}(p_i, \lambda)}{\partial p_i} = -\frac{\alpha_i}{N\mu(1-\epsilon)p_i^2} + \lambda, \tag{3.11a}$$

$$\frac{\partial \mathcal{L}(p_i, \lambda)}{\partial \lambda} = \sum_{i=1}^{N} p_i - 1. \tag{3.11b}$$

Setting (3.11a) and (3.11b) to zero, we get

$$p^*_{i,\text{RND\_NR}} = p^*_{i,\text{RND\_ASQ}} = \sqrt{\alpha_i}, \quad \lambda = \frac{1}{N\mu(1-\epsilon)}. \tag{3.12}$$

Repeating steps (3.10)-(3.11b) for (3.7b) gives $p^*_{i,\text{RND\_ARQ}}$. ■

3.2.2 Round-robin Policy

For the round-robin scheduling policy, transmitting nodes are selected deterministically in order. If the j^{th} packet is successfully delivered, the next source is $m_{j+1} = \{m_j \bmod N\} + 1$. If the j^{th} packet is lost, then we consider same three packet management approaches as in the stationary randomized case. These packet management approaches are denoted as 'RR_NR" (no retransmission, errors are ignored), "RR_ARQ" (the original packet from $\mathcal{S}_{m_j}$ is retransmitted until successfully delivered), and "RR_ASQ" (a fresh packet from $\mathcal{S}_{m_j}$ is transmitted until successfully delivered), respectively.

Theorem 9 presents the average AoI for the round-robin schedule policies.

Theorem 9. *The average AoI Δ_i of the status updates of source $i \in \mathbb{I}$ for the multi-source system with active sources and service completion with error probability ϵ under the round-robin policies is equal to*

$$\Delta_{i,\text{RR\_NR}} = \frac{N + 3 + (N-3)\epsilon}{2\mu(1-\epsilon)}, \tag{3.13a}$$

$$\Delta_{i,\text{RR\_ARQ}} = \frac{N+3}{2\mu(1-\epsilon)}, \tag{3.13b}$$

$$\Delta_{i,\text{RR\_ASQ}} = \frac{N+3-2\epsilon}{2\mu(1-\epsilon)}. \tag{3.13c}$$

Proof sketch. A Markov chain and transition rates for case RR_NR regarding $\Delta_1(t)$ are shown in Fig. 3.4 and Table 3.4, respectively. State m corresponds to $\mathcal{S}_m$ selected to transmit. Links 0 and 1 correspond to successful and unsuccessful transmissions from $\mathcal{S}_1$, respectively. The remaining links are for transmissions from $\mathcal{S}_j$ for all $j \neq 1$ and do not distinguish between successful or unsuccessful transmissions.

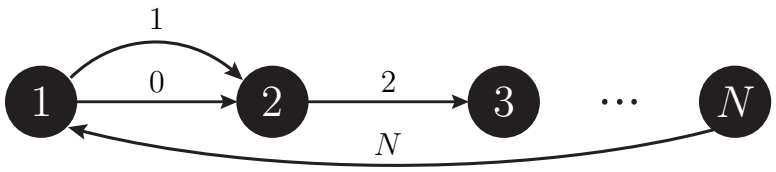

Figure 3.4: The Markov chain for case RR_NR.

Table 3.4: Transition rates and maps for case RR_NR.

ℓ	$q_\ell \to q'_\ell$	$\lambda^{(\ell)}$	$\mathbf{x}\mathbf{A}_\ell$	$\mathbf{A}_\ell$	$\mathbf{v}_{q_\ell}\mathbf{A}_\ell$
0	$1 \to 2$	$\mu(1-\epsilon)$	$[x_1, 0]$	$\mathbf{D}_1$	$[v_{11}, 0]$
1	$1 \to 2$	$\mu\epsilon$	$[x_0, 0]$	$\mathbf{D}_0$	$[v_{10}, 0]$
i	$i \to i+1$	μ	$[x_0, 0]$	$\mathbf{D}_0$	$[v_{i0}, 0]$
N	$N \to 1$	μ	$[x_0, 0]$	$\mathbf{D}_0$	$[v_{N0}, 0]$

Both RR_ARQ and RR_ASQ can be represented by the Markov chain in Fig. 3.5. Here, the even numbered links correspond to unsuccessful transmissions and the odd numbered links correspond to successful transmissions. The transition rates for case RR_ARQ are shown in Table 3.5. Similar to the previous discussion, the only difference between RR_ARQ and RR_ASQ is that the stored age x_1 is reset in link 0 for RR_ASQ. Hence, the transition rate table for case RR_ASQ is the same as Table 3.5 except for link 0 where, for RND_ASQ, we have $\mathbf{A}_0 = \mathbf{D}_0$, $\mathbf{x}\mathbf{A}_0 = [x_0, 0]$, and $\mathbf{v}_{q_0}\mathbf{A}_0 = [v_{10}, 0]$. A similar analysis as above can be applied to solve for $\mathbf{v}_1, \ldots, \mathbf{v}_N$ and then compute $\Delta_i = \sum_{i=1}^{N} v_{i0}$ to get (3.13a)-(3.13c).

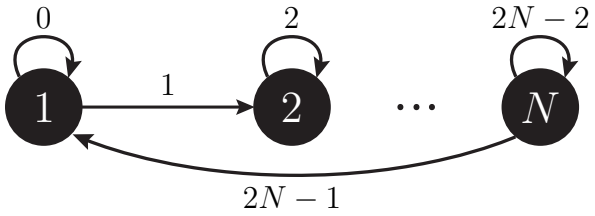

Figure 3.5: The Markov chain for cases RR_ARQ and RR_ASQ.

Table 3.5: Transition rates and maps for case RR_ARQ, $i \in \{2, ..., N-1\}$.

ℓ	$q_\ell \to q'_\ell$	$\lambda^{(\ell)}$	$\mathbf{x}\mathbf{A}_\ell$	$\mathbf{A}_\ell$	$\mathbf{v}_{q_\ell}\mathbf{A}_\ell$
0	$0 \to 0$	$\mu\epsilon$	$[x_0, x_1]$	$\mathbf{D}_2$	$[v_{10}, v_{11}]$
1	$0 \to 1$	$\mu(1-\epsilon)$	$[x_1, 0]$	$\mathbf{D}_1$	$[v_{11}, 0]$
$2i-2$	$i \to i$	$\mu\epsilon$	$[x_0, 0]$	$\mathbf{D}_0$	$[v_{i0}, 0]$
$2i-1$	$i \to i+1$	$\mu(1-\epsilon)$	$[x_0, 0]$	$\mathbf{D}_0$	$[v_{i0}, 0]$
$2N-2$	$N \to N$	$\mu\epsilon$	$[x_0, 0]$	$\mathbf{D}_0$	$[v_{N0}, 0]$
$2N-1$	$N \to 1$	$\mu(1-\epsilon)$	$[x_0, 0]$	$\mathbf{D}_0$	$[v_{N0}, 0]$

3.2.3 Discussion

To compare the RND and the RR policies, we can assume $p_1 = \ldots = p_N = \frac{1}{N}$. From (3.1a)-(3.1c) and (3.13a)-(3.13c) we have

$$\Delta_{i,\text{RND\_NR}} - \Delta_{i,\text{RR\_NR}} = \frac{N-1}{2\mu} \geq 0, \tag{3.14a}$$

$$\Delta_{i,\text{RND\_ARQ}} - \Delta_{i,\text{RR\_ARQ}} = \frac{N-1}{2\mu(1-\epsilon)} \geq 0, \tag{3.14b}$$

$$\Delta_{i,\text{RND\_ASQ}} - \Delta_{i,\text{RR\_ASQ}} = \frac{N-1}{2\mu(1-\epsilon)} \geq 0. \tag{3.14c}$$

The average age gap between RND and RR policies can be intuitively understood by considering the case when $\epsilon = 0$. In this case, the round-robin policy ensures each source is regularly sampled whereas a randomized stationary policy, even when sampled in the same overall proportion as the round-robin schedule, samples each source irregularly. This irregular sampling causes an increase in the average age with respect to the round-robin schedule.

3.3 Average AoI in Multiaccess Channels with Self-Preemptive Sources

Source $\mathcal{S}_i$ generates packets containing status updates at successive times based on a Poisson point process with rate λ_i independently of the other sources and the service times of the server. Packets containing status updates from source $\mathcal{S}_i$ immediately enter service if (i) the

server is idle or (ii) a packet from source $\mathcal{S}_i$ is currently in service. In the latter case, the packet currently in service is dropped and the new packet enters service. If a packet from source $\mathcal{S}_i$ is in service and a new packet from source $\mathcal{S}_j$ with $j \neq i$ arrives at the server, the new packet from source $\mathcal{S}_j$ is discarded.

For notational convenience, we define the normalized rates

$$\rho_i = \frac{\lambda_i}{\mu}, \tag{3.15a}$$

$$\rho = \sum_{i=1}^{N} \rho_i, \text{ and} \tag{3.15b}$$

$$\rho_{-i} = \rho - \rho_i \tag{3.15c}$$

for $i \in \{1, 2, \ldots, N\}$, where ρ_i represents the offered load of source $\mathcal{S}_i$ and ρ represents the total offered load [2].

Theorem 10 provides an expression for the average age of information from source $\mathcal{S}_i$ in the status update system described in Section 3.3.

Theorem 10. *The average age of information Δ_i of the status updates of source $i \in \{1, 2, \ldots, N\}$ for the multi-source system with self preemption in service and service completion with error is equal to*

$$\Delta_i = \frac{\rho_i^3 + \rho_i^2(2\rho_{-i} + 3) + \rho_i[\rho_{-i}^2 + \rho_{-i}(5 - \epsilon) + 3] + (\rho_{-i} + 1)^2}{\mu(1 - \epsilon)\rho_i(\rho_i + 1)(\rho + 1)}. \tag{3.16}$$

The result in Theorem 10 is obtained by following similar steps in the proof of Theorem 7. A Markov chain representation of state $q(t) \in \mathcal{Q}$ of the system from the perspective of source $\mathcal{S}_1$ is shown in Figure 3.6. The states are indexed by $q \in \mathcal{Q} = \{0, 1, \ldots, N\}$, where state 0 indicates the server is idle and state $q \geq 1$ indicates a packet from source q is in service.

In Figure 3.6, link 0 corresponds to a packet arriving from source $\mathcal{S}_1$ when the server is idle. Link 1 corresponds to a packet arriving from source $\mathcal{S}_1$ when the server is currently serving a packet from source $\mathcal{S}_1$ (self preemption in service). Link 2 corresponds to a suc-

cessfully delivered packet and link 3 corresponds to a transmission error. Note that these links are also present for sources $\{\mathcal{S}_2, \ldots, \mathcal{S}_N\}$, but successful and unsuccessful deliveries are lumped into single links to simplify the analysis of the AoI of source $\mathcal{S}_1$. Also note that our self-preemption assumption prevents us from lumping $\{\mathcal{S}_2, \ldots, \mathcal{S}_N\}$ as a single "effective" source as in [68].

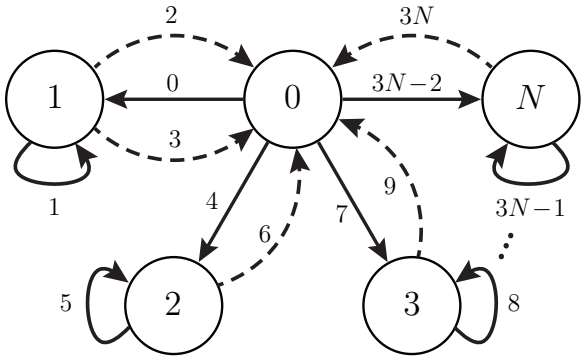

Figure 3.6: The Markov chain representation of the multi-source status update system in Section 3.3 from the perspective of source $\mathcal{S}_1$. States are indexed by $q \in \mathcal{Q} = \{0, \ldots, N\}$. Packet arrivals and service completions are represented by solid and dashed arrows, respectively.

Table 3.6 represents the exponential rates at which state $q(t^-)$ transitions to $q'(t) = q(t^+)$ in the Markov chain in Figure 3.6 and the transition map $\phi(q(t^-), \mathbf{x}(t^-)) = (q'(t), \mathbf{x}'(t)) = (q(t^+), \mathbf{x}(t^+))$ for each link ℓ.

Table 3.6: Transition rates for the Markov chain, $i = \{2, \ldots, N\}$.

link ℓ	$q \to q'$	$\lambda^{(\ell)}$	$\mathbf{x}\mathbf{A}_\ell$	$\mathbf{A}_\ell$	$\mathbf{v}_{q_\ell}\mathbf{A}_\ell$
0	$0 \to 1$	λ_1	$[x_0, 0]$	$\mathbf{D}_0$	$[v_{00}, 0]$
1	$1 \to 1$	λ_1	$[x_0, 0]$	$\mathbf{D}_0$	$[v_{10}, 0]$
2	$1 \to 0$	$(1-\epsilon)\mu$	$[x_1, 0]$	$\mathbf{D}_1$	$[v_{11}, 0]$
3	$1 \to 0$	$\epsilon\mu$	$[x_0, 0]$	$\mathbf{D}_0$	$[v_{10}, 0]$
$3(i-1)+1$	$0 \to i$	λ_i	$[x_0, 0]$	$\mathbf{D}_0$	$[v_{00}, 0]$
$3(i-1)+2$	$i \to i$	λ_i	$[x_0, 0]$	$\mathbf{D}_0$	$[v_{i0}, 0]$
$3i$	$i \to 0$	μ	$[x_0, 0]$	$\mathbf{D}_0$	$[v_{i0}, 0]$

In the absence of packet delivery errors ($\epsilon = 0$), the following Corollary compares self

preemption and global preemption in service (LCFS-S in [68]).

Corollary 4. *In the absence of packet delivery errors, i.e., $\epsilon = 0$, global preemption in service has a lower average AoI than self preemption in service for all sources.*

Proof: From Theorem 2(a) of [68], we have

$$\Delta_{i,\text{glob}} = \frac{1}{\mu}(1+\rho)\frac{1}{\rho_i}. \tag{3.17}$$

Subtracting this from (3.16) results in

$$\Delta_{i,\text{self}} - \Delta_{i,\text{glob}} = \frac{\rho_{-i}}{\mu(\rho_i+1)(\rho+1)} \geq 0, \tag{3.18}$$

since all of the system parameters are non-negative. ■

Finally, considering the average AoI in (3.16), for $\epsilon = 0$ and $\rho_i \to \rho$, we have

$$\lim_{\rho_i \to \rho} \Delta_i = \frac{1}{\mu\rho}(1+\rho) = \frac{1}{\lambda} + \frac{1}{\mu} \tag{3.19}$$

which is identical to the average AoI of a single-source M/M/1 system with LCFS discipline and preemption in service [54].

3.4 Numerical Results

This section presents numerical examples to illustrate the achieved average AoI under various system parameters.

3.4.1 Comparing the Average AoI of Active Sources

Figure 3.7 represents the average age pairs (Δ_1, Δ_2) for $N = 2$ sources, error probability $\epsilon = \{0.15, 0.6\}$ and normalized service rate $\mu = 1$. The results show that $\Delta_1 + \Delta_2$ is minimized under the round-robin policy with retransmissions of fresh samples.

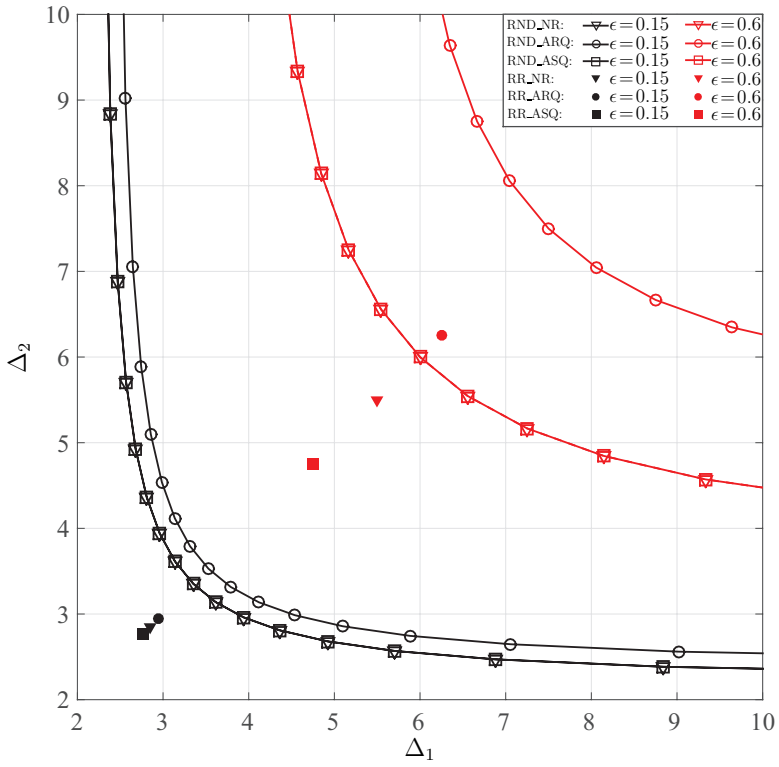

Figure 3.7: Average age pairs (Δ_1, Δ_2) for $N=2$, $\epsilon=\{0.15, 0.6\}$ and $\mu=1$.

Figure 3.8 represents WSAoI versus p_1 for $\alpha_1=0.49$, $\alpha_2=0.09$, $N=2$, $\epsilon=0.6$ and $\mu=1$. For $\alpha_1=0.49$, $\alpha_2=0.09$, the information from source $\mathcal{S}_1$ has a higher weight and intuitively over the long term more packets from $\mathcal{S}_1$ should be delivered to the destination to minimize WSAoI. The simulation results show that the minimum WSAoI is reached when $p^*_{1,\text{RND\_NR}}=p^*_{1,\text{RND\_ARQ}}=p^*_{1,\text{RND\_ASQ}}=0.7$, which agrees with Theorem 8. For the two extreme cases where $p_1\to 0$ ($p_2\to 1$) and $p_1\to 1$ ($p_2\to 0$) we have $\Delta_1\to\infty$ (Δ_2 becomes finite) and Δ_1 becomes finite ($\Delta_2\to\infty$), respectively, giving WSAoI$\to\infty$.

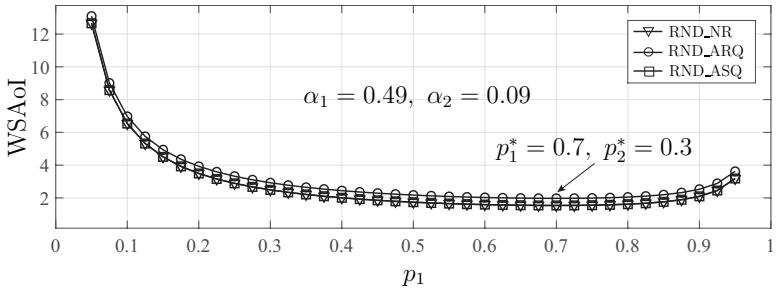

Figure 3.8: Weighted sum average age versus p_1 for $N = 2$, $\epsilon = 0.6$ and $\mu = 1$.

3.4.2 Comparing the Average AoI of Self-Preempting Sources

We first consider a status update system with $N = 2$ sources with a fixed total packet arrival rate $\rho = 1$ and no packet delivery errors ($\epsilon = 0$). Figure 3.9 shows the average AoI pairs (Δ_1, Δ_2) of systems with self preemption in service, global preemption in service, and global preemption in waiting. As expected from Corollary 4, global preemption in service uniformly outperforms self preemption in service. The results also show that when $\rho_1 \to 1$, the average AoI of $\mathcal{S}_1$ for the case with self preemption in service converges to the result in (3.19) and approaches the average AoI of a single-source M/M/1 system with LCFS discipline and preemption in service.

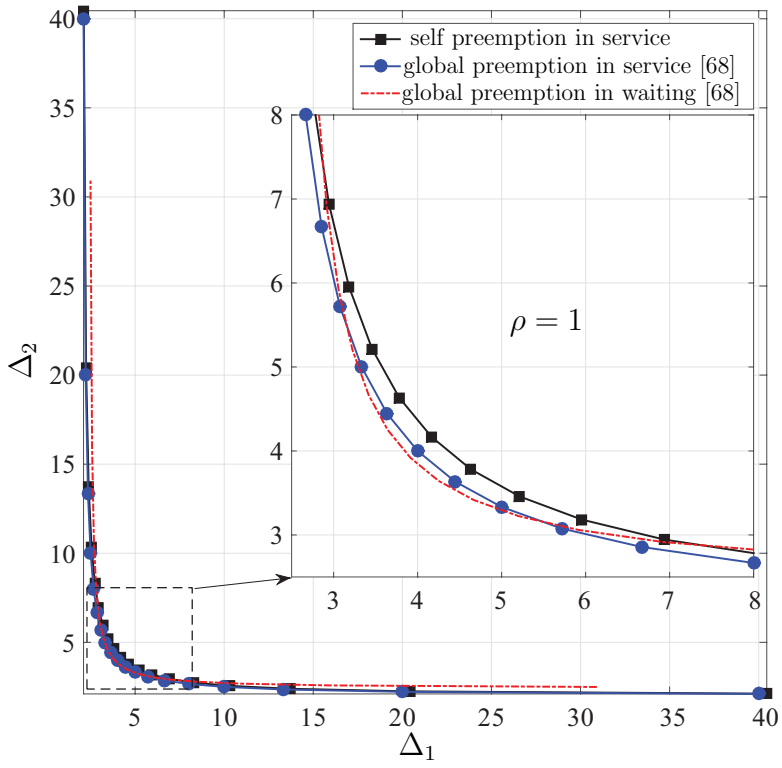

Figure 3.9: Comparison of the achievable age pairs of the proposed scenario with self preemption in service with the global preemption in service and global preemption in waiting cases for $\mu = 1$, $\rho = 1$, and $\epsilon = 0$.

Figure 3.10 considers the same setting except with non-zero packet delivery error probabilities. The results show that the average AoI pairs strictly increase with ϵ. Intuitively, the average number of packets successfully delivered to the destination over any interval decreases as ϵ increases.

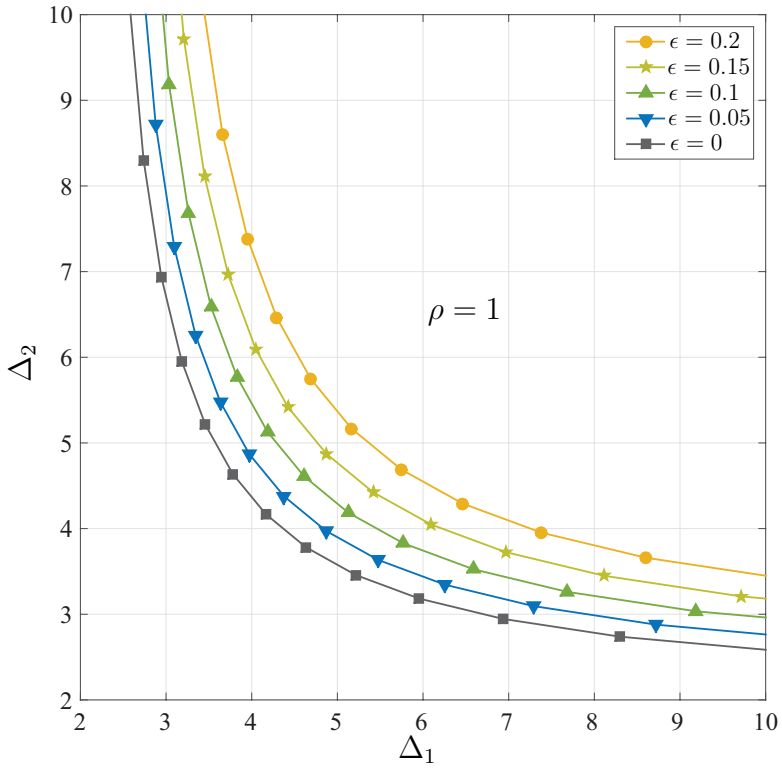

Figure 3.10: Achievable age pairs of the proposed scenario with self preemption in service for $\mu = 1$, $\rho = 1$, and $\epsilon \in \{0, 0.05, 0.1, 0.15, 0.2\}$.

We next consider a system with symmetric loading, i.e., $\rho_i = \frac{\rho}{N}$ for all $i \in \{1, \ldots, N\}$, and no packet delivery errors. Figure 3.11 plots the average AoI versus the total packet arrival rate ρ for $N \in \{2, 10\}$. The results show that average AoI is decreasing in ρ for all three preemption schemes and that global preemption in service uniformly outperforms self preemption in service. For small values of ρ, global preemption in waiting can outperform either preemption in service discipline.

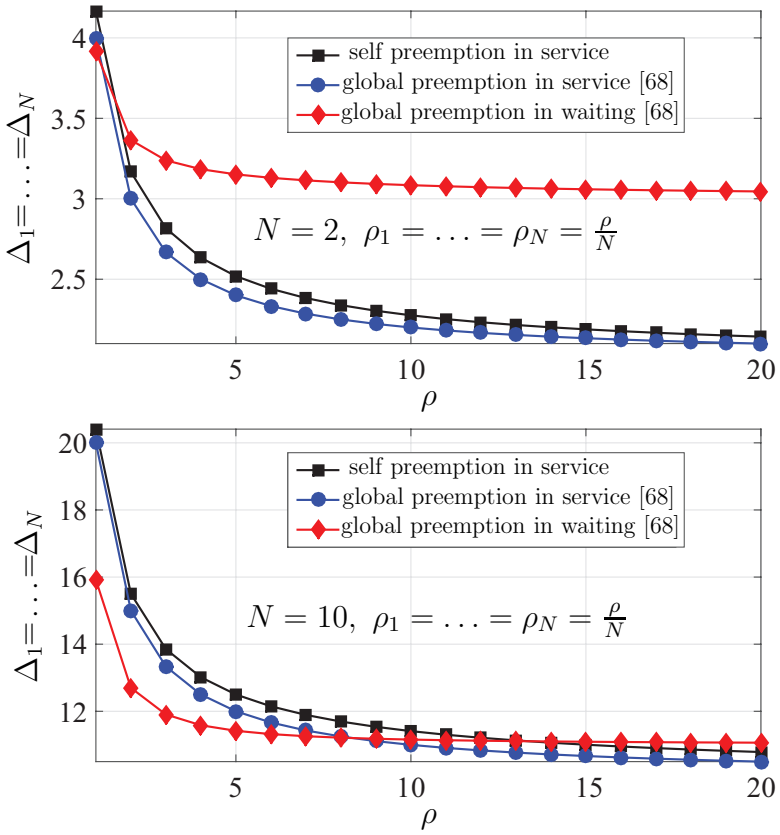

Figure 3.11: Comparison of the achievable average AoI vs ρ where $\rho_1 = \rho_2 = \ldots = \rho_N = \frac{\rho}{N}$ for $\mu = 1$, $\epsilon = 0$, and $N \in \{2, 10\}$.

Finally, we consider a system with asymmetric loading, i.e., $\rho_1 = \frac{\rho}{2}$ and $\rho_i = \frac{\rho}{2(N-1)}$ for $i \in \{2, \ldots, N\}$, and no packet delivery errors. Figure 3.12 represents the achieved average AoI for the three cases versus different total packet arrival rate ρ for $N = 10$. The results show that the average AoI for source $\mathcal{S}_1$ is identical to the symmetric setting with $N = 2$ since source $\mathcal{S}_1$ represents half of the load to the server. The average AoI for the remaining sources is worse than the symmetric setting with $N = 10$ due to each source $i \in \{2, \ldots, 10\}$ receiving smaller fraction of the total load than in the symmetric case.

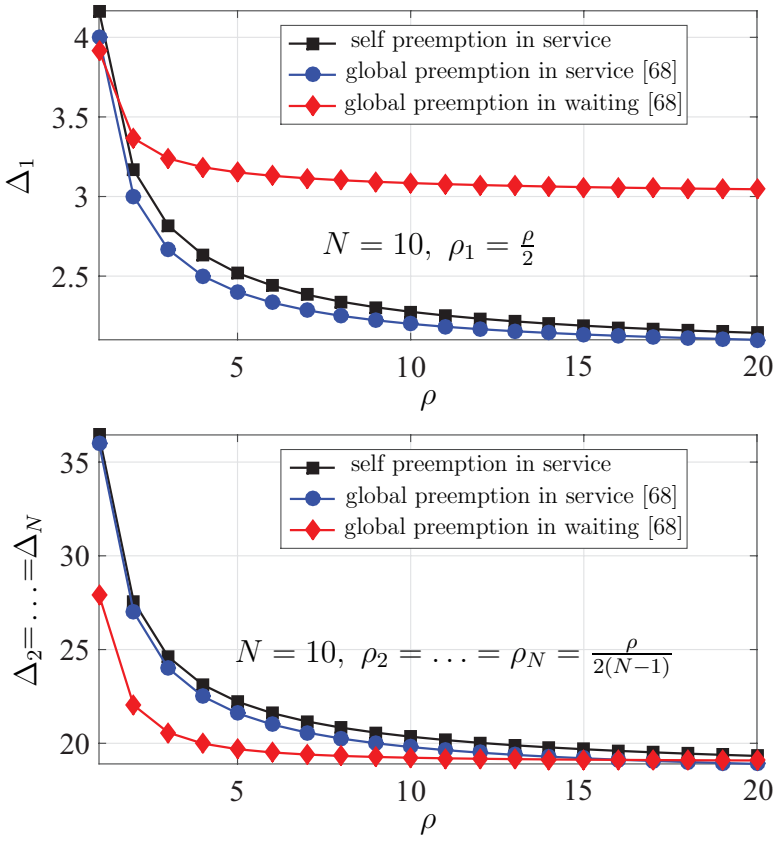

Figure 3.12: Comparison of the achievable average AoI vs ρ where $\rho_1 = \frac{\rho}{2},\ \rho_2 = \ldots = \rho_N = \frac{\rho}{2(N-1)}$ for $\mu = 1$, $\epsilon = 0$, and $N = 10$.

3.5 Conclusion

This chapter studied the AoI problem in a multi-source status update system with transmission errors. Assuming exponential service times, two cases of (i) active sources where they can generate information packets at any point in time and (ii) random packet generation at the sources based on the Poisson process were studied. For the case of active sources, under two scheduling policies, stationary randomized and round-robin, we derived simple closed-form expressions for the average AoI under three different packet management approaches whenever errors occur: no retransmission, retransmission without resampling, and retrans-

mission with resampling. The round-robin policy with retransmission of fresh samples was shown to have the lowest average AoI among the considered cases. It is shown that with equiprobable source selection, the gap between the average AoI of the stationary randomized and round-robin policies under the same packet management approach scales with $\mathcal{O}(N)$. For a general problem where the sources have different priorities, the source selection probabilities were optimized to minimize the weighted sum average AoI for stationary randomized policies. For the Poisson packet arrivals, average AoI expressions were derived assuming that the server allows preemption of the packets in service only by newly-arriving packets from the same source. We showed, somewhat surprisingly, that global preemption in service results in better average AoI than self preemption in service for all sources.

Chapter 4

Age of Information in Energy Harvesting Networks

While there has been considerable work on studying AoI in status update systems without energy constraints, only a handful of recent papers [8, 9, 23–25, 101] have considered AoI in status update systems with energy constraints. This prior work has mainly focused on optimizing the schedule of status updates from the source to minimize the AoI in different scenarios subject to energy constraints. Specifically, [8,9,23,24,101] all assume the source can generate status updates at any time. The goal is to optimize the timing of the status updates from the source to minimize the average age in various settings with energy constraints. Much of this work has focused on the infinite battery regime [8,9,25,101]. Recent work focusing on the finite-battery setting [23,24] assumes always-available source updates and instantaneous service.

In this chapter we study the average AoI for status update systems under energy constraints, taking a somewhat different approach than the previous work in this area. First, we assume that status updates from the source are not always available, but instead arrive at the server at random times. Similarly, energy arrivals and service times are also assumed to be random. Since we do not control the timing of the status updates, we consider a simple, fixed, real-time update policy where new source updates enter service if the server is idle

and has sufficient energy to service the packet. Second, we use tools from stochastic hybrid systems (SHS) [129] to analyze the average age as a function of the arrival/service rates and the battery capacity for four different types of servers [130, 131].

Case A: servers unable to harvest energy while packets are in service, and that block the packets arriving when the server is busy.

Case B: servers able to harvest energy while packets are in service, and that block the packets arriving when the server is busy.

Case C: servers unable to harvest energy while packets are in service, and that accept the packets arriving when the server is busy.

Case D: servers able to harvest energy while packets are in service, and that accept the packets arriving when the server is busy.

Third, our analysis considers both finite and infinite battery regimes without the simplifying assumptions of always-available source updates or instantaneous service. The main contribution is the derivation of closed-form expressions for average age in these settings. Our analysis reveals the effect of each system parameter on the average age: (i) status update arrival rate at the source λ, (ii) energy arrival rate at the server η, (iii) service rate μ, and (iv) server battery capacity B. Simulation results confirm the analysis and numerically demonstrate the performance advantage of servers able to harvest energy while servicing information packets from the source.

Table 4.1 represents a summary of the four possible cases for servers either unable or able to harvest energy while a packet is in service, and also whether preemption of packets in service is allowed or not.

Table 4.1: Different cases with respect to energy harvesting and preemption of the packet in service.

	w/o EH during service	w/ EH during service
w/o preemption	case A	case B
w/ preemption	case C	case D

4.1 System Model

We consider a system with one source node $\mathcal{S}$ and one destination node $\mathcal{D}$ as represented in Fig. 4.1. In the absence of the energy constraints at the server in cases A and B, this system model is identical to the M/M/1/1 case in [12]. In the absence of the energy constraints at the server in cases C and D, this system model is identical to single-source M/M/1 system with last-come-first-served discipline and preemption in service in [68]. The source intends to share information about its *time-varying state* with the destination and generates packets containing status updates at successive times based on a Poisson (point) process with rate λ. The source is assumed to send its packets to the destination through a server with service rate μ. The server is assumed to use energy from a finite capacity battery to service packets from the source. As in [8, 23, 24], we assume that energy units are discrete and normalized so that energy arrivals always correspond to one unit of energy and the service of a packet consumes one unit of energy upon completion of service. The battery is replenished through a random energy harvesting process such that energy units arrive at the server according to a Poisson (point) process with rate η. The server's battery capacity is denoted as B units of energy. The random processes associated with the arrivals of energy units, status update packets, and service times are all assumed to be independent.

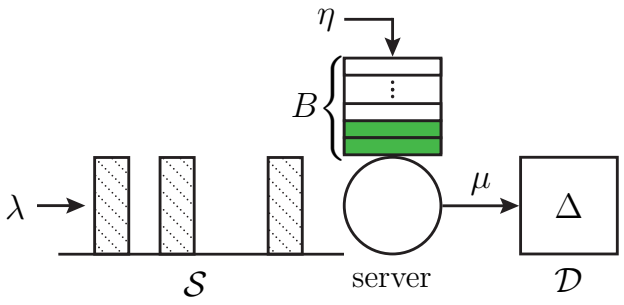

Figure 4.1: The single-source status update system with an energy harvesting server with a battery capacity of B. Status updates arrive at the source with rate λ, energy units arrive at the server with rate η, and packets in service depart the server (complete service) with rate μ.

4.1.1 Energy Harvesting and Preemption Settings

In terms of the server's ability to harvest energy, and also blocking or accepting the arriving packets while a packet is in service, we consider the following four different settings. Observe that in none of the following cases a packet is held in a queue to enter service at a later point.

Case A: Block energy units and information packets while a packet is in service

For this case, packets containing status updates from the source immediately enter service only if (i) the server is idle and (ii) the server's battery is not empty. If either of these conditions are not satisfied when a packet is generated, the packet is ignored by the server and discarded. Energy unit arrivals at the server are stored in the battery only if the battery is not full at the time of arrival and the server is idle. Also, whenever a packet in service is dropped or it completes service, the battery level decreases by one unit.

Case B: Accept energy units and block information packets while a packet is in service

This case is similar to case A, except that energy units that arrive while a packet is in service are stored as long as the battery is not full.

Case C: Block energy units and accept information packets while a packet is in service

This case is similar to case A, except that an arriving information packet while the server is busy and there are at least two energy units in the battery, the packet in service is dropped and the new packet immediately enters service.

Case D: Accept energy units and accept information packets while a packet is in service

This case is similar to case C, except that energy units that arrive while a packet is in service are stored as long as the battery is not full.

For notational convenience, we define the normalized rates

$$\rho \triangleq \frac{\lambda}{\mu}, \tag{4.1a}$$

$$\beta \triangleq \frac{\eta}{\mu}, \tag{4.1b}$$

where ρ represents the *server utilization* [2] and β represents the *energy utilization*, i.e., the rate at which the energy units arrive at the server normalized by the service rate.

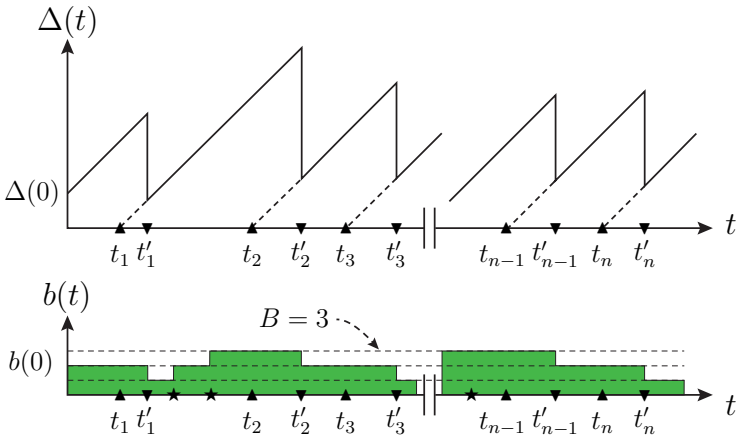

Figure 4.2: An example evolution of the age $\Delta(t)$ and the battery state $b(t)$. Arrival times of the packets that get delivered to the destination are marked by ▲ and departure times of these packets are marked by ▼. We assume at time $t = 0$ the battery of capacity $B = 3$ has $b(0) = 2$ units of energy stored in it and arrival times of the energy units are marked by ★.

4.2 Average Age of Information Analysis

In this section we consider a single-source status update system with energy constraints for the server. We study the four cases A through D that were introduced in section 4.1.1. To simplify the notation, in the following, we refer to the average age expressions of cases X by Δ_{X} for $\mathsf{X} \in \{\mathsf{A}, \mathsf{B}, \mathsf{C}, \mathsf{D}\}$. To compute the average age, we use the SHS approach that was first used in [68] to evaluate the average age in the context of AoI. The SHS method defines a discrete state $q(t) \in \mathcal{Q}$ determining the state of the system with respect to the packets in service and the energy units in the battery. Associated with the SHS method is a continuous state $\mathbf{x}(t)$ that keeps track of the age over time. When a transition $q \to q'$ between two states occurs, the continuous state can have discontinuous jumps $\mathbf{x}(t^-) \to \mathbf{x}'(t) = \mathbf{x}(t^+)$. For more details on the SHS method the reader is referred to [129].

4.2.1 Case A: Server Unable to Harvest Energy While Packet in Service, Preemption of a Packet in Service not Allowed

A Markov chain representation of state $q(t) \in \mathcal{Q}$ of the system is shown in Fig. 4.3. The states are indexed by $q \in \mathcal{Q} = \{0, 1, 2, \ldots, 2B\}$. Each state is also associated with an (i, j) tuple where $i \in \{0, \ldots, B\}$ represents the number of energy units in the server's battery and $j \in \{0, 1\}$ represents the number of packets in service. As seen in Fig. 4.3, when there is a packet in service, i.e., the system is in a positive even indexed state, no energy units are collected. Theorem 11 provides an expression for the average age of the status update system when the server is unable to harvest energy while a packet is in service.

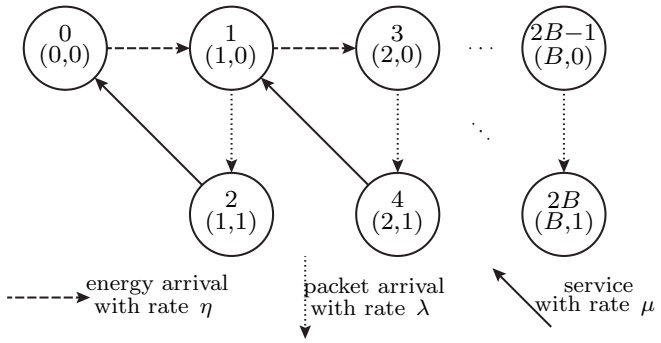

Figure 4.3: The Markov chain representation of the single-source status update system with an energy harvesting server and battery capacity of $B > 1$ units of energy, where the server is unable to harvest energy during service. A dashed line, a dotted line, and a solid line represent the arrival of an energy unit, the arrival of a packet from the source, and departure of the packet in service, respectively. In the (i, j) notation, i and j denote the number of energy units and status updates in the system, respectively. States are indexed by $q \in \mathcal{Q} = \{0, 1, \ldots, 2B\}$.

Theorem 11. *The average age of the status update system where the server is unable to harvest energy while a packet is in service is*

$$\Delta_{\mathsf{A}} = \begin{cases} \dfrac{2B\rho^2 + (2B+2)\rho + B + 2}{\mu[B\rho^2 + (B+1)\rho]} & \beta = \rho \\ \\ \dfrac{(2\rho^2 + 2\rho + 1)\beta^{B+2} - (2\beta^2 + 2\beta + 1)\rho^{B+2}}{\mu[(\rho^2 + \rho)\beta^{B+2} - (\beta^2 + \beta)\rho^{B+2}]} & \beta \neq \rho \end{cases} . \tag{4.2}$$

Table 4.2 represents the exponential rates at which state $q(t^-)$ transitions to $q'(t) = q(t^+)$ in the Markov chain in Fig. 4.3 and the transition map $\phi(q(t^-), \mathbf{x}(t^-)) = (q'(t), \mathbf{x}'(t)) = (q(t^+), \mathbf{x}(t^+))$ for each link ℓ. The result in Theorem 11 is obtained by following similar steps in the proof of Theorem 7.

Note that (4.2) is symmetric with respect to the $\beta = \rho$ line. In other words, for any μ and B, average age is invariant to exchanging β and ρ. This is somewhat surprising since packets and energy are handled differently by the server. Specifically, up to B units of energy can

Table 4.2: Transition rates for the Markov chain in Fig. 4.3, $2 \leq k \leq B$.

ℓ	$q_\ell \to q'_\ell$	$\lambda^{(\ell)}$	$\mathbf{x}\mathbf{A}_\ell$	$\mathbf{A}_\ell$	$\mathbf{v}_{q_\ell}\mathbf{A}_\ell$
0	$0 \to 1$	η	$[x_0, 0]$	$\mathbf{D}_0$	$[v_{00}, 0]$
1	$1 \to 2$	λ	$[x_0, 0]$	$\mathbf{D}_0$	$[v_{10}, 0]$
2	$2 \to 0$	μ	$[x_1, 0]$	$\mathbf{D}_1$	$[v_{21}, 0]$
$3k-3$	$2k-3 \to 2k-1$	η	$[x_0, 0]$	$\mathbf{D}_0$	$[v_{3k-3,0}, 0]$
$3k-2$	$2k-1 \to 2k$	λ	$[x_0, 0]$	$\mathbf{D}_0$	$[v_{3k-2,0}, 0]$
$3k-1$	$2k \to 2k-3$	μ	$[x_1, 0]$	$\mathbf{D}_1$	$[v_{3k-1,1}, 0]$

be stored by the server, whereas only one packet can be in service at any time.

The remainder of this section considers asymptotic results. First, fixing η, μ, and B, when the status update arrival rate becomes large, i.e., $\lambda \to \infty$ or, equivalently, $\rho \to \infty$, we can write

$$\lim_{\rho \to \infty} \Delta_{\mathsf{A}} = \frac{2\beta^2 + 2\beta + 1}{\mu(\beta^2 + \beta)}. \tag{4.3}$$

Second, for fixed λ, μ, and B, when the energy arrival rate becomes large, i.e., $\eta \to \infty$ or, equivalently, $\beta \to \infty$, we can write

$$\lim_{\beta \to \infty} \Delta_{\mathsf{A}} = \frac{2\rho^2 + 2\rho + 1}{\mu(\rho^2 + \rho)}, \tag{4.4}$$

which is identical to the average age expression for the M/M/1/1 case in [12].

Third, for fixed λ, η, and B, when the service rate becomes large, we can write

$$\lim_{\mu \to \infty} \Delta_{\mathsf{A}} = \begin{cases} \dfrac{B+2}{(B+1)\lambda} & \beta = \rho \\ \dfrac{\eta^{B+2} - \lambda^{B+2}}{\lambda\eta^{B+2} - \eta\lambda^{B+2}} & \beta \neq \rho \end{cases}. \tag{4.5}$$

Finally, for fixed λ, η, and μ, when the battery becomes large, we can write

$$\lim_{B \to \infty} \Delta_{\mathsf{A}} = \begin{cases} \dfrac{2\beta^2 + 2\beta + 1}{\mu(\beta^2 + \beta)} & \beta < \rho \\ \dfrac{2\rho^2 + 2\rho + 1}{\mu(\rho^2 + \rho)} & \beta \geq \rho \end{cases}. \tag{4.6}$$

Also, when $\beta \to 0$, $\rho \to 0$, or $\mu \to 0$, we have $\lim_{\beta \to 0} \Delta_{\mathsf{A}} = \infty$, $\lim_{\rho \to 0} \Delta_{\mathsf{A}} = \infty$, and $\lim_{\mu \to 0} \Delta_{\mathsf{A}} = \infty$, respectively.

4.2.2 Case B: Server Able to Harvest Energy While Packet in Service, Preemption of a Packet in Service not Allowed

A Markov chain representation of state $q(t) \in \mathcal{Q}$ is shown in Fig. 4.4. Table 4.3 represents the exponential rates between the states in the Markov chain in Fig. 4.4 and the transition maps for each link ℓ. The difference between this model and the model for case A is that here, while a packet is in service and the battery is not full, an arriving energy unit is harvested. The additional links in Fig. 4.4 cause the SHS analysis to become intractable for general B, however. In this section, we use the SHS method to derive closed-form average age expressions for $B \in \{1, 2\}$ and also derive asymptotic results for all B. The SHS method is also used to efficiently compute numerical results in Section 4.3.

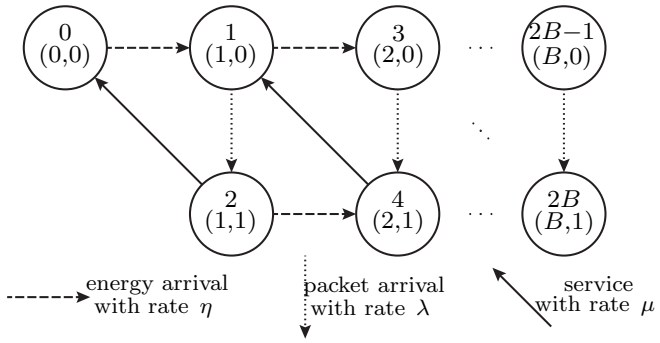

Figure 4.4: The Markov chain representation of the single-source status update system with an energy harvesting server and battery capacity of $B > 1$ units of energy, where the server can harvest energy during service. A dashed line, a dotted line, and a solid line represent the arrival of an energy unit, the arrival of a packet from the source, and departure of the packet in service, respectively. In the (i, j) notation, i and j denote the number of energy units and status updates in the system, respectively. States are indexed by $q \in \mathcal{Q} = \{0, 1, \ldots, 2B\}$.

For $B = 1$, since the Markov chains are identical, the average age is the same for servers

Table 4.3: Transition rates for the Markov chain in Fig. 4.4, $2 \leq k \leq B-1$.

ℓ	$q_\ell \to q'_\ell$	$\lambda^{(\ell)}$	$\mathbf{x}\mathbf{A}_\ell$	$\mathbf{A}_\ell$	$\mathbf{v}_{q_\ell}\mathbf{A}_\ell$
0	$0 \to 1$	η	$[x_0, 0]$	$\mathbf{D}_0$	$[v_{00}, 0]$
1	$1 \to 2$	λ	$[x_0, 0]$	$\mathbf{D}_0$	$[v_{10}, 0]$
2	$1 \to 3$	η	$[x_0, 0]$	$\mathbf{D}_0$	$[v_{10}, 0]$
3	$2 \to 0$	μ	$[x_1, 0]$	$\mathbf{D}_1$	$[v_{21}, 0]$
4	$2 \to 4$	η	$[x_0, x_1]$	$\mathbf{D}_2$	$[v_{20}, v_{21}]$
$4k-3$	$2k-1 \to 2k$	λ	$[x_0, 0]$	$\mathbf{D}_0$	$[v_{2k-1,0}, 0]$
$4k-2$	$2k-1 \to 2k+1$	η	$[x_0, 0]$	$\mathbf{D}_0$	$[v_{2k-1,0}, 0]$
$4k-1$	$2k \to 2k-3$	μ	$[x_1, 0]$	$\mathbf{D}_1$	$[v_{2k,1}, 0]$
$4k$	$2k \to 2k+2$	η	$[x_0, x_1]$	$\mathbf{D}_2$	$[v_{2k,0}, v_{2k,1}]$
$4B-3$	$2B-1 \to 2B$	λ	$[x_0, 0]$	$\mathbf{D}_0$	$[v_{2B-1,0}, 0]$
$4B-2$	$2B \to 2B-3$	μ	$[x_1, 0]$	$\mathbf{D}_1$	$[v_{2B,1}, 0]$

able and unable to harvest energy while a packet is in service. For $B = 2$ the average age can be written as $\Delta_{\mathsf{B}} = X/Y$ where

$$\begin{aligned} X &\triangleq \rho^3(2\beta^4 + 4\beta^3 + 3\beta^2 + 3\beta + 1) + \rho^2(2\beta^5 + 6\beta^4 + 6\beta^3 + 3\beta^2 + \beta) \\ &\quad + \rho(2\beta^3 + \beta^2)(\beta+1)^2 + \beta^3(\beta+1)^2, \\ Y &\triangleq \mu(\beta+1)[\rho^3\beta(\beta^2 + \beta + 1) + \rho^2\beta^2(\beta+1)^2 + \rho(\beta^4 + \beta^3)]. \end{aligned}$$

Note that the symmetry observed in (4.2) is no longer present here. For general B, the average age can be written as

$$\Delta_{\mathsf{B}} = \frac{\rho^{B+1} f_0(\beta) + \rho^B f_1(\beta) + \ldots + \rho f_B(\beta) + f_{B+1}(\beta)}{\mu[\rho^{B+1} g_0(\beta) + \rho^B g_1(\beta) + \ldots + \rho g_B(\beta)]}, \tag{4.7}$$

where $f_i(\beta)$ and $g_j(\beta)$ are polynomial functions of β with degree of at most $2B+1$ for $i \in \{0, 1, \ldots, B+1\}$ and $j \in \{0, 1, \ldots, B\}$.

The form of (4.7) allows us to derive an asymptotic result for the case when the status update arrival rate is large. For fixed η, μ, and B, when $\lambda \to \infty$ or, equivalently, $\rho \to \infty$,

from (4.7) it can be shown that

$$\lim_{\rho\to\infty} \Delta_{\mathsf{B}} = \begin{cases} \dfrac{2\beta^2+2\beta+1}{\mu(\beta^2+\beta)} & B=1 \\ \dfrac{f_0(\beta)}{\mu g_0(\beta)} & B\geq 2 \end{cases}, \tag{4.8}$$

where

$$f_0(\beta) = 2(\beta+1)\sum_{k=0}^{B+1}\beta^k - (\beta^2+\beta+1),$$
$$g_0(\beta) = (\beta+1)\sum_{k=1}^{B+1}\beta^k.$$

For fixed λ, μ, and B, when the energy arrival rate becomes large, i.e., $\eta \to \infty$ or, equivalently, $\beta \to \infty$, the average age of this model is identical to the case when the server is unable to harvest energy while a packet is in service. Intuitively, this follows from the fact that the battery is always either full or one unit less than full when $\beta \to \infty$. In the steady state, the system is always traversing the states at the rightmost end of the Markov chains, i.e., states $2B-3$, $2B-1$, and $2B$, and there is no advantage in being able to harvest energy during service. Similarly, for fixed λ, η, and B, when the service rate becomes large, the average age of this model is identical to the case when the server is unable to harvest energy while a packet is in service. Intuitively, when $\mu \to \infty$, as soon as a packet is presented to the server, it is instantaneously delivered. Hence, the probability of an energy unit arriving during service becomes small and the Markov chains of the two cases become identical, resulting in the same asymptotic average age.

4.2.3 Case C: Server Unable to Harvest Energy While Packet in Service, Preemption of a Packet in Service Allowed

A Markov chain representation of state $q(t) \in \mathcal{Q}$ of the system is shown in Fig. 4.5. The states are indexed by $q \in \mathcal{Q} = \{0, 1, 2, \ldots, 2B\}$. Each state is also associated with an (i, j) tuple where $i \in \{0, \ldots, B\}$ represents the number of energy units in the server's battery and $j \in \{0, 1\}$ represents the number of packets in service. Table 4.4 represents the exponential rates between the states in the Markov chain in Fig. 4.5 and the transition maps for each link ℓ. While the SHS analysis becomes intractable for general B, we use the SHS method to derive closed-form average age expressions for $B \in \{1, 2\}$ and we also derive asymptotic results for all B. The SHS method is also used to efficiently compute numerical results in Section 4.3.

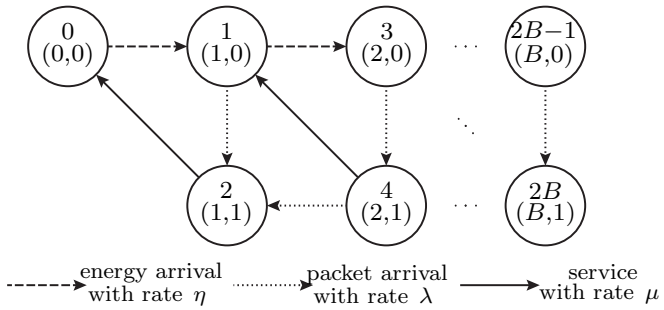

Figure 4.5: The Markov chain representation of the single-source status update system with an energy harvesting server and battery capacity of $B \geq 1$ units of energy, where the server cannot harvest energy during service and preemption of packets in service is allowed. A dashed line, a dotted line and a solid line represent the arrival of an energy unit, the arrival of a packet from the source, and departure of the packet in service, respectively. In the (i, j) notation, i and j denote the number of energy units and status updates in the system, respectively. States are indexed by $q \in \mathcal{Q} = \{0, 1, \ldots, 2B\}$.

For $B = 1$, since the Markov chain is identical to the Markov chains of cases A and B, the average age is the same as Theorem 11. For $B = 2$ the average age can be written as

Table 4.4: Transition rates for the Markov chain in Fig. 4.5, $2 \leq k \leq B$.

ℓ	$q_\ell \to q'_\ell$	$\lambda^{(\ell)}$	$\mathbf{x}\mathbf{A}_\ell$	$\mathbf{A}_\ell$	$\mathbf{v}_{q_\ell}\mathbf{A}_\ell$
0	$0 \to 1$	η	$[x_0, 0]$	$\mathbf{D}_0$	$[v_{00}, 0]$
1	$1 \to 2$	λ	$[x_0, 0]$	$\mathbf{D}_0$	$[v_{10}, 0]$
2	$2 \to 0$	μ	$[x_1, 0]$	$\mathbf{D}_1$	$[v_{21}, 0]$
$3k-3$	$2k-3 \to 2k-1$	η	$[x_0, 0]$	$\mathbf{D}_0$	$[v_{2k-3,0}, 0]$
$3k-2$	$2k-1 \to 2k$	λ	$[x_0, 0]$	$\mathbf{D}_0$	$[v_{2k-1,0}, 0]$
$3k-1$	$2k \to 2k-3$	μ	$[x_1, 0]$	$\mathbf{D}_1$	$[v_{2k,1}, 0]$
$3k$	$2k \to 2k-2$	λ	$[x_0, 0]$	$\mathbf{D}_0$	$[v_{2k,0}, 0]$

$\Delta_{\mathsf{C}} = X/Y$ where

$$\begin{aligned} X &\triangleq \beta^3(2\rho^3 + 3\rho^2 + 3\rho + 1) + \beta^2(2\rho^4 + 6\rho^3 + 4\rho^2 + \rho) \\ &\quad + \beta(2\rho^4 + 4\rho^3 + \rho^2) + \rho^4 + \rho^3, \\ Y &\triangleq \mu[\beta^3(\rho^3 + 2\rho^2 + \rho) + \beta^2(\rho^4 + 3\rho^3 + \rho^2) + \beta(\rho^4 + \rho^3)]. \end{aligned}$$

For general B, the average age can be written as

$$\Delta_{\mathsf{C}} = \frac{\beta^{B+1} f_0(\rho) + \beta^B f_1(\rho) + \ldots + \beta f_B(\rho) + f_{B+1}(\rho)}{\mu[\beta^{B+1} g_0(\rho) + \beta^B g_1(\rho) + \ldots + \beta g_B(\rho)]}, \tag{4.9}$$

where $f_i(\rho)$ and $g_j(\rho)$ are polynomial functions of ρ with degree of at most $2B$ for $i \in \{0, 1, \ldots, B+1\}$ and $j \in \{0, 1, \ldots, B\}$.

The form of (4.9) allows us to derive an asymptotic result for the case when the energy arrival rate is large. For fixed λ, μ, and B, when $\eta \to \infty$ or, equivalently, $\beta \to \infty$, from (4.9) it can be shown that

$$\lim_{\beta \to \infty} \Delta_{\mathsf{C}} = \begin{cases} \dfrac{2\rho^2 + 2\rho + 1}{\mu(\rho^2 + \rho)} & B = 1 \\ \dfrac{f_0(\rho)}{\mu g_0(\rho)} & B \geq 2 \end{cases}, \tag{4.10}$$

where

$$f_0(\rho) = (\rho + 1)^{B+1} + \rho^{B+1}, \quad g_0(\rho) = \rho(\rho + 1)^B.$$

For fixed η, μ, and B, when the status update arrival rate becomes large, i.e., $\lambda \to \infty$ or, equivalently, $\rho \to \infty$, the average age of this case is identical to case A. Intuitively, this follows from the fact that the battery is always either empty or has one energy unit when $\rho \to \infty$. In the steady state, the system is always traversing the states at the leftmost end of the Markov chain, i.e., states 0, 1, and 2, and there is no advantage in being able to preempt the packet in service. Similarly, for fixed λ, η, and B, when the service rate becomes large, the average age of this case is identical to cases A and B where preemption of packets in service is not allowed. Intuitively, when $\mu \to \infty$, as soon as a packet is presented to the server, it is instantaneously delivered. Hence, the probability of a status update arriving during service becomes small and the Markov chain becomes identical to the Markov chains of cases A and B.

4.2.4 Case D: Server Able to Harvest Energy While Packet in Service, Preemption of a Packet in Service Allowed

A Markov chain representation of state $q(t) \in \mathcal{Q}$ of the system is shown in Fig. 4.6. The states are indexed by $q \in \mathcal{Q} = \{0, 1, 2, \ldots, 2B\}$. Theorem 12 provides an expression for the average age of this status update system.

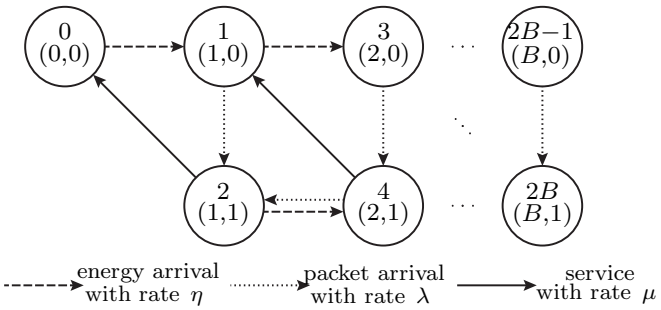

Figure 4.6: The Markov chain representation of the single-source status update system with an energy harvesting server and battery capacity of $B \geq 1$ units of energy, where the server can harvest energy during service and preemption of packets in service is allowed. A dashed line, a dotted line, and a solid line represent the arrival of an energy unit, the arrival of a packet from the source, and departure of the packet in service, respectively. In the (i, j) notation, i and j denote the number of energy units and status updates in the system, respectively. States are indexed by $q \in \mathcal{Q} = \{0, 1, \ldots, 2B\}$.

Theorem 12. *For $B \geq 2$ the average age of the status update system where the server is able to harvest energy while a packet is in service with preemption in service allowed is*

$$\Delta_{\mathsf{D}} = \begin{cases} \dfrac{B\rho^2 + (2B+2)\rho + B + 2}{\mu[B\rho^2 + (B+1)\rho]} & \beta = \rho \\ \dfrac{(\rho+1)^2\beta^{B+2} - (\beta+1)^2\rho^{B+2}}{\mu[(\rho^2+\rho)\beta^{B+2} - (\beta^2+\beta)\rho^{B+2}]} & \beta \neq \rho \end{cases}. \tag{4.11}$$

Table 4.5 represents the exponential rates at which state $q(t^-)$ transitions to $q'(t) = q(t^+)$ in the Markov chain in Fig. 4.6 and the transition map $\phi(q(t^-), \mathbf{x}(t^-)) = (q'(t), \mathbf{x}'(t)) = (q(t^+), \mathbf{x}(t^+))$ for each link ℓ. The result in Theorem 12 is obtained by following similar steps in the proof of Theorem 7.

Similar to (4.2) note that (4.11) is symmetric with respect to the $\beta = \rho$ line. In other words, for any μ and B, average age is invariant to exchanging β and ρ. This is somewhat surprising since packets and energy are handled differently by the server. Specifically, up to

Table 4.5: Transition rates for the Markov chain in Fig. 4.6, $2 \leq k \leq B-1$.

ℓ	$q_\ell \to q'_\ell$	$\lambda^{(\ell)}$	$\mathbf{x}\mathbf{A}_\ell$	$\mathbf{A}_\ell$	$\mathbf{v}_{q_\ell}\mathbf{A}_\ell$
0	$0 \to 1$	η	$[x_0, 0]$	$\mathbf{D}_0$	$[v_{00}, 0]$
1	$1 \to 2$	λ	$[x_0, 0]$	$\mathbf{D}_0$	$[v_{10}, 0]$
2	$1 \to 3$	η	$[x_0, 0]$	$\mathbf{D}_0$	$[v_{10}, 0]$
3	$2 \to 0$	μ	$[x_1, 0]$	$\mathbf{D}_1$	$[v_{21}, 0]$
4	$2 \to 4$	η	$[x_0, x_1]$	$\mathbf{D}_2$	$[v_{20}, v_{21}]$
$5k-5$	$2k-1 \to 2k$	λ	$[x_0, 0]$	$\mathbf{D}_0$	$[v_{2k-1,0}, 0]$
$5k-4$	$2k-1 \to 2k+1$	η	$[x_0, 0]$	$\mathbf{D}_0$	$[v_{2k-1,0}, 0]$
$5k-3$	$2k \to 2k-3$	μ	$[x_1, 0]$	$\mathbf{D}_1$	$[v_{2k,1}, 0]$
$5k-2$	$2k \to 2k-2$	λ	$[x_0, 0]$	$\mathbf{D}_0$	$[v_{2k,0}, 0]$
$5k-1$	$2k \to 2k+2$	η	$[x_0, x_1]$	$\mathbf{D}_2$	$[v_{2k,0}, v_{2k,1}]$
$5B-5$	$2B-1 \to 2B$	λ	$[x_0, 0]$	$\mathbf{D}_0$	$[v_{2B-1,0}, 0]$
$5B-4$	$2B \to 2B-3$	μ	$[x_1, 0]$	$\mathbf{D}_1$	$[v_{2B,1}, 0]$
$5B-3$	$2B \to 2B-2$	λ	$[x_0, 0]$	$\mathbf{D}_0$	$[v_{2B,0}, 0]$

B units of energy can be stored by the server, whereas only one packet can be in service at any time. Comparing the average age expressions for cases A and D, we can write

$$\Delta_{\mathsf{A}} - \Delta_{\mathsf{D}} = \begin{cases} 0 & B = 1 \\ \dfrac{\rho^2\beta^2 \displaystyle\sum_{k=0}^{B-1} \beta^k \rho^{B-k-1}}{\mu\rho\beta \left[(\rho+1) \displaystyle\sum_{k=1}^{B} \beta^k \rho^{B-k} + \rho^B \right]} & B \geq 2 \end{cases},$$

which shows $\Delta_{\mathsf{A}} - \Delta_{\mathsf{D}} \geq 0$ regardless of the system parameters ρ, β, μ, and B. The remainder of this section considers asymptotic results. First, fixing η, μ, and B, when the status update arrival rate becomes large, i.e., $\lambda \to \infty$ (or $\rho \to \infty$), we can write

$$\lim_{\rho \to \infty} \Delta_{\mathsf{D}} = \frac{1}{\mu}\left(1 + \frac{1}{\beta}\right). \tag{4.12}$$

Second, for fixed λ, μ, and B, when the energy arrival rate becomes large, i.e., $\eta \to \infty$ (or $\beta \to \infty$), we can write

$$\lim_{\beta \to \infty} \Delta_{\mathsf{D}} = \frac{1}{\mu}\left(1 + \frac{1}{\rho}\right), \tag{4.13}$$

which is identical to the average age expression of the single-source M/M/1 status update system with last-come-first-served discipline and preemption in service in [68], and also the average age of the best-effort updating policy in [8].

Third, for fixed λ, η, and B, when the service rate becomes large, we can write

$$\lim_{\mu\to\infty} \Delta_{\mathsf{D}} = \begin{cases} \dfrac{B+2}{(B+1)\lambda} & \beta = \rho \\ \dfrac{\eta^{B+2} - \lambda^{B+2}}{\lambda\eta^{B+2} - \eta\lambda^{B+2}} & \beta \neq \rho. \end{cases} \tag{4.14}$$

Observe that when $\mu \to \infty$, all of the four cases A, B, C, and D achieve the same average age.

Finally, for fixed λ, η, and μ, when the battery becomes large, we can write

$$\lim_{B\to\infty} \Delta_{\mathsf{D}} = \begin{cases} \dfrac{1}{\mu}\left(1 + \dfrac{1}{\beta}\right) & \beta < \rho \\ \dfrac{1}{\mu}\left(1 + \dfrac{1}{\rho}\right) & \beta \geq \rho. \end{cases} \tag{4.15}$$

Also, when $\beta \to 0$, $\rho \to 0$, or $\mu \to 0$, we have $\lim_{\beta\to 0} \Delta_{\mathsf{D}} = \infty$, $\lim_{\rho\to 0} \Delta_{\mathsf{D}} = \infty$, and $\lim_{\mu\to 0} \Delta_{\mathsf{D}} = \infty$, respectively.

4.3 Numerical Results

This section provides numerical examples to quantify the average age as a function of the system parameters ρ, β, μ and B. Figures 4.7 and 4.8 represent the contour plots of the average ages Δ_{A} and Δ_{B}, respectively as a function of the system parameters $0.1 \leq \beta \leq 10$, $0.1 \leq \rho \leq 10$, $\mu = 1$ and $B = \{1, 5, 10, 20\}$. From Fig. 4.7, first, the results confirm the symmetric behavior of Δ_{A} with respect to ρ and β as discussed previously. Second, observe that $\lim_{\substack{\rho\to\infty \\ \beta\to\infty}} \Delta_{\mathsf{A}} = 2/\mu = 2$, which agrees with (4.3)–(4.4). Note that the average age in the figures is equivalently a function of η and λ since $\eta = \beta$ and $\lambda = \rho$ for $\mu = 1$.

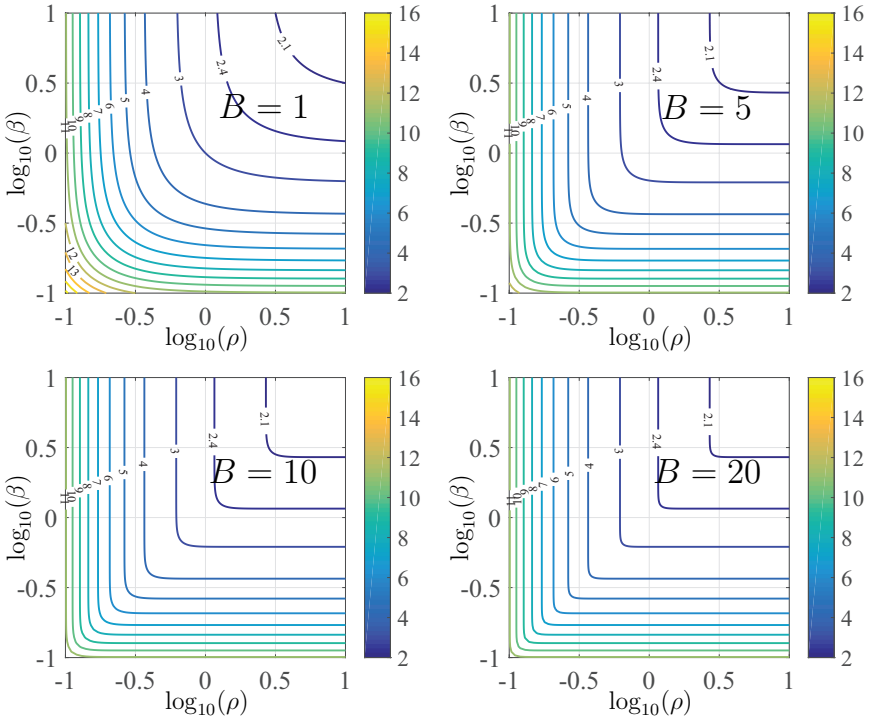

Figure 4.7: Contours of the average age of case A where the server cannot harvest energy during service for $0.1 \leq \beta \leq 10$, $0.1 \leq \rho \leq 10$, $\mu = 1$, and $B = \{1, 5, 10, 20\}$.

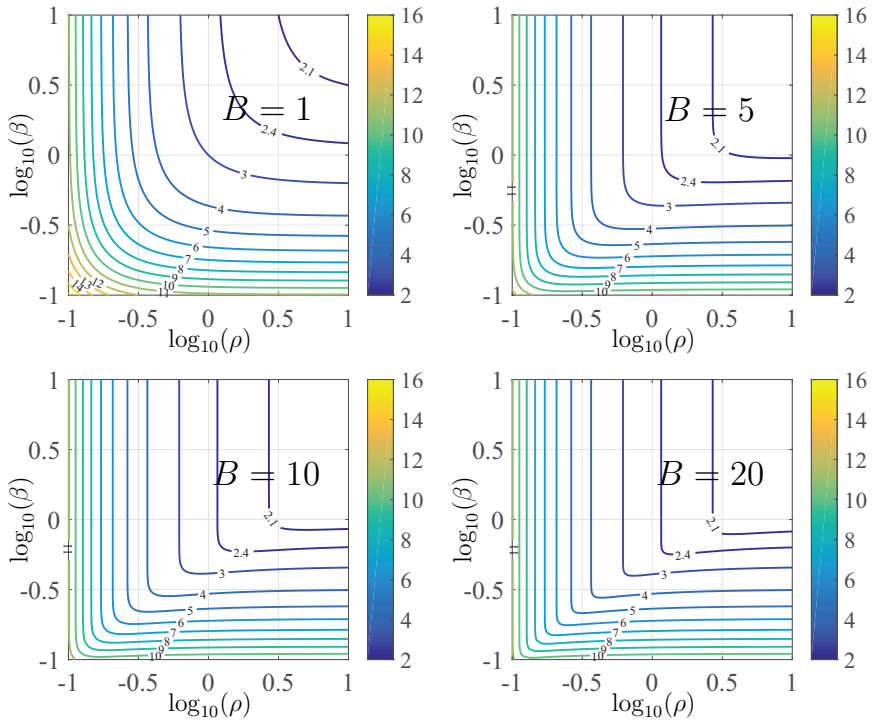

Figure 4.8: Contours of the average age of case B where the server can harvest energy during service for $0.1 \leq \beta \leq 10$, $0.1 \leq \rho \leq 10$, $\mu = 1$, and $B = \{1, 5, 10, 20\}$.

Figure 4.9 represents the ratio of the average age in case B and case A for $B = \{2, 5, 10, 20\}$ and shows the performance improvement in terms of average AoI reduction when the server is able to harvest energy while servicing packets. The results show that as β increases, both cases have the same average age, but when β decreases case B leads to a considerably better average age. When the server can harvest energy during service, as long as the battery is not full, no energy unit is wasted. Consequently we expect case B to have a better average age performance than case A. Since $\Delta_{\mathsf{B}}/\Delta_{\mathsf{A}} \leq 1$ regardless of any of the system parameters, case A provides an upper bound on the average age of case B.

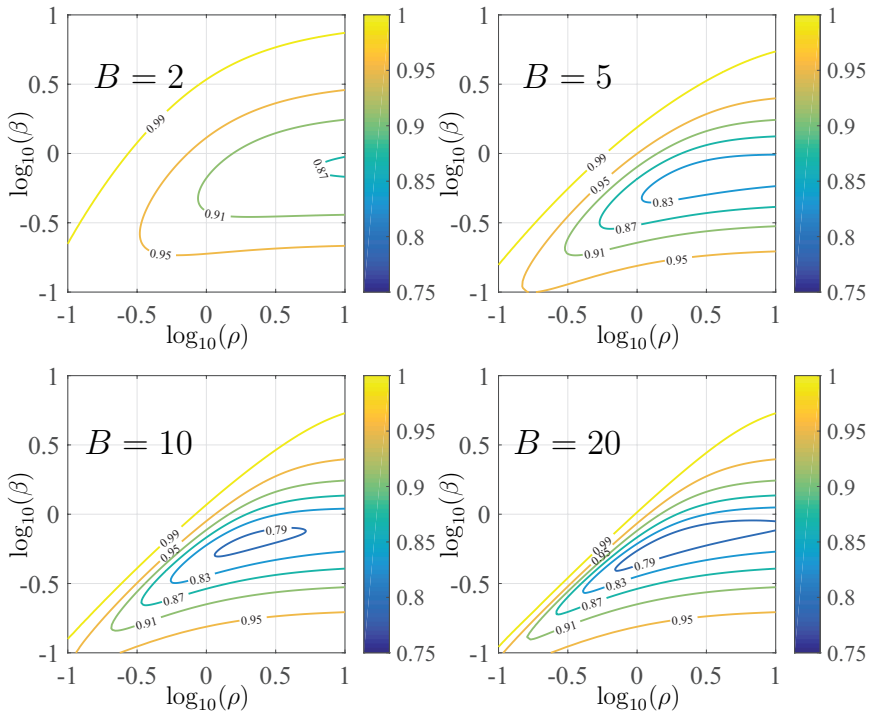

Figure 4.9: Contours of the ratio of the average age of cases B and A, i.e., $\Delta_{\mathsf{B}}/\Delta_{\mathsf{A}}$, for $0.1 \leq \beta \leq 10$, $0.1 \leq \rho \leq 10$, $\mu = 1$, and $B = \{2, 5, 10, 20\}$.

Figure 4.10 represents the average age of cases A and B for $\mu = 1$, $\beta = 0.1$, and $B = \{5, 20\}$. The results show that for case A, Δ_{A} is monotonically decreasing with ρ and independent of B. But, for case B, as ρ and B increase, there exists an optimal choice of ρ that minimizes Δ_{B}. This result is similar to a result in [54] where an optimal server utilization rate was shown to minimize the average age. Also, as B increases the average age of the same case decreases monotonically. This is because in general more energy units are stored in the battery and the number of packets that are dropped because of an empty battery is reduced, resulting in more status updates being delivered to the destination, which reduces the average age. Observe that when ρ is comparable to β, $\beta < \rho \ll 1$, the servers ability to harvest energy while a packet is in service for case B leads to a considerable advantage over case A.

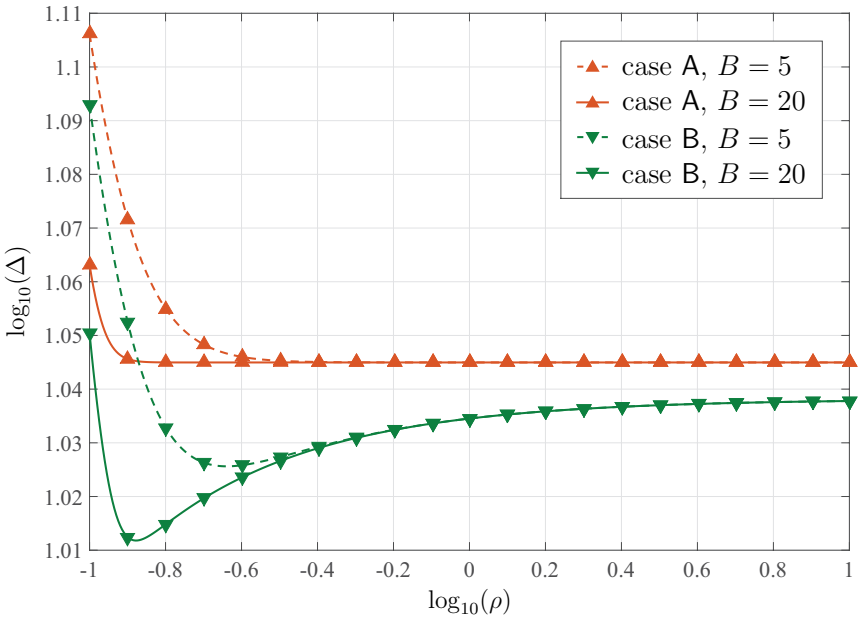

Figure 4.10: The average age of cases A and B for $0.1 \leq \rho \leq 10$, $\beta = 0.1$, $\mu = 1$, and $B = \{5, 20\}$.

Figure 4.11 plots the ratio $\Delta_{\mathsf{C}}/\Delta_{\mathsf{A}}$, where the server is unable to harvest energy while a packet is in service, and the ratio $\Delta_{\mathsf{D}}/\Delta_{\mathsf{B}}$, where the server is able to harvest energy while a packet is in service. Regions shaded in green and yellow correspond to improved or degraded performance, respectively, with preemption.

In the yellow shaded areas, preemption results in degraded performance. Intuitively, the yellow shaded area corresponds to an "energy starved" operating regime, where energy arrivals are relatively infrequent with respect to the rate of information arrivals and the service rate. Preemption of packets in service leads to faster depletion of the battery which increases the probability of new status updates being dropped because of an empty battery. This in turn leads to less frequent delivery of status updates to the destination and degraded performance.

In the green shaded areas, preemption improves performance. Intuitively, the green shaded area corresponds to an "energy rich" operating regime. In this regime, the probability of the battery becoming depleted is small and the effect of the energy constraint is

less significant. Similar to [54], which analyzed the average age of a server that allowed preemption without energy constraints, we see that the performance achieved by preemption is better than the average age achieved by a server that does not allow preemption of packets in service in the "energy rich" regime. We also observe that the average age reduction due to preemption becomes more considerable when the server is able to harvest energy while a packet is in service compared to cases where the server is unable to harvest energy while a packet is in service. Intuitively, this is because the server's ability to harvest energy while a packet is in service helps avoid wasting the arriving energy units as long as the battery in not full.

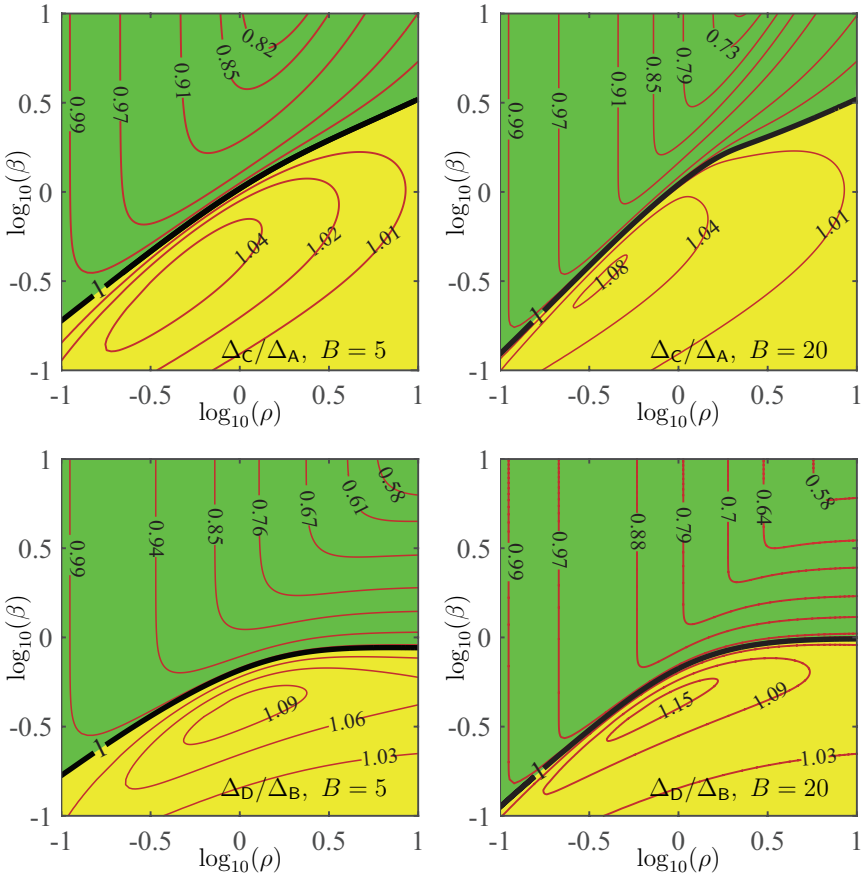

Figure 4.11: Contours of the ratio of the average age of cases with or without preemption, for $0.1 \leq \beta \leq 10$, $0.1 \leq \rho \leq 10$, $\mu = 1$, and $B = \{5, 20\}$. The green and yellow regions represent the areas where the ratio is less than one, and the ratio is greater than one, respectively.

4.4 Conclusion

In this chapter we studied the AoI problem in a single-source status update system with an energy harvesting server with finite battery capacity. Four cases based on the server's ability to harvest energy while the server is busy and also allowing preemption of the packets in service were considered. Expressions for the average AoI were derived as a function of the system parameters. Asymptotic average age expressions were also derived for several cases. Numerical results were provided to quantify the average age in terms of the system parameters and numerically demonstrate the performance advantage of servers with simultaneous service and energy harvesting, and to illustrate the operating regimes where preemption of packets in service achieves a lower average age compared to a server that does not allow preemption of packets in service. The results showed that in general preemption of the packets in service is not the best packet management policy all the times, and the best policy depends on the system parameters and the servers ability to harvest energy while a packet is in service.

Chapter 5

Age of Channel State Information in Wireless Networks

In wireless networks, knowledge of channel state information (CSI) by the nodes in the network can often be used to improve one or more performance characteristics of the network, e.g., increase data rates, reduce interference, and/or improve energy efficiency. In point-to-point links, knowledge of the channel state information at the transmitter (CSIT) can improve performance through techniques such as Tomlinson-Harashima precoding [132], waterfilling [133, 134], and/or adaptive transmission over fading channels [135]. In multiple-input multiple-output (MIMO) channels, CSIT allows for coherent transmission techniques like beamforming and can also provide multiplexing gains [136–138]. CSIT can also be used in MIMO systems for interference mitigation, e.g., zero-forcing beamforming [138], nullforming [139], and interference alignment [140].

While the value of CSIT is well-established in the literature, there are also many examples of systems where the nodes in the wireless network benefit from having a more comprehensive view of the channel states in the network beyond just CSIT. For example, optimum power allocation [141–143], zero-forcing beamforming [144], nullforming [145], and interference alignment [146], and scheduling in multihop wireless networks generally require global CSI [147, 148].

Global knowledge of CSI also permits nodes to opportunistically determine an appropriate network structure and communication strategy for efficient operation under the current channel state. Furthermore, availability of global CSI allows nodes to change roles over time, perhaps participating in a coherent transmit cluster at one point in time, then serving as a relay at another point in time, with the current role dynamically determined by the evolving global channel state.

This chapter derives lower bounds and develop schedules for estimation and dissemination of global CSI in fully-connected wireless networks with reciprocal channels. By "global CSI", we mean that each node maintains its own table of estimates for *all* $L = \frac{N(N-1)}{2}$ reciprocal channels in the network, not just the $N-1$ channels to which a given node is directly connected. Nodes obtain estimates of channels to which they are not directly connected via CSI "dissemination". Specifically, nodes disseminate CSI by embedding one or more CSI estimate(s) in each transmission so other nodes can learn the states of channels to which they are not directly connected. Over time, each node in the network directly estimates the $N-1$ channels to which it is directly connected and "indirectly estimates" the remaining $L-N+1$ channels in the network by collecting disseminated CSI. While some recent studies have considered the problem of estimating and tracking so-called "global CSI", e.g., [149–151], the notion of global CSI in these papers is not the same as the notion of global CSI considered here. In that prior work, the roles of the nodes are fixed and the focus is on providing estimates of all transmit-receive channels to all transmit nodes in the network, i.e., global *CSIT*. We emphasize that our notion of global CSI does not presume roles for the nodes in the network and allows nodes to dynamically adapt their roles by estimating and tracking *all* of the L reciprocal channels in the network.

Nevertheless, there is a gap in solidly understanding the overhead and tradeoffs involved in tracking global CSI throughout a network, particularly in cases where N is small and global CSI may be feasible.

The focus of this chapter is on wireless networks with reciprocal channels. In this setting,

there are two sources of error in the global CSI at each node in the network: (i) channel estimation error, typically governed by fundamental bounds such as the Cramer-Rao lower bound (CRLB) and (ii) error caused by time-variation and staleness, i.e., the delay from when the time-varying channel was estimated and the current time n. In this chapter, we assume the type (ii) error is dominant. The value of stale (sometimes called delayed or outdated) CSIT has been considered only recently in [152–154]. While it was shown that even completely stale CSIT can still be useful in certain scenarios [152], there is generally a loss of performance with respect to perfect CSI knowledge as CSI becomes more stale [154]. Moreover, the focus of these studies has been on maximizing degrees of freedom in conventional MIMO channels with delayed CSIT, and not on cooperative, distributed, or multihop scenarios where a more comprehensive knowledge of CSI is necessary. In these types of scenarios, performance can be highly sensitive to the accuracy of the CSI, which is directly related to its age [143, 155].

In this chapter, first, we develop a new and general framework for quantifying the age of global CSI in packetized fully-connected wireless networks. This framework accounts for the number of channel states disseminated in each packet as well as the additional data and overhead in each packet which contribute to the age of the CSI. We then develop lower bounds on the peak and average AoI metrics [156–158]. Subsequently, we develop a greedy CSI dissemination schedule based on minimizing the instantaneous average age of CSI parameters. Next, we derive a lower bound on the average age of random CSI dissemination schedules [159].

5.1 System Model

Consider a fully-connected network with N single-antenna nodes communicating over time-varying reciprocal channels. The complex channel gain between two nodes i and j at time n is denoted by $h_{i,j}[n]$ and assuming reciprocity, we have $h_{i,j}[n] = h_{j,i}[n]$. The network's

topology is described by a complete graph with $N \geq 3$ vertices and $L = (N^2 - N)/2$ edges, representing all of the N nodes and L reciprocal channels in the network, respectively. Each node in the network maintains its own local table of estimates of these L complex channel gains. During each time slot, one node transmits a packet of length P words which includes $M \in \{1, 2, 3, \ldots, N-1\}$ *disseminated* CSI estimates.

Figure 5.1: Example fixed-length packet showing overhead, data, and CSI dissemination. The CSI dissemination consists of M channel estimates and each channel estimate (including its associated timestamp) has a length of one word. The data and overhead consists of D words. The total packet length is $P = D + M$ words.

Fig. 5.1 represents the general structure of a packet exchanged among the nodes in the network. All packets are assumed to be received reliably. Each fixed-length packet contains overhead, data, and M disseminated CSI estimates. Since node k cannot estimate a channel to which it is not directly connected, i.e., the channel between nodes i and j for $i \neq j \neq k$, it uses the disseminated CSI information embedded in the transmitted packets by either nodes i or j, to obtain an estimate of the (i, j) channel. Assuming a length of D words for the data plus overhead, each packet has a length of $P = D + M$ words. Although Fig. 5.1 shows a particular packet structure, the position of the overhead, data, and disseminated CSI within any packet does not affect our results.

Each node that receives the transmitted packet by node i does two things:

1. It directly estimates the channel $h_{i,j}[n]$, which can be obtained via a known training sequence in the packet, e.g., a known preamble embedded in the overhead, and/or through blind channel estimation techniques.
2. It extracts the disseminated CSI and uses it to update any "staler" CSI in its local table.

Note that every disseminated CSI also includes a timestamp of when it was obtained. This

allows each node to determine if the disseminated CSI is fresher than any CSI in its table.

We denote the k^{th} node's estimate of the (i,j) channel measured directly from a packet transmitted at time n as $\hat{h}_{i,j}^{(k)}[n]$. Since each node $i \in \{1,\dots,N\}$ maintains its own table of L global CSI estimates, the total number of CSI estimates in the network is NL.

As an explicit example of CSI estimation and dissemination, suppose at time $n=1$ node 6 directly estimates the $(5,6)$ channel and updates its local CSI table with $\hat{h}_{5,6}^{(6)}[1]$. Then, at time $n=2$ suppose node 6 disseminates this estimate to other nodes in the network. In the process of this dissemination, each node $j \neq 6$ updates its *direct* CSI estimate, i.e., stores $\hat{h}_{6,j}^{(j)}[2]$ in its local CSI table, and also checks its local CSI table to determine if its estimate of the $(5,6)$ channel has a timestamp prior to the timestamp of the disseminated $(5,6)$ estimate from node 6. Each node j with a staler $(5,6)$ estimate stores the indirectly obtained CSI estimate $\hat{h}_{5,6}^{(j)}[1]$ in its local CSI table.

Similar to Chapter 2 here we define a schedule alongside the peak and average age metrics. A schedule represents a sequence of transmitting nodes and the "channel indices" they disseminate.

Definition 7 (Age)**.** *The age $\Delta_{i,j}^{(k)}[n]$ of the CSI estimate $\hat{h}_{i,j}^{(k)}[n']$ with timestamp n' at time $n \geq n'$ is $(n-n')P$ words.*

Directly estimated CSI has a age of zero in the timeslot in which it is estimated. All indirectly estimated CSI has a minimum age of P words. If a given CSI estimate is not updated in a timeslot, either due to direct estimation or dissemination, then its age increases by P words in that timeslot.

Using any ordering of the individual age terms $\Delta_{i,j}^{(k)}[n]$, we can denote a global age vector $\boldsymbol{\Delta}[n] \in \mathbb{Z}^{NL}$. It is not difficult to see that, given a transmitting node and disseminated channel indices, the age vector obeys a simple time-varying linear update equation

$$\boldsymbol{\Delta}[n+1] = \boldsymbol{A}[n]\left(\boldsymbol{\Delta}[n] + \mathbf{1}P\right) \tag{5.1}$$

where $\boldsymbol{A}[n] \in \mathbb{Z}^{NL \times NL}$ is a time-varying update matrix with entries equal to either zero or one. As an explicit example, and omitting the time index for notational convenience, we can define the global age vector in an $N = 3$ node network as

$$\boldsymbol{\Delta} = \left[\Delta_{1,2}^{(1)}, \Delta_{1,3}^{(1)}, \Delta_{2,3}^{(1)}, \Delta_{1,2}^{(2)}, \Delta_{1,3}^{(2)}, \Delta_{2,3}^{(2)}, \Delta_{1,2}^{(3)}, \Delta_{1,3}^{(3)}, \Delta_{2,3}^{(3)}\right]^\top.$$

Suppose node 1 disseminates the $(1,3)$ link at time n. Then

$$\boldsymbol{A}[n] = \begin{bmatrix} 1 & 0 & 0 & 0 & 0 & 0 & 0 & 0 & 0 \\ 0 & 1 & 0 & 0 & 0 & 0 & 0 & 0 & 0 \\ 0 & 0 & 1 & 0 & 0 & 0 & 0 & 0 & 0 \\ 0 & 0 & 0 & 0 & 0 & 0 & 0 & 0 & 0 \\ 0 & 1 & 0 & 0 & 0 & 0 & 0 & 0 & 0 \\ 0 & 0 & 0 & 0 & 0 & 1 & 0 & 0 & 0 \\ 0 & 0 & 0 & 0 & 0 & 0 & 1 & 0 & 0 \\ 0 & 0 & 0 & 0 & 0 & 0 & 0 & 0 & 0 \\ 0 & 0 & 0 & 0 & 0 & 0 & 0 & 0 & 1 \end{bmatrix} = \begin{bmatrix} \boldsymbol{e}_1^\top \\ \boldsymbol{e}_2^\top \\ \boldsymbol{e}_3^\top \\ \boldsymbol{0}^\top \\ \boldsymbol{e}_2^\top \\ \boldsymbol{e}_6^\top \\ \boldsymbol{e}_7^\top \\ \boldsymbol{0}^\top \\ \boldsymbol{e}_9^\top \end{bmatrix}$$

where $\boldsymbol{e}_m$ is the m^{th} standard unit vector. Rows 1-3 of $\boldsymbol{A}[n]$ reflect the fact that node 1 was transmitting and, as such, no updates are made to its local CSI table (the age of all CSI at node 1 increases by P). Row 4, being all zeros, reflects the direct estimation of the $(1,2)$ link at node 2. Row 5 reflects the indirect estimation of the $(1,3)$ link at node 2 from the CSI disseminated by node 1, i.e., node 2 now has the same estimate and the same age of the $(1,3)$ link as node 1. The remaining rows are similar, but it is worth mentioning row 8. In this case, node 3 receives the disseminated CSI of the $(1,3)$ link from node 1 but also directly estimates the $(1,3)$ link. Since the direct estimate is fresher than any disseminated estimate, node 3 ignores the disseminated CSI. This is reflected in the all-zero row 8. Some basic properties of $\boldsymbol{A}[n]$ will be listed in Section 5.1.2.

5.1.1 Age of Information Metrics

In this section, we define the peak and average age statistics used in the remainder of the chapter.

Definition 8 (Peak age at time n)**.** *The peak age at time n is defined as*

$$\Delta_{\text{peak}}[n] = \max \boldsymbol{\Delta}[n].$$

Definition 9 (Average age at time n)**.** *The average age at time n is defined as*

$$\Delta_{\text{avg}}[n] = \frac{1}{NL}\mathbf{1}^{\top}\boldsymbol{\Delta}[n].$$

Definition 10 (Peak age)**.** *The peak age Δ_{peak} is defined as*

$$\Delta_{\text{peak}} = \max_{n \geq \bar{n}} \Delta_{\text{peak}}[n]$$

for $\bar{n}$ sufficiently large such that the effect of any initial age state can be ignored.

Definition 11 (Average age)**.** *The average age Δ_{avg} is defined as*

$$\Delta_{\text{avg}} = \mathrm{E}\left[\Delta_{\text{avg}}[n]\right]$$

where the expectation is over $n \geq \bar{n}$ for $\bar{n}$ sufficiently large such that the effect of any initial age state can be ignored.

5.1.2 Basic properties of $\mathbf{A}[n]$

From (5.1) and the description of how each node updates its local CSI table through direct estimation and disseminated CSI estimates, observe that $\boldsymbol{A}[n]$ has the following properties:

- Each row of $\boldsymbol{A}[n]$ is either equal to zero or has a single non-zero entry equal to one.

- Row m of $\boldsymbol{A}[n]$ is equal to zero if the corresponding CSI estimate is directly estimated in timelot n.
- Since $N-1$ CSI estimates are directly estimated in each timeslot, exactly $N-1$ rows of $\boldsymbol{A}[n]$ are zero for all n.
- Row m of $\boldsymbol{A}[n]$ is equal to $\boldsymbol{e}_m^\top$, i.e., the transposed m^{th} standard unit vector, if the corresponding CSI estimate is not updated.
- Row m of $\boldsymbol{A}[n]$ is equal to $\boldsymbol{e}_\ell^\top$, i.e., the transposed ℓ^{th} standard unit vector, if the corresponding CSI estimate is updated to match the disseminated CSI estimate corresponding to row ℓ. Since the M disseminated CSI are received by $N-1$ nodes, it is easy to see that there are at most $(N-1)M$ such rows in $\boldsymbol{A}[n]$. In fact, due to the fact that some disseminated CSI is also directly estimated, as was illustrated in the $N=3$ example, there will be at most $(N-1)M-M$ such rows in $\boldsymbol{A}[n]$.

This last basic property allows us to characterize the dimension of the nullspace of $\boldsymbol{A}[n]$. Observe that the dimension of the nullspace of $\boldsymbol{A}[n]$, i.e., $\text{nullity}(\boldsymbol{A}[n])$, satisfies

$$N-1 \leq \text{nullity}(\boldsymbol{A}[n]) \leq N-1+(N-1)M-M. \tag{5.2}$$

The $N-1$ term on both sides corresponds to the $N-1$ rows of $\boldsymbol{A}[n]$ that must be zero due to direct estimation at all nodes except the transmitting node. On the right hand side, the $(N-1)M-M=(N-2)M$ term corresponds to the "useful" disseminated CSI, i.e., each node except the transmitting node receives M disseminated CSI estimates and a total of M of these are discarded due to direct estimation. The upper bound in (5.2) is tight, as seen in the $N=3$ node example above, and is the key result that facilitates the development of the lower bounds on the peak and average age in the following section.

5.2 Age of Global CSI Dissemination in Fully-Connected Networks

In this section we derive lower bounds on the peak and average age metrics for global CSI dissemination in fully-connected networks. Also, we develop algorithms that generate schedules for CSI dissemination throughout the network.

5.2.1 Lower Bounds on Peak and Average Age for General $M \in \{1, 2, 3, \ldots, N-1\}$ in Fully-Connected Networks

In this section we derive lower bounds on the peak and average age metrics for global CSI dissemination in fully-connected networks. These lower bounds hold for any schedule, whether deterministic or random, and any fixed $M \in \{1, 2, 3, \ldots, N-1\}$. Since the network is fully-connected, each node has at most $N-1$ useful directly estimated CSI parameters to disseminate in its packet. As shown by simulations in section 5.3, the achievable peak and average age are not necessarily minimized by either of the extreme choices $M \in \{1, N-1\}$ CSI estimates disseminated in each packet, and the best choice of M depends on the number of nodes N and the amount of data plus overhead D in each packet. Intuitively, as M increases, more CSI is disseminated in each packet and each node updates more entries in its local CSI table. This improves the age metrics. On the other hand, the packet length P increases with M, which has a negative impact on age. Thus, there are two competing forces in choosing the optimal amount of CSI to disseminate per packet.

From (5.1) and given an initial state at time n_0, we can write

$$\boldsymbol{\Delta}[n] = \boldsymbol{\Phi}[n, n_0]\boldsymbol{\Delta}[n_0] + P\sum_{t=n_0}^{n-1} \boldsymbol{\Phi}[n, t]\mathbf{1} \tag{5.3}$$

where

$$\boldsymbol{\Phi}[n,\tau] = \begin{cases} \boldsymbol{A}[n-1]\boldsymbol{A}[n-2]\cdots\boldsymbol{A}[\tau] & n-\tau > 0 \\ \boldsymbol{I}_{NL} & n-\tau = 0 \\ \text{undefined} & n-\tau < 0. \end{cases}$$

Observe that, like $\boldsymbol{A}[n]$, each row of $\boldsymbol{\Phi}[n,t]$ for $n \geq t$ is either all zeros or contains a single non-zero element equal to one.

In order to develop the lower bounds on the peak and average age, we begin with a basic but useful Lemma.

Lemma 5. *For any matrices* $\boldsymbol{A} \in \mathbb{R}^{n\times n}$ *and* $\boldsymbol{B} \in \mathbb{R}^{n\times n}$,

$$\text{nullity}(\boldsymbol{AB}) \leq \text{nullity}(\boldsymbol{A}) + \text{nullity}(\boldsymbol{B})$$

Proof. From [160], we have $\text{rank}(\boldsymbol{AB}) \geq \text{rank}(\boldsymbol{A}) + \text{rank}(\boldsymbol{B}) - n$. Since the rank and nullity of any $n \times n$ matrix must sum to n, we can write

$$n - \text{nullity}(\boldsymbol{AB}) \geq n - \text{nullity}(\boldsymbol{A}) + n - \text{nullity}(\boldsymbol{B}) - n$$

which simplifies directly to the desired result. □

The utility of this result is that it can be used to provide a convenient upper bound on the dimension of the nullspace of the transition matrix $\boldsymbol{\Phi}[n,\tau]$ in terms of the dimension of the nullspaces of the constituent matrices $\boldsymbol{A}[n-1]$, $\boldsymbol{A}[n-2]$, ..., $\boldsymbol{A}[\tau]$ for $n > \tau$.

We now derive a useful property of the transition matrices in the following Lemma.

Lemma 6. $\mathbf{1}^\top \boldsymbol{\Phi}[n,\tau]\mathbf{1} > 0$ *for all* $n - \tau$ *satisfying*

$$0 \leq n - \tau < \Delta^* = \lceil \Delta \rceil$$

where

$$\Delta := \frac{NL}{N-1+(N-2)M}.$$

Proof. Since $\mathbf{\Phi}[n,\tau] \in \mathbb{R}^{NL\times NL}$ is composed of elements equal to zero or one for all $n > \tau$, then $\mathbf{1}^\top \mathbf{\Phi}[n,\tau]\mathbf{1} > 0$ if and only if

$$\text{nullity}(\mathbf{\Phi}[n,\tau]) < NL.$$

From Lemma 5 and (5.2), we have

$$\text{nullity}(\mathbf{\Phi}[n,\tau]) \leq (n-\tau)(N-1+(N-2)M).$$

Hence, to satisfy $\text{nullity}(\mathbf{\Phi}[n,\tau]) < NL$ for integer n and τ, it is sufficient for $0 \leq n-\tau < \left\lceil \frac{NL}{N-1+(N-2)M} \right\rceil$, which shows the desired result. □

We present one additional Lemma that will also be used in the development of the bounds.

Lemma 7. $\mathbf{0} \preceq \mathbf{\Phi}[n,t-1]\mathbf{1} \preceq \mathbf{\Phi}[n,t]\mathbf{1} \preceq \mathbf{1}$ *for all* $n \geq t$ *where* $\preceq$ *corresponds to element-wise inequality.*

Proof. The inequality $\mathbf{\Phi}[n,t]\mathbf{1} \preceq \mathbf{1}$ follows directly from the fact that each row of $\mathbf{\Phi}[n,\tau]$ for $n \geq \tau$ is either all zeros or contains a single non-zero element equal to one. Given any $\mathbf{0} \preceq \boldsymbol{u} \preceq \boldsymbol{v}$, this fact also implies $\mathbf{0} \preceq \mathbf{\Phi}[n,\tau]\boldsymbol{u} \preceq \mathbf{\Phi}[n,\tau]\boldsymbol{v}$ for all $n \geq \tau$. Then, setting $\boldsymbol{u} = \boldsymbol{A}[t-1]\mathbf{1}$ and $\boldsymbol{v} = \mathbf{1}$ and noting that $\mathbf{0} \preceq \boldsymbol{u} \preceq \boldsymbol{v}$, we can write

$$\mathbf{0} \preceq \mathbf{\Phi}[n,t-1]\mathbf{1} = \mathbf{\Phi}[n,t]\boldsymbol{u} \preceq \mathbf{\Phi}[n,t]\boldsymbol{v} = \mathbf{\Phi}[n,t]\mathbf{1} \preceq \mathbf{1}$$

which is the desired result. □

An implication of this result is that if, for some fixed $\tau < n$, a particular element of $\mathbf{\Phi}[n,\tau]\mathbf{1}$ is equal to one, then that same element must also be equal to one for all $\mathbf{\Phi}[n,\tau+\ell]\mathbf{1}$ for all $\ell = 1,\ldots,n-\tau$.

The following two Theorems present the lower bounds on peak and average age.

Theorem 13 (Lower bound on peak age)**.** *The peak age of any schedule is lower bounded by*

$$\Delta_{\text{peak}} \geq \Delta^*_{\text{peak}} = (\Delta^* - 1)\, P. \tag{5.4}$$

Proof. From Definition 8 and (5.3), we can write

$$\begin{aligned}
\Delta_{\text{peak}}[n] &= \max \boldsymbol{\Delta}[n] && \text{(5.5a)}\\
&= \max \left(\boldsymbol{\Phi}[n, n_0]\boldsymbol{\Delta}[n_0] + P \sum_{t=n_0}^{n-1} \boldsymbol{\Phi}[n,t]\mathbf{1} \right) && \text{(5.5b)}\\
&\geq \max \left(P \sum_{t=n_0}^{n-1} \boldsymbol{\Phi}[n,t]\mathbf{1} \right) && \text{(5.5c)}
\end{aligned}$$

where the inequality results from the fact that $\boldsymbol{\Phi}[n, n_0]\boldsymbol{\Delta}[n_0]$ only contains non-negative elements. Note that the sum contains $n - n_0$ terms. Lemma 6 implies that at least $\boldsymbol{\Phi}[n, n-1]\mathbf{1}, \ldots, \boldsymbol{\Phi}[n, n-\Delta^*+1]\mathbf{1}$ must be non-zero. Hence

$$\Delta_{\text{peak}}[n] \geq \max \left(P \sum_{t=n-\Delta^*+1}^{n-1} \boldsymbol{\Phi}[n,t]\mathbf{1} \right) = (\Delta^* - 1)\, P. \tag{5.6}$$

The final equality follows from the fact that there are $\Delta^* - 1$ terms in the summation and, according to Lemma 7, at least one consistent element of each term is equal to one. The desired result then follows directly from Definition 10. □

Theorem 14 (Lower bound on average age)**.** *The average age of any schedule is lower bounded by*

$$\Delta_{\text{avg}} \geq \Delta^*_{\text{avg}} = \lambda(\Delta^* - 1)P \tag{5.7}$$

where $\lambda := 1 - \frac{\Delta^*}{2\Delta}$.

Proof. From Definition 9 and following a similar approach as in the proof of Theorem 13, we can write

$$\Delta_{\text{avg}}[n] = \frac{1}{NL}\mathbf{1}^\top \boldsymbol{\Delta}[n] \tag{5.8a}$$

$$\geq \frac{P}{NL} \sum_{t=n-\Delta^*+1}^{n-1} \mathbf{1}^\top \boldsymbol{\Phi}[n,t]\mathbf{1} \tag{5.8b}$$

$$\geq \frac{P}{NL} \sum_{t=n-\Delta^*+1}^{n-1} \operatorname{rank}\left(\boldsymbol{\Phi}[n,t]\right) \tag{5.8c}$$

$$\geq \frac{P}{NL} \sum_{t=n-\Delta^*+1}^{n-1} NL - (n-t)(N-1+(N-2)M) \tag{5.8d}$$

$$= P \sum_{t=n-\Delta^*+1}^{n-1} 1 - \frac{n-t}{\Delta} \tag{5.8e}$$

where the final inequality follows from Lemma 5 and the properties of $\boldsymbol{\Phi}[n,t]$. This result can be simplified by reindexing the sum to write

$$\Delta_{\text{avg}}[n] \geq P \sum_{m=1}^{\Delta^*-1} 1 - \frac{m}{\Delta} \tag{5.9a}$$

$$= P\left(\Delta^* - 1 - \frac{1}{\Delta}\sum_{m=1}^{\Delta^*-1} m\right) \tag{5.9b}$$

$$= P\left(\Delta^* - 1 - \frac{1}{\Delta}\cdot\frac{(\Delta^*-1)\Delta^*}{2}\right) \tag{5.9c}$$

$$= P(\Delta^*-1)\left(1 - \frac{\Delta^*}{2\Delta}\right) \tag{5.9d}$$

$$= \lambda(\Delta^*-1)P. \tag{5.9e}$$

Since this result does not depend on n, we have

$$\Delta_{\text{avg}} \geq \Delta^*_{\text{avg}} = \lambda(\Delta^*-1)P \tag{5.10}$$

which is the desired result. □

5.2.2 Greedy CSI Dissemination Schedule Design for Fully-Connected Networks

In general, for $M \in \{1, 2, 3, 4, \ldots, N-1\}$, the resulting combinatorics are challenging, and it is not obvious how to construct an efficient schedule to disseminate global CSI throughout the network. That is, it is not clear how to make the best choice of transmitting node in each time slot, and the choice of which CSI should be disseminated among the $\binom{N-1}{M} = \frac{(N-1)!}{(N-1-M)!M!}$ different sets of direct estimates from its table to disseminate. Hence, in this section we present a "greedy" schedule that minimizes the instantaneous average age throughout the network, and generates schedules for any choice of N and M.

Algorithm 4: One-Step Greedy Schedule

1 initialize time, $n \leftarrow 0$;
2 each of the N nodes shares its table with the rest of the network;
3 compute the average age improvement over all combinations:
4 **for** $i_{\text{node}} = 1 : N$ **do**
5 **for** $j_{\text{set}} = 1 : \binom{N-1}{M}$ **do**
6 compute $\Delta_{\text{avg,improve}}(i_{\text{node}}, j_{\text{set}})$, which represents the average age improvement throughout the network, given that node i_{node} disseminates its $j_{\text{set}}^{\text{th}}$ set of M direct estimates;
7 **end**
8 **end**
9 choose the node and its set of M estimates that maximize the average age improvement, and resolve ties:
10 **if** there is a tie between two different nodes **then**
11 select the node that has least recently transmitted;
12 **else**
13 **if** there is a tie between two different sets of M direct estimates at the same node **then**
14 select the set that updates greater number of staler estimates throughout the network;
15 **end**
16 **end**
17 the selected node disseminates it selected set of M direct estimates;
18 all nodes update their local tables with any disseminated CSI that is fresher than the CSI currently in their table;
19 $n \leftarrow n + 1$;
20 go to line 3;

The one-step greedy schedule can be run in parallel at all nodes in a distributed fashion.

We note that the schedule could omit the initialization step to minimize startup overhead, if desired, by assuming that all nodes have no CSI knowledge. Although sharing the tables at the beginning takes some time, it permits the schedule to make use of the existing CSI knowledge throughout the network, and therefore may lead to an overall age improvement at startup. In the long run, however, this initial CSI is insignificant since the CSI tables are continually updated. Finally, we note that the resulting greedy schedule for a given choice of N, M, and D could be precomputed offline and saved in a lookup table at all nodes.

Since in each time slot, the greedy schedule determines the transmitting node and its set of M direct estimates based on maximizing the average age during only the current time slot, it is called one-step greedy schedule. Using a schedule that minimizes the instantaneous age in each time slot is somewhat myopic, and may not lead to the best schedule in terms of minimizing steady-state age. Thus, this one-step greedy schedule could be extended to minimize the average age improvement over a window of two or more consecutive time slots, leading to a possible improvement in steady-state age. However, the amount of combinations to search over (i.e., node order and CSI to disseminate) increases exponentially with the window size.

Note that the schedules generated by the one-step greedy schedule eventually result in a periodic schedule since, for any fixed N, there are a finite number of parameters throughout the network, i.e., NL CSI parameters, and they can be modeled as a finite state-space system. The resulting periodic schedule, however, is dependent on the initial conditions (i.e., the age values throughout the network at startup). Interestingly, for the $M \geq (N-1)/2$ region, always the greedy schedule generates a N-periodic round-robin schedule regardless of initialization, and in the resulting schedule each transmitting node always disseminates its M freshest directly estimated CSI parameters. Intuitively, for the $M \geq (N-1)/2$ region, all CSI parameters throughout the network can be updated at least once when during every N consecutive time slots, each of the N nodes transmits exactly once and disseminates its M freshest estimates.

5.2.3 Average Age of Global CSI Dissemination with Random Schedules in Fully-Connected Networks

In this section, the average age of CSI dissemination with equiprobable random node selection is analyzed for two schedules: (i) dissemination of the single freshest channel estimate in each packet, and (ii) dissemination of all directly estimated CSI in each packet. These cases correspond to $M = 1$ and $M = N - 1$, respectively.

Nodes Disseminate Freshest Single CSI ($M = 1$)

For $n \geq 1$, the transmitting node i_n disseminates its single freshest CSI estimate. By "freshest", we mean the channel state estimate with the least age. This freshest CSI estimate at time n corresponds to the (i_{n-1}, i_n) channel directly estimated by node i_n at time $n-1$. This CSI estimate has an age of P words (one packet).

Theorem 15. *The average age of freshest CSI dissemination with equiprobable transmit node selection is equal to*

$$\Delta_{\text{avg}} = \frac{N(N-1)}{2}(D+1). \tag{5.11}$$

Proof. Since the network is assumed to be fully connected and nodes transmit equiprobably, the age statistics are identical at each node in the network. Hence, we focus specifically on the age of channel estimates from the perspective of node i. Consider the age of the direct channel estimate (i, j) at node i for $j \neq i$. The age of this channel estimate follows

$$\Delta_{i,j}^{(i)}[n] = \begin{cases} 0 & \text{w.p. } \frac{1}{N} \\ \Delta_{i,j}^{(i)}[n-1] + P & \text{w.p. } \frac{N-1}{N} \end{cases}$$

where the first case corresponds to node j transmitting at time n and the second case corresponds to any node except node j transmitting at time n. Observe that the age of the (i, j) channel estimate from the perspective of node i is a Markov chain with an infinite number

of states. Let $q \in \{0, 1, 2, \dots\}$ be the state index corresponding to the age $\Delta_{i,j}^{(i)}[n] = qP$ of the (i, j) channel estimate at node i. Denoting $\pi_q = \text{Prob}\left(\Delta_{i,j}^{(k)}[n] = qP\right)$, the probability of state 0 can be computed as $\pi_0 = \sum_{q=0}^{\infty} \frac{1}{N}\pi_q = \frac{1}{N}$, since $\sum_{q=0}^{\infty} \pi_q = 1$ by definition of the state probabilities. The remaining state probabilities π_q for $q \in \{1, 2, 3, \dots\}$ can be straightforwardly computed from the fact that $\pi_q = \frac{N-1}{N}\pi_{q-1}$. Hence, the steady-state distribution of the age states of the direct channel estimate (i, j) at node i is

$$\pi_q = \frac{(N-1)^q}{N^{q+1}}$$

for $q \in \{0, 1, 2, \dots\}$. The average age of the direct channel estimate (i, j) at node i follows as

$$\Delta_{\text{avg,direct}} = \sum_{q=0}^{\infty} q\pi_q P = (N-1)P. \tag{5.12}$$

Consider now the age of the indirectly estimated (j, k) channel at node i for $j \neq k \neq i$. Observe that the age of this channel estimate can only be reduced at node i if node j or node k disseminates the CSI corresponding to the (j, k) channel. This event can only occur in the freshest CSI dissemination schedule when either node j transmits immediately after node k or vice-versa. If this event occurs, the age of the (j, k) channel estimate at node i becomes one, otherwise the age of the (j, k) channel estimate at node i increments. Fig. 5.2 shows a Markov chain representation of the state transitions of the age of the (j, k) channel estimate at node i. For notational convenience, for $\ell \in \{1, \dots, N\}$, denote

$$\pi_{q,\ell} = \text{Prob}\left(\Delta_{j,k}^{(i)}[n] = qP, i_n = \ell\right) \tag{5.13a}$$

$$\pi_{q,\star} = \text{Prob}\left(\Delta_{j,k}^{(i)}[n] = qP, i_n \neq j, i_n \neq k\right). \tag{5.13b}$$

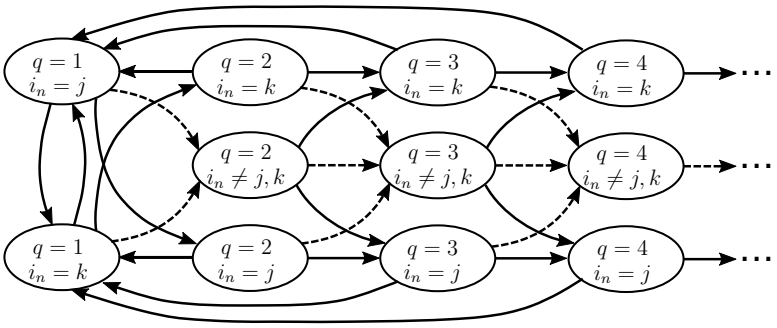

Figure 5.2: A Markov chain representation of the age of the (j,k) channel estimate from the perspective of node i, where solid lines represent transition probability of $\frac{1}{N}$ and dashed lines represent transition probability of $\frac{N-2}{N}$. Also, q represents the state index corresponding to the age $\Delta_{j,k}^{(i)}[n] = qP$ of the (j,k) channel estimate at node i and i_n represents the index of the transmitting node at time n.

Further, the steady state probability distribution of the age states is defined as

$$\pi_q = \sum_{\ell=1}^{N} \pi_{q,\ell} = 2\pi_{q,j} + \pi_{q,\star} \tag{5.14}$$

where the second equality results from the fact that $\pi_{q,j} = \pi_{q,k}$ for all $q \in \{1, 2, \dots\}$, which can be seen from the symmetry of the states in Fig. 5.2. From Fig. 5.2, for $q = 1$, we can write

$$\pi_{1,j} = \frac{1}{N} \sum_{q=1}^{\infty} \pi_{q,j}, \quad \pi_{1,\star} = 0 \tag{5.15}$$

and hence $\pi_1 = 2\pi_{1,j}$. For $q \in \{2, 3, 4, \dots\}$, we can write

$$\pi_{q,j} = \frac{1}{N} \left(\pi_{q-1,j} + \pi_{q-1,\star}\right) \tag{5.16a}$$

$$\pi_{q,\star} = \frac{N-2}{N} \left(2\pi_{q-1,j} + \pi_{q-1,\star}\right). \tag{5.16b}$$

Combining the linear equations (5.13a)-(5.16b), the final steady state probabilities can then

be computed as $\pi_0 = 0$, $\pi_1 = 2\pi_{1,j} = 2/N^2$, $\pi_2 = 2\pi_{2,j} + \pi_{2,\star} = 2(N-1)/N^3$ and $\pi_q = 2\pi_{q,j} + \pi_{q,\star} = \mathbf{A}\mathbf{B}^{q-2}\mathbf{C} \quad \forall q \geq 3$, where

$$\mathbf{A} = \begin{bmatrix} \frac{1}{N^3} & \frac{2(N-2)}{N^3} \end{bmatrix}, \mathbf{B} = \begin{bmatrix} \frac{1}{N} & \frac{2(N-2)}{N} \\ \frac{1}{N} & \frac{N-2}{N} \end{bmatrix}, \mathbf{C} = \begin{bmatrix} 2 \\ 1 \end{bmatrix}. \tag{5.17a}$$

The average age of the indirect estimate of the (j,k) channel at node i follows as

$$\Delta_{\text{avg,indirect}} = \sum_{q=0}^{\infty} q\pi_q P = \frac{(N-1)(N+2)P}{2}. \tag{5.18}$$

Since the age statistics are identical for all nodes in the network, we can use (5.12) and (5.18) to compute the average age as

$$\Delta_{\text{avg}} = \frac{2L\Delta_{\text{avg,direct}} + L(N-2)\Delta_{\text{avg,indirect}}}{LN} \tag{5.19a}$$

$$= \frac{N(N-1)}{2}P \tag{5.19b}$$

where the result in (5.11) follows from the fact that $P = D+1$ with single-CSI dissemination.

□

Nodes Disseminate All Directly Estimated CSI ($M = N-1$)

For $n \geq 1$, the transmitting node i_n disseminates *all* of its directly estimated CSI ($M = N-1$ words of CSI dissemination). Note that node i_n does not disseminate indirectly estimated CSI since the age of indirectly estimated CSI at node i_n is the same or worse than the age of these channel estimates at all other nodes in the fully-connected network.

Theorem 16. *The average age of all directly estimated CSI dissemination with equiprobable transmit node selection is equal to*

$$\Delta_{\text{avg}} = \frac{3N-4}{2}(D+N-1). \tag{5.20}$$

Proof. Similar to the case with single freshest CSI dissemination, we consider the average age of the directly estimated and indirectly estimated CSI separately. The age of the direct estimate (i,j) at node i for $j \neq i$ is the same as the freshest CSI dissemination case since the age of these channels do not depend on the disseminated CSI. Hence, the average age of the (i,j) channel, considered from the perspective of node i, is identical to (5.12).

Consider now the age of the indirect estimates (j,k) at node i for $j \neq k \neq i$. To facilitate analysis, define the vector state $[\Delta_{j,k}^{(i)}[n], m[n]]^\top$ where $m[n]$ denotes the number of packets since either node j or node k last transmitted at time n. Under our equiprobable transmit node assumption, the vector state follows

$$\begin{bmatrix} \Delta_{j,k}^{(i)}[n] \\ m[n] \end{bmatrix} = \begin{cases} \begin{bmatrix} \Delta_{j,k}^{(i)}[n-1] + P \\ m[n-1] + 1 \end{bmatrix} & \text{w.p. } \frac{N-2}{N} \\ \begin{bmatrix} \Delta_{j,k}^{(i)}[n-1] + P \\ 0 \end{bmatrix} & \text{w.p. } \frac{1}{N} \\ \begin{bmatrix} (m[n-1]+1)P \\ 0 \end{bmatrix} & \text{w.p. } \frac{1}{N} \end{cases} \tag{5.21a}$$

where the first case corresponds to neither node j nor node k transmitting at time n. The second case corresponds to node j (resp. node k) transmitting, but node j (resp. node k) was the most recent node to transmit among node j and node k. This case does not immediately reduce the age at node i because the disseminating node is not disseminating anything new about the (j,k) channels. The third case corresponds to node j (resp. node k) transmitting, and node k (resp. node j) was the most recent node to transmit among node j and node k. When this event occurs, the age of channel estimate (j,k) at node i becomes $\Delta_{j,k}^{(i)}[n] = (m[n-1]+1)P$ since node j or node k disseminates all of its directly estimated CSI at time n and the (j,k) channel estimate has age $(m[n-1]+1)P$ at the disseminating node at time n. Fig. 5.3 shows a Markov chain representation of the age of the (j,k) channel

estimate from the perspective of node i. For notational convenience, define

$$\pi_{q,m} = \text{Prob}\left(m[n] = m, \Delta_{j,k}^{(i)}[n] = qP\right). \tag{5.22}$$

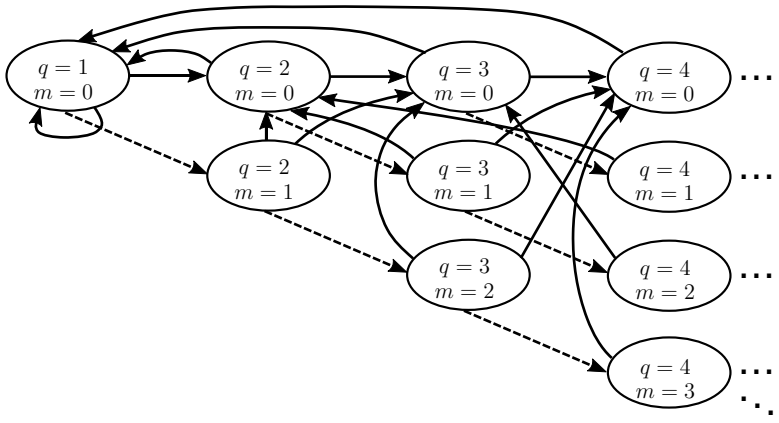

Figure 5.3: A Markov chain representation of the age of the indirect estimate (j,k) from the perspective of node i, where solid lines represent transition probability of $\frac{1}{N}$ and dashed lines represent transition probability of $\frac{N-2}{N}$. The quantity q represents the state index corresponding to the age $\Delta_{j,k}^{(i)}[n] = qP$ of the (j,k) channel estimate at node i and the quantity m represents the number of packets since either node j or node k last transmitted.

With knowledge of the transition probabilities, the steady state probability distribution of the age states are calculated as

$$\pi_q = \sum_{m=0}^{q-1} \pi_{q,m} = \frac{2}{N}\left\{\left(\frac{N-1}{N}\right)^q - \left(\frac{N-2}{N}\right)^q\right\} \tag{5.23a}$$

for all $q \in \{1, 2, 3, \dots\}$ with $\pi_0 = 0$. The average age of the (j,k) channel considered from the view of node i is obtained as

$$\Delta_{\text{avg,indirect}} = \sum_{q=0}^{\infty} q\pi_q P = \frac{(3N-2)P}{2}. \tag{5.24}$$

Finally, since the age statistics are identical for all nodes in the network, using (5.12) and

(5.24), the average age is computed as

$$\Delta_{\text{avg}} = \frac{2L\Delta_{\text{avg,direct}} + L(N-2)\Delta_{\text{avg,indirect}}}{LN} \tag{5.25a}$$

$$= \frac{(3N-4)}{2}P. \tag{5.25b}$$

where the result in (5.20) follows from the fact that $P = D + N - 1$ when nodes disseminate all directly estimated CSI. □

5.3 Numerical Results

This section provides numerical examples to verify the analysis in the previous section and to quantify the peak and average age of information as a function of the network parameters N, D and M. Figures 5.4, 5.5 and 5.6 compare the achievable peak and average age of the greedy schedule with the lower bounds in Theorems 13 and 14 for $N = 8$, versus the number of CSI estimates per packet M for $D \in \{0, 2, 10\}$. The $D = 0$ case can be considered a schedule with no data or overhead where each packet is dedicated solely to CSI dissemination. Since the greedy schedule is sensitive to the initial age values throughout the network, for each M the schedule is run for 1000 random initializations and the minimum and maximum age values are chosen as the best and worst achievable age of the greedy schedule, respectively. The area between the best and worst achievable age of the greedy schedule is shaded, which represents achievable peak and average age of the greedy schedule for different initializations.

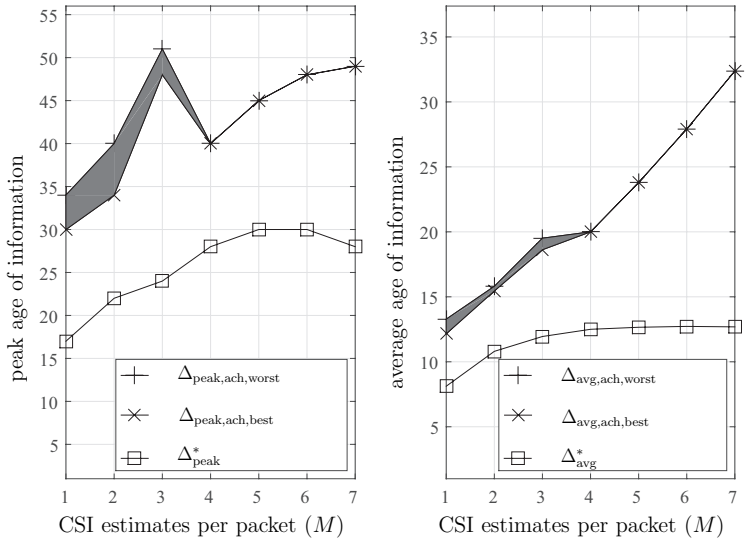

Figure 5.4: Age versus M for $N = 8$ and $D = 0$.

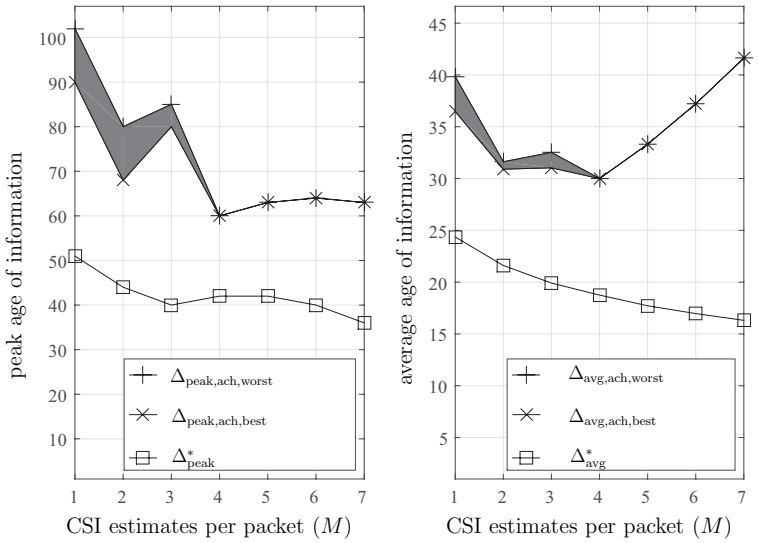

Figure 5.5: Age versus M for $N = 8$ and $D = 2$.

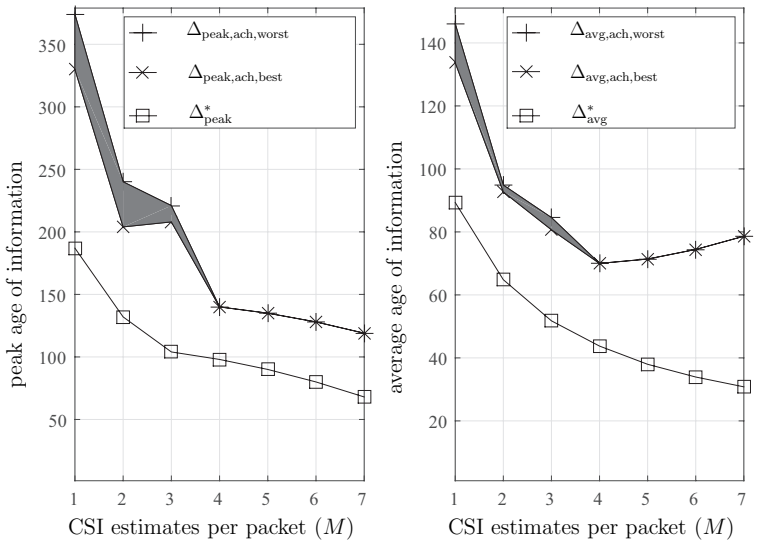

Figure 5.6: Age versus M for $N = 8$ and $D = 10$.

Figures 5.4 and 5.6 confirm that for small and large values of D, to minimize the achievable peak age it is optimal to disseminate $M = 1$ and $M = N - 1$ CSI estimates in each packet, respectively, but as Fig. 5.5 shows for an intermediate value of D, i.e., $D = 2$, the achievable peak age is minimized when $M = 4$ CSI estimate are disseminated in each packet.

Figures 5.7 and 5.8 represent the average age of global CSI dissemination with equiprobable random node selection. Figures5.7 plots the average age of single/all CSI dissemination versus the number of nodes N for $D \in \{0, 10\}$. These results show that single CSI dissemination ($M = 1$) provides better age when $D = 0$ but all directly estimated CSI dissemination ($M = N - 1$) provides better age when $D = 10$.

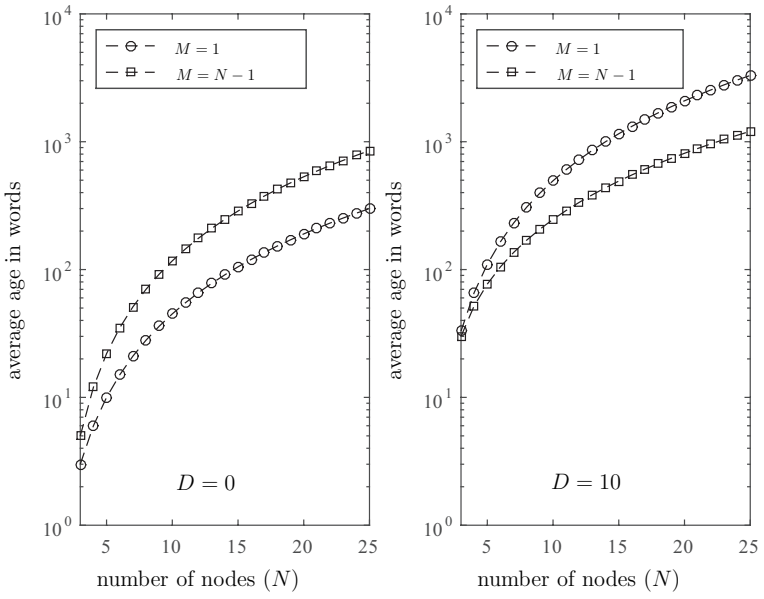

Figure 5.7: Average age versus number of nodes N.

Figure 5.8 plots the average age versus the packet data and overhead D for $N \in \{5, 25\}$. These results show that single CSI dissemination ($M = 1$) tends to be more efficient only for very small values of D, especially in the $N = 25$ case. Intuitively, when the amount of data and overhead in each packet is large, it is more efficient to disseminate all directly estimated CSI ($M = N - 1$) since the additional incurred age is relatively small. In fact, in the $N = 25$ case, we see that "all" CSI dissemination provides better average age than single CSI dissemination for $D \geq 3$.

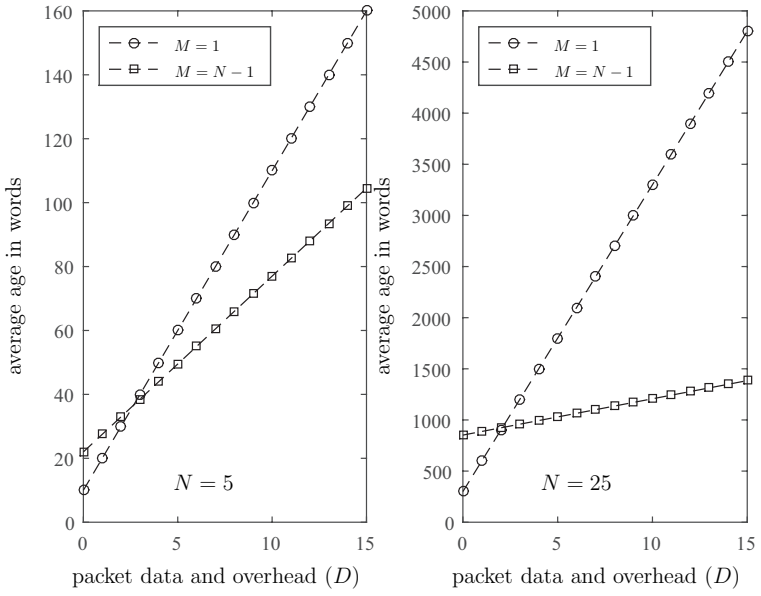

Figure 5.8: Average age versus packet data and overhead D.

5.4 Conclusion

This chapter studied the application of the age of information in quantifying the age of global channel state information in fully-connected wireless networks with packetized transmissions and time-varying reciprocal channels. Lower bounds on the peak and average age of global CSI dissemination were derived as a function of the number of nodes, CSI estimates and data plus overhead per packet. A one-step greedy algorithm that generates CSI dissemination schedules for any choice of number of nodes and number of CSI estimates per packet was developed based on maximizing the instantaneous average age improvement throughout the network. The results show that for small packet data plus overhead, the age is minimized when the number of CSI estimates per packet is small, too. On the other hand, for large packet data plus overhead, the age is minimized when all CSI estimates are disseminated in each packet.

Chapter 6

Conclusion and Future Work

In this final chapter the main ideas of this dissertation are summarized and future research directions are provided.

6.1 Conclusion

In this dissertation we studied the Age of Information problem in different status update systems under various settings. In Chapter 2 a general multi-source multi-hop partially-connected wireless network with time slotted transmissions was considered. We derived lower bounds on the instantaneous peak and average age of information under three different interference cases: (i) global interference model (ii) interference free model, and (iii) topologically-dependent interference model. We showed that these lower bounds are a function of fundamental parameters of the graph representing the network topology. We developed an algorithm that generates minimum-length periodic schedules for dissemination of the status updates among the nodes in the network with a connected topology, given the global interference model. In presence of transmission errors, a lower bound on the average peak age of information was derived considering repetitive transmissions by the nodes in the flooding tree that disseminates statuses throughout the network.

In Chapter 3 we considered the multi-source status update system with transmission

errors. Two cases of (i) active sources where they can generate information packets at any point in time and (ii) random packet generation at the sources based on the Poisson process were studied. For two scheduling policies, stationary randomized and round-robin, closed-form expressions were derived for the case of active sources. Further, three different packet management approaches whenever errors occur: no retransmission, retransmission without resampling, and retransmission with resampling were considered for each scheduling policy. For the Poisson packet arrivals, average AoI expressions were derived assuming that the server only allows self preemption of the packets in service.

In Chapter 4 the single-source status update system with an energy harvesting server with finite battery capacity was considered. Expressions for the average AoI were derived as a function of the system parameters for four different scenarios based on the server's ability to harvest energy while the server is busy and also allowing preemption of the packets in service. It was shown that in general preemption of the packets in service is the best packet management when the rate of energy arrivals is higher than the packet arrival rate.

In Chapter 5 the age of channel state information in fully-connected wireless networks with time slotted transmissions over time-varying reciprocal channels was considered. Fundamental bounds on the peak and average age of global CSI dissemination were derived as a function of the number of nodes, CSI estimates and data plus overhead disseminated in each packet. A one-step greedy algorithm was developed that generates scheduling policies for any choice of number of nodes and number of CSI estimates per packet based on maximizing the instantaneous average age improvement throughout the network.

6.2 Future Work

There are numerous interesting future directions of work on the age of information to consider. Given the general multi-source multi-hop scenario with a fixed network topology in Chapter 2, the minimum-length periodic schedule has been shown to be peak age optimal. However, it is not the case regarding the average age. An interesting problem is to opti-

mize the scheduling policy that minimizes the average age. Another interesting problem is to study the achievable average age of the schedules with repetitive transmissions by the disseminating nodes in presence of errors. The setting in Chapter 2 assumed that each node has direct access to its local process. An interesting problem is to investigate the optimal flooding trees that minimize the age metrics when multiple nodes in the network have zero-delay access to the same process. For energy harvesting status update systems, generalizing the results in Chapter 4 to multiple sources would be an interesting problem.

Appendix A

List of Notation and Acronyms

Table A.1: List of Notation and Acronyms

Notation	Description
$\mathcal{G}$	an undirected graph representing the wireless network
$\mathcal{E}$	set of the edges in $\mathcal{G}$ representing the channels in the network
$\mathcal{V}$	set of the vertices in $\mathcal{G}$ representing the nodes in the network
$\mathcal{G}[\mathcal{U}]$	the graph induced by a vertex set $\mathcal{U} \subseteq \mathcal{V}$
N	number of the nodes in the network, i.e., $N = \lvert\mathcal{V}\rvert$
$d(i,j)$	shortest path length between two vertices i and j
$\bar{d}$	average shortest path length between all vertices in $\mathcal{G}$
δ_i	degree of vertex i
$\delta_{\max}$	maximum degree over all vertices in $\mathcal{G}$
$\mathcal{N}_k(i)$	set of vertices $j \in \mathcal{V}$ such that $1 \leq d(i,j) \leq k$
γ_c	connected domination number, i.e., cardinality of any MCDS
$\mathcal{L}$	set of pseudoleaf vertices, i.e., all vertices not in any MCDS
$H_j^{(i)}(t)$	the H_j process at node i
$\tau_j^{(i)}(t)$	timestamp of the most recent H_j process at node i

$\Delta_j^{(i)}(t)$	the age of the H_j process at node i at time t
mod	modulus operator
CSI	channel state information
FCFS	first-come first-served
LCFS	last-come first-served
SHS	Stochastic Hybrid Systems

Bibliography

[1] S. Kaul, M. Gruteser, V. Rai, and J. Kenney, "Minimizing age of information in vehicular networks," in *Sensor, Mesh and Ad Hoc Communications and Networks (SECON), 2011 Annual IEEE Communications Society Conference on*, Jun. 2011, pp. 350–358.

[2] S. Kaul, R. Yates, and M. Gruteser, "Real-time status: How often should one update?" in *IEEE Conference on Computer Communications (INFOCOM)*, Mar. 2012, pp. 2731–2735.

[3] C. Kam, S. Kompella, and A. Ephremides, "Age of information under random updates," in *IEEE International Symposium on Information Theory (ISIT)*, Jul. 2013, pp. 66–70.

[4] M. Costa, M. Codreanu, and A. Ephremides, "Age of information with packet management," in *IEEE International Symposium on Information Theory (ISIT)*, Jun. 2014, pp. 1583–1587.

[5] C. Kam, S. Kompella, and A. Ephremides, "Effect of message transmission diversity on status age," in *IEEE International Symposium on Information Theory (ISIT)*, Jun. 2014, pp. 2411–2415.

[6] M. Costa, S. Valentin, and A. Ephremides, "On the age of channel information for a finite-state markov model," in *IEEE International Conference on Communications (ICC)*, 2015, pp. 4101–4106.

[7] M. Costa, S. Valentin, and A. Ephremides, "On the age of channel state information for non-reciprocal wireless links," in *IEEE International Symposium on Information Theory (ISIT)*, Jun. 2015, pp. 2356–2360.

[8] R. D. Yates, "Lazy is timely: Status updates by an energy harvesting source," in *IEEE International Symposium on Information Theory (ISIT)*, Jun. 2015, pp. 3008–3012.

[9] B. T. Bacinoglu, E. T. Ceran, and E. Uysal-Biyikoglu, "Age of information under energy replenishment constraints," in *Proc. Information Theory and Applications Workshop (ITA)*, Feb. 2015, pp. 25–31.

[10] E. Najm and R. Nasser, "Age of information: The gamma awakening," in *IEEE International Symposium on Information Theory (ISIT)*, Jul. 2016, pp. 2574–2578.

[11] K. Chen and L. Huang, "Age-of-information in the presence of error," in *IEEE International Symposium on Information Theory (ISIT)*, Jul. 2016, pp. 2579–2583.

[12] M. Costa, M. Codreanu, and A. Ephremides, "On the age of information in status update systems with packet management," *IEEE Transactions on Information Theory*, vol. 62, no. 4, pp. 1897–1910, 2016.

[13] A. M. Bedewy, Y. Sun, and N. B. Shroff, "Optimizing data freshness, throughput, and delay in multi-server information-update systems," in *IEEE International Symposium on Information Theory (ISIT)*, Jul. 2016, pp. 2569–2573.

[14] Y. Sun, E. Uysal-Biyikoglu, R. D. Yates, C. E. Koksal, and N. B. Shroff, "Update or wait: How to keep your data fresh," *IEEE Transactions on Information Theory*, vol. 63, no. 11, pp. 7492–7508, Aug. 2017.

[15] A. Kosta, N. Pappas, A. Ephremides, and V. Angelakis, "Age and value of information: Non-linear age case," in *IEEE International Symposium on Information Theory (ISIT)*, Jun. 2017, pp. 326–330.

[16] E. Najm, R. Yates, and E. Soljanin, "Status updates through M/G/1/1 queues with HARQ," in *IEEE International Symposium on Information Theory (ISIT)*, Aug. 2017, pp. 131–135.

[17] Y. Sang, B. Li, and B. Ji, "The power of waiting for more than one response in minimizing the age-of-information," in *IEEE Global Communications Conference (GLOBECOM)*, Dec. 2017, pp. 1–6.

[18] Y. Inoue, H. Masuyama, T. Takine, and T. Tanaka, "The stationary distribution of the age of information in fcfs single-server queues," in *IEEE International Symposium on Information Theory (ISIT)*, Aug. 2017, pp. 571–575.

[19] R. D. Yates, E. Najm, E. Soljanin, and J. Zhong, "Timely updates over an erasure channel," in *IEEE International Symposium on Information Theory (ISIT)*, Jun. 2017.

[20] J. Zhong, R. D. Yates, and E. Soljanin, "Backlog-adaptive compression: Age of information," in *IEEE International Symposium on Information Theory (ISIT)*, Aug. 2017, pp. 566–570.

[21] Y. Sun, Y. Polyanskiy, and E. Uysal-Biyikoglu, "Remote estimation of a wiener process over a channel with random delay," in *IEEE International Symposium on Information Theory (ISIT)*, Aug. 2017, pp. 321–325.

[22] L. Huang and L. P. Qian, "Age of information for transmissions over markov channels," in *IEEE Global Communications Conference (GLOBECOM)*, Dec. 2017, pp. 1–6.

[23] X. Wu, J. Yang, and J. Wu, "Optimal status updating to minimize age of information with an energy harvesting source," in *IEEE International Conference on Communications (ICC)*, Jul. 2017, pp. 1–6.

[24] B. T. Bacinoglu and E. Uysal-Biyikoglu, "Scheduling status updates to minimize age of information with an energy harvesting sensor," in *IEEE International Symposium on Information Theory (ISIT)*, Aug. 2017, pp. 1122–1126.

[25] A. Arafa and S. Ulukus, "Age minimization in energy harvesting communications: Energy-controlled delays," in *Asilomar Conference on Signals, Systems and Computers (ACSSC)*, Oct. 2017.

[26] C. Kam, S. Kompella, G. D. Nguyen, J. E. Wieselthier, and A. Ephremides, "On the age of information with packet deadlines," *IEEE Transactions on Information Theory*, 2018.

[27] Y.-P. Hsu, "Age of information: Whittle index for scheduling stochastic arrivals," in *IEEE International Symposium on Information Theory (ISIT)*, Jun. 2018, pp. 2634–2638.

[28] C. Kam, S. Kompella, G. D. Nguyen, J. E. Wieselthier, and A. Ephremides, "Towards an "effective age" concept," in *IEEE International Workshop on Signal Processing Advances in Wireless Communications (SPAWC)*. IEEE, 2018, pp. 1–5.

[29] S. Bhambay, S. Poojary, and P. Parag, "Fixed length differential encoding for real-time status updates," *IEEE Transactions on Communications*, 2018.

[30] R. Devassy, G. Durisi, G. C. Ferrante, O. Simeone, and E. Uysal-Biyikoglu, "Delay and peak-age violation probability in short-packet transmissions," in *IEEE International Symposium on Information Theory (ISIT)*, Jun. 2018, pp. 2471–2475.

[31] B. T. Bacinoglu, Y. Sun, E. Uysal-Biyikoglu, and V. Mutlu, "Achieving the age-energy tradeoff with a finite-battery energy harvesting source," in *IEEE International Symposium on Information Theory (ISIT)*, Jun. 2018, pp. 876–880.

[32] J. Zhang and C.-C. Wang, "On the rate-cost of gaussian linear control systems with random communication delays," in *IEEE International Symposium on Information Theory (ISIT)*. IEEE, 2018, pp. 2441–2445.

[33] Z. Jiang, B. Krishnamachari, X. Zheng, S. Zhou, and Z. Niu, "Timely status update in massive iot systems: Decentralized scheduling for wireless uplinks," in *IEEE International Symposium on Information Theory (ISIT)*. IEEE, 2018, pp. 1–6.

[34] Y. Xiao and Y. Sun, "A dynamic jamming game for real-time status updates," in *IEEE Conference on Computer Communications Workshops (INFOCOM WKSHPS)*, Apr. 2018, pp. 354–360.

[35] S. Feng and J. Yang, "Optimal status updating for an energy harvesting sensor with a noisy channel," in *IEEE Conference on Computer Communications Workshops (INFOCOM WKSHPS)*, Apr. 2018, pp. 348–353.

[36] J. Gong, X. Chen, and X. Ma, "Energy-age tradeoff in status update communication systems with retransmission," in *IEEE Global Communications Conference (GLOBECOM)*. IEEE, 2018.

[37] A. Arafa, J. Yang, and S. Ulukus, "Age-minimal online policies for energy harvesting sensors with random battery recharges," in *IEEE International Conference on Communications (ICC)*, Jul. 2018.

[38] A. Arafa, J. Yang, S. Ulukus, and H. V. Poor, "Age-minimal transmission for energy harvesting sensors with finite batteries: Online policies," *IEEE Transactions on Information Theory*, 2019.

[39] A. Arafa and S. Ulukus, "Timely updates in energy harvesting two-hop networks: Offline and online policies," *IEEE Transactions on Wireless Communications*, vol. 18, no. 8, pp. 4017–4030, 2019.

[40] A. Arafa, J. Yang, S. Ulukus, and H. V. Poor, "Online timely status updates with erasures for energy harvesting sensors," in *2018 56th Annual Allerton Conference on Communication, Control, and Computing (Allerton)*, 2018, pp. 966–972.

[41] B. Wang, S. Feng, and J. Yang, "When to preempt? age of information minimization under link capacity constraint," *Journal of Communications and Networks*, vol. 21, no. 3, pp. 220–232, 2019.

[42] P. Zou, O. Ozel, and S. Subramaniam, "On the benefits of waiting in status update systems," in *IEEE Conference on Computer Communications Workshops (INFOCOM WKSHPS)*, 2019, pp. 171–176.

[43] R. Talak and E. Modiano, "Age-delay tradeoffs in single server systems," in *IEEE International Symposium on Information Theory (ISIT)*, 2019, pp. 340–344.

[44] J. Gong, Q. Kuang, X. Chen, and X. Ma, "Reducing age-of-information for computation-intensive messages via packet replacement," in *International Conference on Wireless Communications and Signal Processing (WCSP)*, 2019, pp. 1–6.

[45] A. Arafa, J. Yang, S. Ulukus, and H. V. Poor, "Using erasure feedback for online timely updating with an energy harvesting sensor," in *IEEE International Symposium on Information Theory (ISIT)*, 2019, pp. 607–611.

[46] Y. Lu, K. Xiong, P. Fan, Z. Zhong, and K. B. Letaief, "Online transmission policy in wireless powered networks with urgency-aware age of information," in *International Wireless Communications & Mobile Computing Conference (IWCMC)*, 2019, pp. 1096–1101.

[47] E. T. Ceran, D. Gündüz, and A. György, "Average age of information with hybrid arq under a resource constraint," in *IEEE Wireless Communications and Networking Conference (WCNC)*, 2018, pp. 1–6.

[48] G. D. Nguyen, S. Kompella, C. Kam, and J. E. Wieselthier, "Information freshness over a markov channel: The effect of channel state information," *Ad Hoc Networks*, vol. 86, pp. 63–71, 2019.

[49] I. Krikidis, "Average age of information in wireless powered sensor networks," *IEEE Wireless Communications Letters*, 2019.

[50] M. Wang, W. Chen, and A. Ephremides, "Real-time reconstruction of counting process through queues," *arXiv preprint arXiv:1901.08197*, 2019.

[51] P. Zou, O. Ozel, and S. Subramaniam, "Relative age of information: A new metric for status update systems," *arXiv preprint arXiv:1901.05428*, 2019.

[52] Z. Liu and B. Ji, "Towards the tradeoff between service performance and information freshness," in *IEEE International Conference on Communications (ICC)*, 2019, pp. 1–6.

[53] R. D. Yates and S. Kaul, "Real-time status updating: Multiple sources," in *IEEE International Symposium on Information Theory (ISIT)*, Jul. 2012, pp. 2666–2670.

[54] S. K. Kaul, R. D. Yates, and M. Gruteser, "Status updates through queues," in *Annual Conference on Information Sciences and Systems (CISS)*, Mar. 2012, pp. 1–6.

[55] N. Pappas, J. Gunnarsson, L. Kratz, M. Kountouris, and V. Angelakis, "Age of information of multiple sources with queue management," in *IEEE International Conference on Communications (ICC)*, Jun. 2015, pp. 5935–5940.

[56] B. Li, A. Eryilmaz, and R. Srikant, "On the universality of age-based scheduling in wireless networks," in *IEEE Conference on Computer Communications (INFOCOM)*, Apr. 2015, pp. 1302–1310.

[57] I. Kadota, E. Uysal-Biyikoglu, R. Singh, and E. Modiano, "Minimizing the age of information in broadcast wireless networks," in *Annual Allerton Conference on Communication, Control, and Computing (Allerton)*, Sep. 2016, pp. 844–851.

[58] L. Huang and E. Modiano, "Optimizing age-of-information in a multi-class queueing system," in *IEEE International Symposium on Information Theory (ISIT)*, Jun. 2015, pp. 1681–1685.

[59] Q. He, D. Yuan, and A. Ephremides, "On optimal link scheduling with min-max peak age of information in wireless systems," in *IEEE International Conference on Communications (ICC)*, May 2016, pp. 1–7.

[60] Q. He, D. Yuan, and A. Ephremides, "Optimizing freshness of information: On minimum age link scheduling in wireless systems," in *Modeling and Optimization in Mobile, Ad Hoc, and Wireless Networks (WiOpt), 2016 14th International Symposium on*, May 2016, pp. 1–8.

[61] R. D. Yates and S. K. Kaul, "Status updates over unreliable multiaccess channels," in *IEEE International Symposium on Information Theory (ISIT)*, Aug. 2017, pp. 331–335.

[62] Y.-P. Hsu, E. Modiano, and L. Duan, "Age of information: Design and analysis of optimal scheduling algorithms," in *IEEE International Symposium on Information Theory (ISIT)*, Aug. 2017, pp. 561–565.

[63] V. Tripathi and S. Moharir, "Age of information in multi-source systems," in *IEEE Global Communications Conference (GLOBECOM)*, Dec. 2017, pp. 1–6.

[64] R. D. Yates, P. Ciblat, A. Yener, and M. Wigger, "Age-optimal constrained cache updating," in *IEEE International Symposium on Information Theory (ISIT)*, Aug. 2017, pp. 141–145.

[65] Y.-P. Hsu, E. Modiano, and L. Duan, "Scheduling algorithms for minimizing age of information in wireless broadcast networks with random arrivals," *IEEE Transactions on Mobile Computing*, 2019.

[66] C. Kam, S. Kompella, G. D. Nguyen, J. E. Wieselthier, and A. Ephremides, "Information freshness and popularity in mobile caching," in *IEEE International Symposium on Information Theory (ISIT)*, Aug. 2017, pp. 136–140.

[67] R. Deng, Z. Jiang, S. Zhou, and Z. Niu, "How often should csi be updated for massive mimo systems with massive connectivity?" in *IEEE Global Communications Conference (GLOBECOM)*. IEEE, 2017, pp. 1–6.

[68] R. D. Yates and S. K. Kaul, "The age of information: Real-time status updating by multiple sources," *IEEE Transactions on Information Theory*, vol. 65, no. 3, pp. 1807–1827, 2018.

[69] Q. He, D. Yuan, and A. Ephremides, "Optimal link scheduling for age minimization in wireless systems," *IEEE Transactions on Information Theory*, vol. 64, no. 7, pp. 5381–5394, Jul. 2018.

[70] Q. He, D. Yuan, and A. Ephremides, "Optimal link scheduling for age minimization in wireless systems," *IEEE Transactions on Information Theory*, vol. 64, no. 7, pp. 5381–5394, 2018.

[71] I. Kadota, A. Sinha, E. Uysal-Biyikoglu, R. Singh, and E. Modiano, "Scheduling policies for minimizing age of information in broadcast wireless networks," *IEEE/ACM Transactions on Networking*, vol. 26, no. 6, pp. 2637–2650, 2018.

[72] Y.-P. Hsu, "Age of information: Whittle index for scheduling stochastic arrivals," in *IEEE International Symposium on Information Theory (ISIT)*. IEEE, 2018, pp. 2634–2638.

[73] Z. Jiang, B. Krishnamachari, X. Zheng, S. Zhou, and Z. Niu, "Decentralized status update for age of information optimization in wireless multiaccess channels," in *IEEE International Symposium on Information Theory (ISIT)*, Jun. 2018, pp. 2276–2280.

[74] J. Zhong, R. D. Yates, and E. Soljanin, "Two freshness metrics for local cache refresh," in *IEEE International Symposium on Information Theory (ISIT)*, Jun. 2018.

[75] J. Zhong, R. D. Yates, and E. Soljanin, "Multicast with prioritized delivery: How fresh is your data?" in *IEEE International Workshop on Signal Processing Advances in Wireless Communications (SPAWC)*, Jun. 2018.

[76] I. Kadota, A. Sinha, and E. Modiano, "Optimizing age of information in wireless networks with throughput constraints," in *IEEE Conference on Computer Communications (INFOCOM)*, Apr. 2018, pp. 1844–1852.

[77] I. Kadota, A. Sinha, and E. Modiano, "Scheduling algorithms for optimizing age of information in wireless networks with throughput constraints," *IEEE/ACM Transactions on Networking*, vol. 27, no. 4, pp. 1359–1372, 2019.

[78] Y. Sun, E. Uysal-Biyikoglu, and S. Kompella, "Age-optimal updates of multiple information flows," in *IEEE Conference on Computer Communications Workshops (INFOCOM WKSHPS)*, Apr. 2018, pp. 136–141.

[79] J. Zhong, R. D. Yates, and E. Soljanin, "Minimizing content staleness in dynamo-style replicated storage systems," in *IEEE Conference on Computer Communications Workshops (INFOCOM WKSHPS)*, Apr. 2018, pp. 361–366.

[80] Q. He, G. Dan, and V. Fodor, "Minimizing age of correlated information for wireless camera networks," in *IEEE Conference on Computer Communications Workshops (INFOCOM WKSHPS)*, Apr. 2018, pp. 547–552.

[81] G. D. Nguyen, S. Kompella, C. Kam, J. E. Wieselthier, and A. Ephremides, "Information freshness over an interference channel: A game theoretic view," in *IEEE Conference on Computer Communications (INFOCOM)*. IEEE, 2018, pp. 908–916.

[82] S. Gopal and S. K. Kaul, "A game theoretic approach to dsrc and wifi coexistence," in *IEEE Conference on Computer Communications Workshops (INFOCOM WKSHPS)*, Apr. 2018, pp. 565–570.

[83] M. Costa and Y. E. Sagduyu, "Age of information with network coding," *Ad Hoc Networks*, vol. 86, pp. 15–22, 2019.

[84] B. Sombabu and S. Moharir, "Poster: Age-of-information aware scheduling for heterogeneous sources," in *Proceedings of the Annual International Conference on Mobile Computing and Networking*. ACM, 2018, pp. 696–698.

[85] A. Kosta, N. Pappas, A. Ephremides, and V. Angelakis, "Age of information performance of multiaccess strategies with packet management," *Journal of Communications and Networks*, vol. 21, no. 3, pp. 244–255, 2019.

[86] M. K. Abdel-Aziz, C.-F. Liu, S. Samarakoon, M. Bennis, and W. Saad, "Ultra-reliable low-latency vehicular networks: Taming the age of information tail," in *IEEE Global Communications Conference (GLOBECOM)*. IEEE, 2018, pp. 1–7.

[87] E. T. Ceran, D. Gündüz, and A. György, "A reinforcement learning approach to age of information in multi-user networks," in *IEEE International Symposium on Personal, Indoor and Mobile Radio Communications (PIMRC)*. IEEE, 2018, pp. 1967–1971.

[88] Z. Jiang, S. Zhou, Z. Niu, and C. Yu, "A unified sampling and scheduling approach for status update in multiaccess wireless networks," in *IEEE Conference on Computer Communications (INFOCOM)*. IEEE, 2019, pp. 208–216.

[89] C. Joo and A. Eryilmaz, "Wireless scheduling for information freshness and synchrony: Drift-based design and heavy-traffic analysis," *IEEE/ACM Transactions on Networking*, vol. 26, no. 6, pp. 2556–2568, 2018.

[90] A. Alabbasi and V. Aggarwal, "Joint information freshness and completion time optimization for vehicular networks," *arXiv preprint arXiv:1811.12924*, 2018.

[91] A. E. Kalør and P. Popovski, "Minimizing the age of information from sensors with correlated observations," *arXiv preprint arXiv:1811.06453*, 2018.

[92] B. Zhou and W. Saad, "Minimizing age of information in the internet of things with non-uniform status packet sizes," in *IEEE International Conference on Communications (ICC)*. IEEE, 2019, pp. 1–6.

[93] A. Maatouk, M. Assaad, and A. Ephremides, "Age of information with prioritized streams: When to buffer preempted packets?" in *IEEE International Symposium on Information Theory (ISIT)*. IEEE, 2019, pp. 325–329.

[94] Y.-H. Tseng and Y.-P. Hsu, "Online energy-efficient scheduling for timely information downloads in mobile networks," in *IEEE International Symposium on Information Theory (ISIT)*. IEEE, 2019, pp. 1022–1026.

[95] A. Maatouk, M. Assaad, and A. Ephremides, "Minimizing the age of information: Noma or oma?" in *IEEE Conference on Computer Communications Workshops (INFOCOM WKSHPS)*. IEEE, 2019, pp. 102–108.

[96] C. Xu, H. H. Yang, X. Wang, and T. Q. Quek, "On peak age of information in data preprocessing enabled iot networks," in *IEEE Wireless Communications and Networking Conference (WCNC)*. IEEE, 2019, pp. 1–6.

[97] B. Zhou and W. Saad, "Minimum age of information in the internet of things with non-uniform status packet sizes," *IEEE Transactions on Wireless Communications*, 2019.

[98] A. Maatouk, M. Assaad, and A. Ephremides, "Minimizing the age of information in a csma environment," *arXiv preprint arXiv:1901.00481*, 2019.

[99] S. Kaul, R. Yates, and M. Gruteser, "On piggybacking in vehicular networks," in *IEEE Global Communications Conference (GLOBECOM)*, Dec. 2011, pp. 1–5.

[100] J. Selen, Y. Nazarathy, L. L. Andrew, and H. L. Vu, "The age of information in gossip networks," in *International Conference on Analytical and Stochastic Modeling Techniques and Applications*. Springer, 2013, pp. 364–379.

[101] A. Arafa and S. Ulukus, "Age-minimal transmission in energy harvesting two-hop networks," in *IEEE Global Communications Conference (GLOBECOM)*, Dec. 2017, pp. 1–6.

[102] R. D. Yates, "Age of information in a network of preemptive servers," in *IEEE Conference on Computer Communications Workshops (INFOCOM WKSHPS)*, Apr. 2018, pp. 118–123.

[103] B. Buyukates, A. Soysal, and S. Ulukus, "Age of information in multihop multicast networks," *Journal of Communications and Networks*, vol. 21, no. 3, pp. 256–267, 2019.

[104] A. M. Bedewy, Y. Sun, and N. B. Shroff, "Age-optimal information updates in multihop networks," in *IEEE International Symposium on Information Theory (ISIT)*, Aug. 2017, pp. 576–580.

[105] A. M. Bedewy, Y. Sun, and N. B. Shroff, "The age of information in multihop networks," *IEEE/ACM Transactions on Networking*, vol. 27, no. 3, pp. 1248–1257, 2019.

[106] R. Talak, S. Karaman, and E. Modiano, "Minimizing age-of-information in multi-hop wireless networks," in *Annual Allerton Conference on Communication, Control, and Computing (Allerton)*, Oct. 2017, pp. 486–493.

[107] R. Talak, S. Karaman, and E. Modiano, "Optimizing information freshness in wireless networks under general interference constraints," *IEEE/ACM Transactions on Networking*, 2019.

[108] R. Talak, I. Kadota, S. Karaman, and E. Modiano, "Scheduling policies for age minimization in wireless networks with unknown channel state," in *IEEE International Symposium on Information Theory (ISIT)*, Jun. 2018, pp. 2564–2568.

[109] R. Talak, S. Karaman, and E. Modiano, "Optimizing age of information in wireless networks with perfect channel state information," in *International Symposium on Modeling and Optimization in Mobile, Ad Hoc, and Wireless Networks (WiOpt)*, May 2018.

[110] R. Talak, S. Karaman, and E. Modiano, "Distributed scheduling algorithms for optimizing information freshness in wireless networks," in *IEEE International Workshop on Signal Processing Advances in Wireless Communications (SPAWC)*, Jun. 2018.

[111] Q. Liu, H. Zeng, and M. Chen, "Minimizing age-of-information with throughput constraints in multi-path network communication," *arXiv preprint arXiv:1811.12605*, 2018.

[112] V. Tripathi, R. Talak, and E. Modiano, "Age optimal information gathering and dissemination on graphs," in *IEEE Conference on Computer Communications (INFOCOM)*. IEEE, 2019, pp. 2422–2430.

[113] T. Shreedhar, S. K. Kaul, and R. D. Yates, "Acp: An end-to-end transport protocol for delivering fresh updates in the internet-of-things," *arXiv preprint arXiv:1811.03353*, 2018.

[114] S. Farazi, A. G. Klein, J. A. McNeill, and D. R. Brown III, "On the age of information in multi-source multi-hop wireless status update networks," in *IEEE International Workshop on Signal Processing Advances in Wireless Communications (SPAWC)*, Jun. 2018.

[115] S. Farazi, A. G. Klein, and D. R. Brown III, "Fundamental bounds on the age of information in multi-hop global status update networks," *Journal of Communications and Networks*, vol. 21, no. 3, pp. 268–279, 2019.

[116] S. Farazi, A. G. Klein, and D. R. Brown III, "Fundamental bounds on the age of information in general multi-hop interference networks," in *IEEE Conference on Computer Communications Workshops (INFOCOM WKSHPS)*, Apr. 2019, pp. 96–101.

[117] S. Farazi, A. G. Klein, and D. R. Brown III, "Age of information with unreliable transmissions in multi-source multi-hop status update systems," in *Asilomar Conference on Signals, Systems and Computers (ACSSC)*, Nov. 2019, pp. 2017–2021.

[118] D. B. West, *Introduction to Graph Theory*, 2nd ed. Prentice Hall, 2000.

[119] E. Sampathkumar and H. Walikar, "The connected domination number of a graph," *J. Math. Phys*, 1979.

[120] B. Das and V. Bharghavan, "Routing in ad-hoc networks using minimum connected dominating sets," in *IEEE International Conference on Communications (ICC)*, 1997, pp. 376–380.

[121] H. Lim and C. Kim, "Flooding in wireless ad hoc networks," *Computer Communications*, vol. 24, no. 3-4, pp. 353–363, 2001.

[122] A. Brandstadt, J. P. Spinrad *et al.*, *Graph classes: a survey*. Siam, 1999, vol. 3.

[123] J. A. Gallian, "A dynamic survey of graph labeling," *The electronic journal of combinatorics*, vol. 16, no. 6, pp. 1–219, 2009.

[124] B. McKay, "Database of connected simple graphs." [Online]. Available: http://users.cecs.anu.edu.au/~bdm/data/graphs.html

[125] S. Feng and J. Yang, "Age of information minimization for an energy harvesting source with updating erasures: With and without feedback," *arXiv preprint arXiv:1808.05141*, 2018.

[126] V. Tripathi and E. Modiano, "A whittle index approach to minimizing functions of age of information," *arXiv preprint arXiv:1908.10438*, 2019.

[127] S. Farazi, A. G. Klein, and D. R. Brown III, "Average age of information in update systems with active sources and packet delivery errors," 2020, in Wireless Communications Letters.

[128] S. Farazi, A. G. Klein, and D. R. Brown III, "Average age of information in multi-source self-preemptive status update systems with packet delivery errors," in *Asilomar Conference on Signals, Systems and Computers (ACSSC)*, Nov. 2019, pp. 396–400.

[129] J. P. Hespanha, "Modelling and analysis of stochastic hybrid systems," *IEE Proceedings-Control Theory and Applications*, vol. 153, no. 5, pp. 520–535, 2006.

[130] S. Farazi, A. G. Klein, and D. R. Brown III, "Average age of information for status update systems with an energy harvesting server," in *IEEE Conference on Computer Communications Workshops (INFOCOM WKSHPS)*, Apr. 2018, pp. 112–117.

[131] S. Farazi, A. G. Klein, and D. R. Brown III, "Age of information in energy harvesting status update systems: When to preempt in service?" in *IEEE International Symposium on Information Theory (ISIT)*, Jun. 2018, pp. 2436–2440.

[132] M. Tomlinson, "New automatic equaliser employing modulo arithmetic," *Electronics Letters*, vol. 7, no. 5/6, pp. 138–139, Mar. 1971.

[133] R. G. Gallager, *Information Theory and Reliable Communication*. New York: John Wiley, 1971.

[134] P. Chow, J. Cioffi, and J. Bingham, "A practical discrete multitone transceiver loading algorithm for data transmission over spectrally shaped channels," *IEEE Transactions on Communications*, vol. 43, no. 234, pp. 773–775, Feb/Mar/Apr 1995.

[135] R. A. Berry and R. G. Gallagher, "Communication over fading channels with delay constraints," *IEEE Transactions on Information Theory*, vol. 48, no. 5, pp. 1135–1149, May 2002.

[136] B. Vojcic and W. M. Jang, "Transmitter precoding in synchronous multiuser communications," *IEEE Transactions on Communications*, vol. 46, no. 10, pp. 1346–1355, Oct. 1998.

[137] A. Scaglione, P. Stoica, S. Barbarossa, G. Giannakis, and H. Sampath, "Optimal designs for space-time linear precoders and decoders," *IEEE Transactions on Signal Processing*, vol. 50, no. 5, pp. 1051–1064, May 2002.

[138] Q. Spencer, A. Swindlehurst, and M. Haardt, "Zero-forcing methods for downlink spatial multiplexing in multiuser MIMO channels," *IEEE Transactions on Signal Processing*, vol. 52, no. 2, pp. 461–471, Feb. 2004.

[139] D. R. Brown III and D. Love, "On the performance of MIMO nullforming with random vector quantization limited feedback," *IEEE Transactions on Wireless Communications*, vol. 13, no. 5, pp. 2884–2893, May 2014.

[140] A. Sendonaris, E. Erkip, and B. Aazhang, "Interference alignment and degrees of freedom of the k-user interference channel," *IEEE Transactions on Information Theory*, vol. 54, no. 8, pp. 3425–3441, Aug. 2008.

[141] A. Sendonaris, E. Erkip, and B. Aazhang, "User cooperation diversity, Part I: System description," *IEEE Transactions on Communications*, vol. 51, no. 11, pp. 1927–1938, Nov. 2003.

[142] J. N. Laneman, D. N. Tse, and G. W. Wornell, "Cooperative diversity in wireless networks: Efficient protocols and outage behavior," *IEEE Transactions on Information Theory*, vol. 50, no. 12, pp. 3062–3080, Dec. 2004.

[143] Y. Li, Q. Yin, W. Xu, and H.-M. Wang, "On the design of relay selection strategies in regenerative cooperative networks with outdated CSI," *IEEE Transactions on Wireless Communications*, vol. 10, no. 9, pp. 3086–3097, Sep. 2011.

[144] D. R. Brown III, P. Bidigare, S. Dasgupta, and U. Madhow, "Receiver-coordinated zero-forcing distributed transmit nullforming," in *IEEE Statistical Signal Processing Workshop (SSP)*, Aug. 2012, pp. 269–272.

[145] D. R. Brown III, U. Madhow, S. Dasgupta, and P. Bidigare, "Receiver-coordinated distributed transmit nullforming with channel state uncertainty," in *Annual Conference on Information Sciences and Systems (CISS)*, Mar. 2012.

[146] V. Cadambe and S. Jafar, "Interference alignment and degrees of freedom of the k-user interference channel," *IEEE Transactions on Information Theory*, vol. 54, no. 8, pp. 3425–3441, Aug. 2008.

[147] X. Lin, N. B. Shroff, and R. Srikant, "A tutorial on cross-layer optimization in wireless networks," *IEEE Journal on Selected areas in Communications*, vol. 24, no. 8, pp. 1452–1463, Aug. 2006.

[148] L. Georgiadis, M. J. Neely, and L. Tassiulas, *Resource allocation and cross-layer control in wireless networks*. Now Publishers Inc, 2006.

[149] P. de Kerret and D. Gesbert, "CSI sharing strategies for transmitter cooperation in wireless networks," *IEEE Wireless Communications Magazine*, vol. 20, no. 1, pp. 43–49, Feb. 2013.

[150] A. Adhikary, M. Kobayashi, P. Piantanida, H. Papadopoulos, and G. Caire, "CSI dissemination for MU-MIMO schemes based on outdated CSI," in *Annual Allerton Conference on Communication, Control, and Computing (Allerton)*, Oct. 2012, pp. 1672–1679.

[151] S. Ramanan and J. Walsh, "Distributed estimation of channel gains in wireless sensor networks," *IEEE Transactions on Signal Processing*, vol. 58, no. 6, pp. 3097–3107, Jun. 2010.

[152] M. Maddah-Ali and D. Tse, "Completely stale transmitter channel state information is still very useful," *IEEE Transactions on Information Theory*, vol. 58, no. 7, pp. 4418–4431, Jul. 2012.

[153] J. Chen, S. Yang, A. Ozgur, and A. Goldsmith, "Outdated CSIT can achieve full DoF in heterogeneous parallel channels," in *IEEE International Symposium on Information Theory (ISIT)*, Jun. 2014, pp. 2564–2568.

[154] J. Xu, J. Andrews, and S. Jafar, "MISO broadcast channels with delayed finite-rate feedback: Predict or observe?" *IEEE Transactions on Wireless Communications*, vol. 11, no. 4, pp. 1456–1467, Apr. 2012.

[155] L. Ying and S. Shakkottai, "On throughput optimality with delayed network-state information," *IEEE Transactions on Information Theory*, vol. 57, no. 8, pp. 5116–5132, 2011.

[156] A. G. Klein, S. Farazi, W. He, and D. R. Brown III, "Staleness bounds and efficient protocols for dissemination of global channel state information," *IEEE Transactions on Wireless Communications*, vol. 16, no. 9, pp. 5732–5746, Sep. 2017.

[157] S. Farazi, D. R. Brown III, and A. G. Klein, "On global channel state estimation and dissemination in ring networks," in *Asilomar Conference on Signals, Systems and Computers (ACSSC)*, Nov. 2016, pp. 1122–1127.

[158] S. Farazi, A. G. Klein, and D. R. Brown III, "Bounds on the age of information for global channel state dissemination in fully-connected networks," in *International Conference on Computer Communication and Networks (ICCCN)*, Jul. 2017, pp. 1–7.

[159] S. Farazi, A. G. Klein, and D. R. Brown III, "On the average staleness of global channel state information in wireless networks with random transmit node selection," in *In Proceedings Acoustics, Speech and Signal Processing (ICASSP), 2016 IEEE International Conference on*, Mar. 2016, pp. 3621–3625.

[160] R. A. Horn and C. R. Johnson, *Matrix analysis*. Cambridge university press, 2012.